APPENDIX D

Acoustic Modelling Report

Modelling Underwater Sound Associated with Scotian Basin Exploration Drilling Project

Acoustic Modelling Report

Submitted to:
Heather Giddens
Stantec Consulting Ltd.
Agreement: Nova Scotia Drilling ESIA
(121413516) 9 Oct 2015

Author:
Mikhail M. Zykov

26 May 2016

P001299-001
Document 01112
Version 2.0

JASCO Applied Sciences (Canada) Ltd.
202–32 Troop Avenue
Dartmouth, NS B3B 1Z1 Canada
Tel: +1-902-405-3336
Fax: +1-902-405-3337
www.jasco.com

Document Version Control

Version	Date	Name	Change
1.0	2015 Dec 21	M. Zykov	Draft released to client for review.
2.0	2016 Feb 09	M. Zykov	Final report released to client for review. Expanded frequency band for Airgun source array (up to 25 kHz) and Vessels (up to 63 kHz). Added level vs range analysis.

Suggested citation:

Zykov, M.M. 2016. *Modelling Underwater Sound Associated with Scotian Basin Exploration Drilling Project: Acoustic Modelling Report*. JASCO Document 01112, Version 2.0. Technical report by JASCO Applied Sciences for Stantec Consulting Ltd..

Contents

Figures

Tables

1. Introduction

1.1. Project Overview

Stantec Consulting Ltd. (Stantec), by request from BP Canada Energy Group ULC (BP), has engaged JASCO Applied Sciences (JASCO) to perform acoustic field modelling of underwater sound levels associated exploratory well activities within the Scotian Basin Exploration Drilling Project (the Project). The area of interest spans exploratory license blocks EL-2431, 2432, 2433, and 2434.

Two hypothetical well sites on the continental slope in water deeper than 2000 m were modelled (Figure 1). Proposed activities at the sites that would generate underwater sound, and that are modelled in this study, are exploratory well drilling and Vertical Seismic Profiling (VSP). The specifics of vessels and the seismic source are unknown at this time. A drillship (DS) or a semi-submersible platform (SS) could be used; therefore, both of these sound sources were modelled. A support vessel (SV) that will be present during drilling was also modelled. The VSP survey will be performed with a VSP airgun source array.

Multiple scenarios were modelled at each of the two sites to cover different configurations of the acoustic sources, as well as the seasonal variations of the propagation conditions. The modelling methodology accounts for source characteristics and for local environmental properties. Model results are presented as root-mean-square (rms) sound pressure levels (SPLs), peak SPL, and cumulative sound exposure levels (cSELs). The SELs were calculated after the M-weighting filters of Southall et al. (2007) and NOAA (2015) were applied. The acoustic modelling results were compared to various sound level threshold criteria associated with potential injury and behavioral disturbance in order to assess the ranges from the source at which such potential effects may occur, based on:

- Injury
  - Southall et al. 2007 metrics, in both, peak SPL and cSEL
  - NOAA 2015 draft metrics, in both peak SPL and cSEL
- Behavioural
  - NOAA interim 120 dB rms SPL for non-pulse/continuous acoustic sources (i.e., vessels)
  - NOAA interim 160 dB rms SPL for pulse/impulsive sources (i.e., VSP)

Section 1.2 presents background information on various metrics commonly used to characterise underwater sound. The acoustic threshold criteria associated with potential impacts are discussed in Section 1.3. Section 2 discusses the methods used to estimate the source levels and model the sound propagation. Section 3 details the acoustic sources that were modelled and describes the environmental parameters used in the propagation model. Section 4 presents the model results in two formats: (1) tables of distances to sound level thresholds and (2) sound field contour maps showing the directivity of the various sound level threshold contours. Section 5 provides a discussion of model prediction validity and the factors influencing sound propagation.

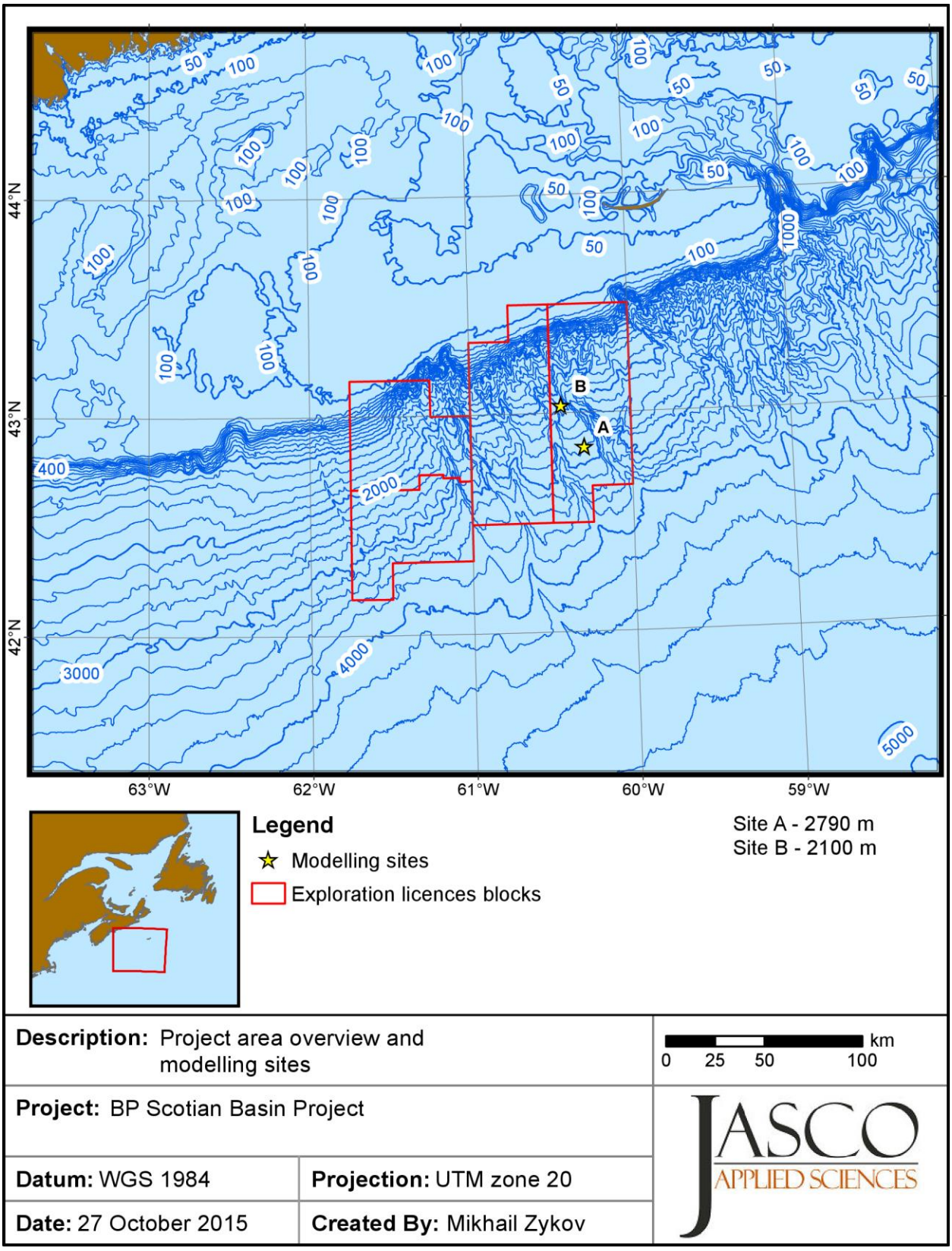

Figure 1. Modelling area overview and modelling sites (yellow stars). Blue lines show bathymetry (m).

1.2. Background–Underwater Acoustics

1.2.1. Types of Sound

Numerous scientific reviews and workshops over the past 40 years have focused on how anthropogenic sounds can affect marine life (e.g., Payne and Webb 1971, Fletcher and Busnel 1978, Richardson et al. 1995, MMC 2007, Nowacek et al. 2007, Southall et al. 2007, Weilgart 2007, Tyack 2008). When assessing potential impacts of anthropogenic sound on marine life, sounds are commonly divided into two main categories: pulsed (with pulses further split into single and multiple pulses) and non-pulsed sounds (Southall et al. 2007).

Pulsed sounds include impact pile driving, airgun pulses, and some types of sonar. Non-pulsed sounds include vessel propulsion sound and some types of sonar. Numerous definitions and mathematical expressions (e.g., Burdic 1984) distinguish pulsed and non-pulsed sounds from one another.

1.2.1.1. Vessel Sounds

Underwater sound that radiates from vessels is produced mainly by propeller and thruster cavitation, with a smaller fraction of sound produced by sound transmitted through the hull, such as by engines, gearing, and other mechanical systems. Sound levels tend to be the highest when thrusters are used to position the vessel and when the vessel is transiting at high speeds. A vessel's sound signature depends on the vessel's size, power output, propulsion system, and the design characteristics of the given system (e.g., blade shape and size). A vessel produces broadband acoustic energy with most of the energy emitted below a few kilohertz. Sound from onboard machinery, particularly sound below 200 hertz (Hz), dominates the sound spectrum before cavitation begins—normally around 8–12 knots on many commercial vessels (Spence et al. 2007). Under higher speeds and higher propulsion system load, the acoustic output from the cavitation processes on the propeller blades dominates other sources of sound on the vessel (Leggat et al. 1981).

1.2.1.2. Seismic Airgun Source Arrays

Seismic airguns generate pulsed acoustic energy by releasing a highly compressed air bubble into the water that expands and then collapses. Seismic airgun source arrays are comprised of multiple individual source elements, which are activated together to produce an output with frequencies ranging from several hertz to several kilohertz. Larger individual source element volumes producing lower frequencies and higher sound levels.

A single source element produces an approximately omnidirectional sound field, emitting acoustic energy equally in all directions. Multiple element seismic source arrays exhibit directivity due to geometric separation of the elements. The geometric separation translates into phase shift during the superposition of acoustic waves emitted by individual elements. The phase shift depends not only on the value of the geometrical separation, but also on the frequency. The effect of the superposition can be constructive or destructive. For VSP surveys, source array layouts are configured to achieve higher sound energy emission levels in the vertical direction where at far-field the pulses from all elements add in-phase, since there is virtually no geometric shift along the z-axis for the array elements. Lower levels of sound energy are emitted in other directions. Airgun source arrays might show significant directionality in the horizontal direction due to the phase delay between pulses because the elements are horizontally separated. The directivity pattern of an airgun source array is different at different frequencies.

1.2.2. Acoustic Metrics

Underwater sound amplitude is measured in decibels (dB) relative to a fixed reference pressure of p_0 = 1 µPa. Because the perceived loudness of sound, especially impulsive sound, is not generally

proportional to the instantaneous acoustic pressure, several sound level metrics are commonly used to evaluate sound and its effects on marine life.

The acoustic impact criteria considered in this report use the metrics:

- peak SPL,
- rms SPL,
- SEL, and
- cumulative SEL (cSEL)

The zero-to-peak SPL, or peak SPL (dB re 1 µPa), is the maximum instantaneous sound pressure level in a stated frequency band attained by an acoustic pressure signal, $p(t)$:

$$\text{Peak SPL} = 10\log_{10}\left[\frac{\max\left(\left|p^2(t)\right|\right)}{p_0^2}\right] \quad (1)$$

At high intensities, the peak SPL can be a valid metric for assessing whether potential injury may occur due to a sound signal or event; however, because the peak SPL does not account for the duration of a sound event, it is a poor indicator of perceived loudness.

The root-mean-square (rms) SPL (dB re 1 µPa) is the rms sound pressure level in a stated frequency band over a time window (T, s) containing the acoustic event:

$$\text{rms SPL} = 10\log_{10}\left(\frac{1}{T}\int_T p^2(t)dt \Big/ p_0^2\right) \quad (2)$$

The rms SPL is a measure of the average pressure or of the effective pressure over the duration of an acoustic event, such as the emission of one acoustic pulse, a marine mammal vocalization, the passage of a vessel, or a fixed duration. Because the window length, T, is the divisor, events more spread out in time will have a lower rms SPL for the same total acoustic energy density. For characterization of continuous sound, such as that from vessels, the time window T, over which the acoustic energy integration occurs, is taken as 1 s. In this case, the rms SPL is equal to the SEL.

In studies of impulsive sound, T is often defined as the "90% energy pulse duration" (T_{90}): the interval over which the pulse energy curve rises from 5% to 95% of the total energy. The SPL computed over this T_{90} interval is commonly called the 90% rms SPL (dB re 1 µPa):

$$\text{90\% rms SPL} = 10\log_{10}\left(\frac{1}{T_{90}}\int_{T_{90}} p^2(t)dt \Big/ p_0^2\right) \quad (3)$$

The sound exposure level (SEL, dB re 1 µPa^2·s) is a measure of the total acoustic energy contained in one or more acoustic events. The SEL for a single event is computed from the time-integral of the squared pressure over the full event duration (T_{100}):

$$\text{SEL} = 10\log_{10}\left(\int_{T_{100}} p^2(t)dt \Big/ T_0 p_0^2\right) \quad (4)$$

where T_0 is a reference time interval of 1 s. The SEL represents the total acoustic energy received at one location during an acoustic event; it measures the total sound energy to which an organism at that location would be exposed.

SEL is a cumulative metric if it is calculated over periods with multiple acoustic events or over a fixed period of time. For multiple events, the cumulative SEL (dB re 1 µPa^2·s) can be computed by summing (in

linear units) the SELs of the *N* individual events (5). For a fixed duration, the pressure is summed over the duration of interest (4).

$$\text{Cumulative SEL} = 10\log_{10}\left(\sum_{i=1}^{N} 10^{\frac{\text{SEL}_i}{10}}\right) \tag{5}$$

Because the rms SPL and SEL are both computed from the integral of square pressure, these metrics are related by the following expression, which depends only on the duration of the energy time window, *T*:

$$\text{rms SPL} = \text{SEL} - 10\log_{10}(T) \tag{6}$$

$$\text{rms SPL} = \text{SEL} - 10\log_{10}(T_{90}) - 0.458 \tag{7}$$

where the 0.458 dB factor accounts for the rms SPL containing 90% of the total energy from the per-pulse SEL.

1.2.3. 1/3-Octave-Band Modelling

The distribution of a sound's power with frequency is described by the frequency spectrum, which shows the fine-scale features of the frequency distribution of a sound. The broadband or total frequency spectrum of a sound can be split into a series of adjacent frequency bands. Splitting a spectrum into 1 Hz wide bands, called passbands, yields the "power spectral density" of the sound. This splitting of the spectrum into passbands of a constant width of 1 Hz does not, however, represent how animals perceive sound.

Because animals perceive exponential increases in frequency rather than linear increases, analyzing a sound spectrum with passbands that increase exponentially in size gives a more meaningful representation of how an animal might perceive sound. In underwater acoustics, a spectrum is commonly split into 1/3-octave-bands, which are one-third of an octave wide; each octave represents a doubling in sound frequency. The centre frequency of the *i*th 1/3-octave-band, $f_c(i)$, is defined as:

$$f_c(i) = 10^{i/10}, \tag{8}$$

and the low (f_{lo}) and high (f_{hi}) frequency limits of the *i*th 1/3-octave-band are defined as:

$$f_{lo}(i) = 10^{-i/20} f_c(i) \text{ and } f_{lo}(i) = 10^{i/20} f_c(i) \ . \tag{9}$$

The 1/3-octave-bands become wider with increasing frequency and on a logarithmic scale the bands appear equally spaced (Figure 2).

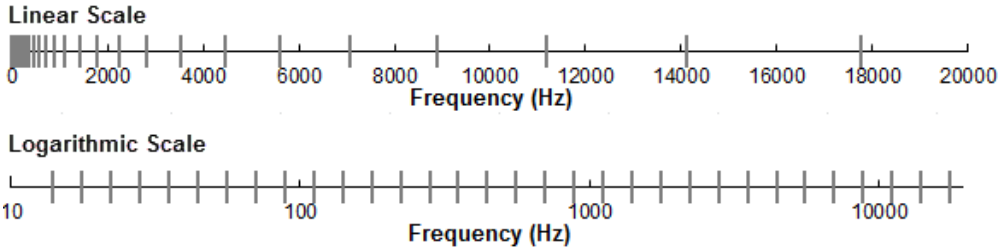

Figure 2. One-third-octave-bands shown on a linear frequency scale and on a logarithmic scale.

The sound pressure level in the *i*th 1/3-octave-band $(L_b^{(i)})$ is computed from the power spectrum $S(f)$ between f_{lo} and f_{hi}:

$$L_{\mathrm{b}}^{(i)} = 10\log_{10}\left(\int_{f_{lo}}^{f_{hi}} S(f)\,df\right). \tag{10}$$

Summing the sound pressure level of all the 1/3-octave-bands yields the broadband SEL:

$$\text{Broadband SEL} = 10\log_{10}\sum_{i} 10^{L_{\mathrm{b}}^{(i)}/10}. \tag{11}$$

Figure 3 shows an example of how the 1/3-octave-band sound pressure levels compare to the power spectrum of an ambient sound signal (continuous noise). Because the 1/3-octave-bands are wider with increasing frequency, the 1/3-octave-band SEL (or, equivalently, rms SPL) is higher than the power spectrum, especially at higher frequencies. Acoustic modelling of 1/3-octave-bands require less computation time than 1 Hz bands and still resolves the frequency dependence of the sound source and the propagation environment.

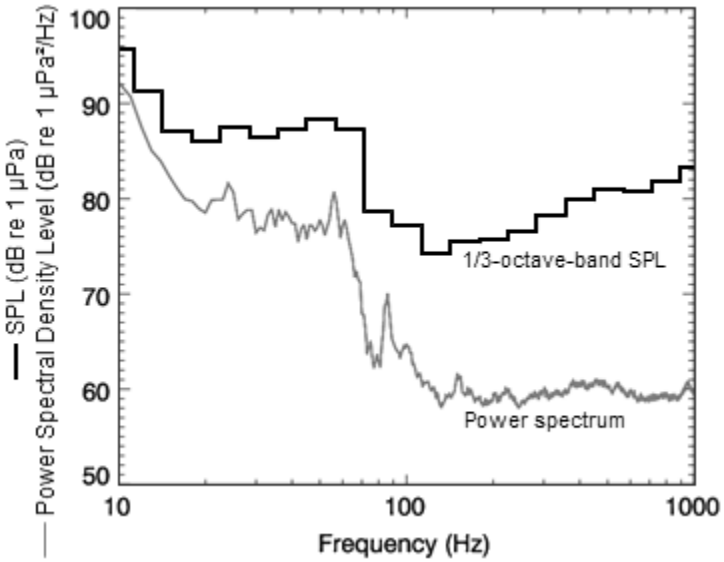

Figure 3. A power spectrum and the corresponding 1/3-octave-band rms SPL of example ambient sound shown on a logarithmic frequency scale.

1.2.4. Received Levels

The received level (RL) at a receiver location can be calculated in decibels (dB) by:

$$\text{RL} = \text{SL} - \text{TL} \tag{12}$$

where SL is the effective SPL or SEL of the source at a reference distance of 1 m (dB re 1 µPa @ 1 m and dB re 1 µPa^2·s @ 1 m, respectively), RL is the SPL or SEL received at the given location (dB re 1 µPa or dB re 1 µPa^2·s, respectively), and TL is the transmission loss (i.e., decrease in sound level measured in dB) that occurs between the source and that location. For prediction of the received levels at a receiver caused by an acoustic source in the environment, one therefore needs to estimate both the source level and the transmission loss.

Geometric spreading of acoustic waves is the predominant way by which transmission loss occurs. Transmission loss also happens when the sound is absorbed and scattered by the seawater, and absorbed, scattered, and reflected at the water surface and within the seabed. The amount of transmission loss therefore depends on the acoustic properties of the ocean and seabed; its value changes with frequency.

1.3. Acoustic Impact Criteria

1.3.1. Current NMFS Criteria

NMFS has historically used relatively simple criteria for potential injury exposure—190 dB re 1 µPa rms SPL for pinnipeds and 180 dB re 1 µPa rms SPL for cetaceans (NMFS 2016). These thresholds are conservative estimates of the sound levels that could potentially cause permanent threshold shift (PTS), which is considered a physical injury to an animal's hearing organs. These historic criteria are applied to all impulsive and non-impulsive sounds. NMFS criteria for behavioural response to impulse sounds is an rms SPL of 160 dB re 1 µPa for both pinnipeds and cetaceans (NMFS 2016). For non-impulsive noise sources, NMFS implemented a lower threshold of 120 dB re 1 µPa rms SPL.

Expressed in rms SPLs, these criteria account for the energy and duration of the acoustic event. They do not, however, account for exposure duration, frequency composition of the sound, repetition rate, or the hearing ability of animals.

1.3.2. Noise Criteria Group Recommendations

The Noise Criteria Group, sponsored by NMFS, was established in 2005 to address shortcomings of the 190–160 dB rms SPL injury criteria mentioned above. The goal of the Group was to review the literature on marine mammal hearing and their behavioural and physiological responses to anthropogenic sound and to propose new sound exposure criteria. In 2007, the findings were published by an assembly of experts (Southall et al. 2007).

The potential for sound to affect animals depends, in part, on how well the animals can hear it. Sounds are less likely to disturb or injure an animal if they are at frequencies that the animal cannot hear well. An exception occurs when the sound pressure is so high that it can physically injure an animal by non-auditory means (i.e., barotrauma). For sound levels below such extremes, the importance of sound components at particular frequencies can be scaled by frequency weighting relevant to an animal's sensitivity to those frequencies (Nedwell and Turnpenny 1998, Nedwell et al. 2007).

To address the variation of marine mammals' hearing sensitivity at different frequencies. Four functional hearing groups of marine mammals in water were defined (Southall et al. 2007):

- Low-frequency cetaceans—mysticetes (baleen whales)
- Mid-frequency cetaceans—some odontocetes (toothed whales)
- High-frequency cetaceans—odontocetes specialized for using high-frequencies
- Pinnipeds—seals, sea lions, and walrus

Southall et al. (2007) propose auditory weighting functions for marine mammals—called *M-weighting* functions—to be considered for each group when assessing sound exposure.

1.3.2.1. Auditory Weighting Functions by Southall et al. (2007)

The M-weighting functions have unity gain (0 dB) through the passband and their high and low frequency roll-offs are approximately –12 dB per octave. The amplitude response in the frequency domain of each M-weighting function is defined by:

$$G(f) = -20\log_{10}\left[\left(1+\frac{a^2}{f^2}\right)\left(1+\frac{f^2}{b^2}\right)\right] \quad (13)$$

where $G(f)$ is the weighting function amplitude (in dB) at the frequency f (in Hz), and a and b are the estimated lower and upper hearing limits, respectively, which control the roll-off and passband of the

weighting function. The parameters *a* and *b* are defined uniquely for each functional hearing group (Table 1).

Figure 4 shows the auditory weighting functions recommended by Southall et al. (2007).

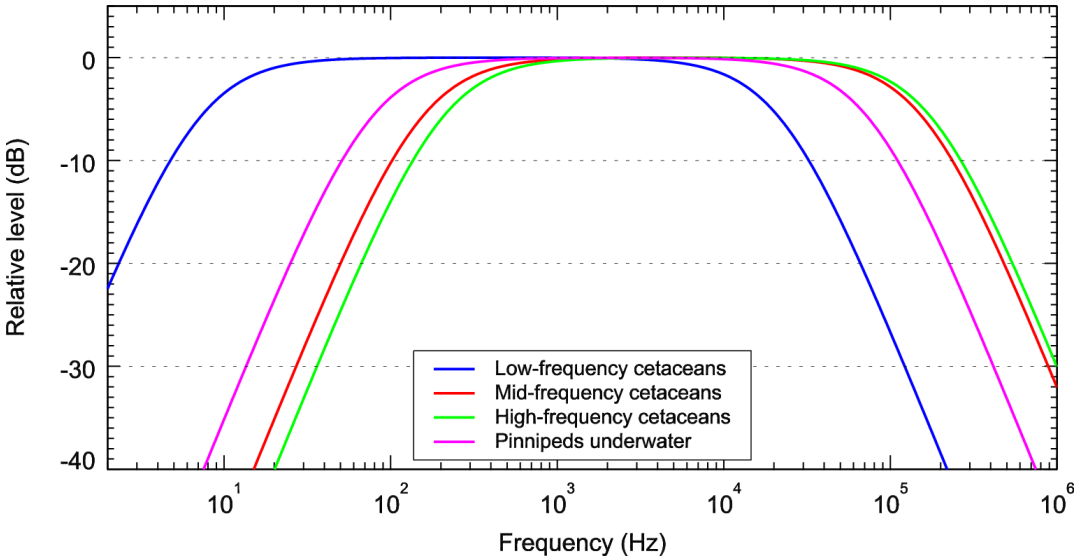

Figure 4. Auditory weighting functions for functional marine mammal hearing groups as recommended by Southall et al. (2007).

Table 1. The estimated lower (a) and upper (b) hearing limit parameters for the auditory weighting functions recommended by Southall et al. (2007).

Functional hearing group	a (Hz)	b (Hz)
Low-frequency cetaceans	7	22,000
Mid-frequency cetaceans	150	160,000
High-frequency cetaceans	200	180,000
Pinnipeds in water	75	75,000

1.3.2.2. Acoustic Thresholds by Southall et al. (2007)

Southall et al. (2007) introduced dual injury criteria consisting of both zero-to-peak (peak) SPL thresholds, expressed in dB re 1 µPa, and cumulative SEL thresholds, expressed in dB re 1 µPa^2·s (Table 2). A PTS-onset (injury) is assumed to occur if a received sound exposure exceeds the peak SPL criterion, the SEL criterion, or both. The peak SPL is not frequency weighted whereas the SEL is frequency-weighted using the m-weighting function related to the specific marine mammal functional hearing group.

Table 2. Peak SPL (dB re 1 µPa) and auditory-weighted cumulative SEL (dB re 1 $\mu Pa^2 \cdot s$) dual acoustic thresholds for permanent threshold shift (PTS) from impulsive and non-impulsive sounds proposed by Southall et al. (2007).

Functional hearing group	Impulsive sound		Non-impulsive sound	
	Peak SPL	Weighted SEL	Peak SPL	Weighted SEL
Low-frequency cetaceans	230	198	230	215
Mid- frequency cetaceans	230	198	230	215
High-frequency cetaceans	230	198	230	215
Pinnipeds in water	218	186	218	203

The PTS-onset thresholds based on peak SPL metric were estimated by adding 6 dB to the known or assumed peak SPL onset of elicit Temporary Threshold Shift (TTS). The PTS-onset thresholds based on the cumulative SEL metric were estimated by adding 15 dB (for impulsive sounds) and 20 dB (for non-impulsive sounds) to the known or assumed cumulative SEL of elicit TTS-onset.

Unlike NMFS criteria (Section 1.3.1), Southall et al. (2007) criteria consider not only the factor of individual pulses impact, but also a temporal factor, i.e., the history of the exposure to the sound over a specific period of time. For impulsive sound, the shape of the pulse is not considered, only the maximum amplitude.

1.3.3. NOAA Draft Acoustic Guidelines

NOAA has developed Draft Acoustic Guidelines (NOAA and US Dept. of Commerce 2013, NOAA 2015) to improve upon and ultimately replace their previous interim criteria for auditory injury (Section 1.3.1). Like the recommendations by Southall et al. (2007), these guidelines include peak SPL and cumulative SEL thresholds as the criteria for the PTS-onset (injury) in marine mammals.

Similar to Southall et al. (2007), the NOAA Draft Acoustic Guidelines also take into account the different hearing abilities of marine mammals by considering marine mammal hearing groups. Three groups are defined for the cetaceans; however, pinnipeds are subdivided into phocid and otariid groups. The cut-off frequencies for the weighting functions were redefined; a variable roll off coefficient was introduced. Consequently, the thresholds for sound exposure criteria assessment were adjusted (Table 4).

Instead of relying on a static model, in which both the source and receivers are stationary, the NOAA Draft Acoustic Guidelines suggest the cumulative SEL should be assessed based on modelling full animal movement during the whole assessment time period. The individual-based, or *animat*, models are suggested for predicting animal movement.

For exposure modelling that consider animal movement, the integration period for cumulative SEL calculation was suggested to be the lesser of 24 h or the length of the acoustic activity. The Guidelines recognise that, in some circumstances, the source and animal movements cannot be modelled. In these cases, a simplified approach is suggested, for which static source and receivers are considered and a 1-hour accumulation time should be used.

1.3.3.1. Auditory Weighting Functions by NOAA (2015)

The proposed auditory weighting functions and thresholds are based primarily on two studies: Southall et al. (2007) and Finneran and Jenkins (2012).

NOAA (2015) defines the amplitude response in the frequency domain of each M-weighting function with an equation somewhat different than Southall et al. (2007):

$$G(f) = -C - 10\log_{10}\left[\frac{(f/f_1)^{2a}}{\left[1+(f/f_1)^2\right]^a\left[1+(f/f_2)^2\right]^b}\right] \quad (14)$$

where $G(f)$ is the weighting function amplitude (in dB) at the frequency f (in Hz), f_1 and f_2 are the estimated lower and upper hearing limits, respectively, which control the passband of the weighting function, a and b control the rate at which the weighting function amplitude declines with frequency at the lower and upper frequencies respectively, and C is the weighting function gain used to set the maximum amplitude of the weighting function to 0 dB. The parameters f_1, f_2, a, and b are defined uniquely for each functional hearing group (Table 3).

Figure 5 shows the auditory weighting functions recommended by NOAA (2015).

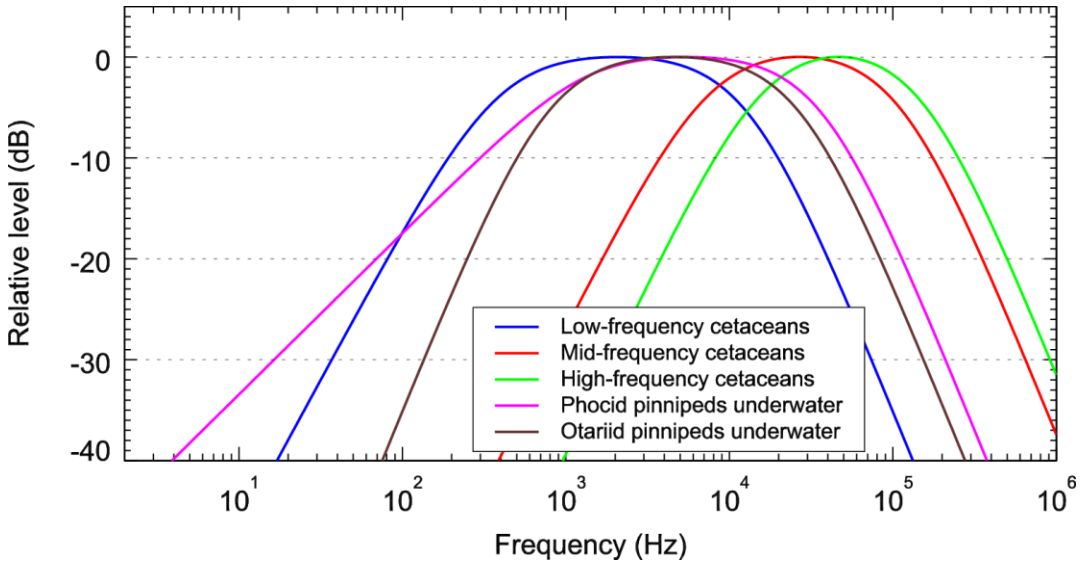

Figure 5. Auditory weighting functions for functional marine mammal hearing groups as recommended by NOAA (2015).

Table 3. Parameters for the auditory weighting functions recommended by NOAA (2015).

Functional hearing group	*a*	*b*	f_1 (Hz)	f_2 (Hz)	*c* (dB)
Low-frequency cetaceans	1.5	2	380	13,000	0.43
Mid-frequency cetaceans	1.6	2	7400	110,000	1.02
High-frequency cetaceans	1.7	2	16,000	150,000	1.63
Phocid pinnipeds in water	0.8	2	1300	27,000	0.49
Otariid pinnipeds in water	2	2	770	37,000	0.38

1.3.3.2. Acoustic Thresholds by NOAA (2015)

The NOAA Draft Acoustic Guidelines' thresholds for the onset of PTS are given in Table 4. The most significant change was in the peak SPL threshold for high-frequency cetaceans group. The threshold was

lowered by 28 dB to 202 dB re µPa from 230 dB re µPa in Southall et al. (2007). On the contrary, the peak SPL threshold for both pinniped groups was increased to 230 dB re µPa from 218 dB re µPa in Southall et al. (2007).

The criteria threshold for weighted SEL cannot be compared directly with the ones in Southall et al. (2007) as the weighting functions are defined differently.

Table 4. Peak SPL (dB re 1 µPa) and auditory-weighted cumulative SEL (dB re 1 $\mu Pa^2 \cdot s$) dual acoustic thresholds for permanent threshold shift (PTS) from impulsive and non-impulsive sounds proposed by the NOAA Draft Acoustic Guidelines (NOAA 2015).

Functional hearing group	Impulsive sound		Non-impulsive sound	
	Peak SPL	Weighted SEL	Peak SPL	Weighted SEL
Low-frequency cetaceans	230	192	230	207
Mid- frequency cetaceans	230	187	230	199
High-frequency cetaceans	202	154	202	171
Phocid pinnipeds in water	230	186	230	201
Otariid pinnipeds in water	230	203	230	218

2. Methods

2.1. Source Models

2.1.1. Airgun Source Array Model

The source levels and directivity of the airgun source array were predicted with JASCO's Airgun Array Source Model (AASM; MacGillivray 2006). This model is based on the physics of oscillation and radiation of airgun bubbles described by Ziolkowski (1970). The model solves the set of parallel differential equations that govern bubble oscillations. AASM also accounts for nonlinear pressure interactions between airguns, port throttling, bubble damping, and generator-injector (GI) gun behaviour discussed by Dragoset (1984), Laws et al. (1990), and Landro (1992). AASM includes four empirical parameters that were tuned so model output matches observed airgun behaviour. The model parameters fit to a large library of empirical airgun data using a "simulated annealing" global optimization algorithm. These airgun data are measurements of the signatures of Bolt 600/B guns ranging in volume from 5 to 185 in^3 (Racca and Scrimger 1986).

While source elements signatures are highly repeatable at the low frequencies, which are used for seismic imaging, their sound emissions have a large random component at higher frequencies that cannot be predicted using a deterministic model. Therefore, AASM uses a stochastic simulation to predict the high-frequency (560−25,000 Hz) sound emissions of individual source elements, using a data-driven multiple-regression model. The multiple-regression model is based on a statistical analysis of a large collection of high quality seismic source signature data recently obtained from the Joint Industry Program (JIP) on Sound and Marine Life (Mattsson and Jenkerson 2008). The stochastic model uses a Monte-Carlo simulation to simulate the random component of the high-frequency spectrum of each airgun in an array. The mean high-frequency spectra from the stochastic model augment the low-frequency signatures from the physical model, allowing AASM to predict individual source elements' source levels at frequencies up to 25,000 Hz.

AASM produces a set of "notional" signatures for each array element based on:

- Array layout
- Volume, tow depth, and firing pressure of each airgun
- Interactions between different airguns in the array

These notional signatures are the pressure waveforms of the individual airguns at a standard reference distance of 1 m; they account for the interactions with the other airguns in the array. The signatures are summed with the appropriate phase delays to obtain the far-field source signature of the entire array in all directions. This far-field array signature is filtered into 1/3-octave-bands to compute the source levels of the array as a function of frequency band and azimuthal angle in the horizontal plane (at the source depth), after which it is considered a directional point source in the far field.

A seismic airgun source array consists of many elements and the point-source assumption is invalid in the near field where the array elements add incoherently. The maximum extent of the near field of an array (R_{nf}) is:

$$R_{\mathrm{nf}} < \frac{l^2}{4\lambda} \tag{15}$$

where λ is the sound wavelength and l is the longest dimension of the array (Lurton 2002, §5.2.4). For example, an airgun source array length of l = 16 m yields a near-field range of 85 m at 2 kHz and 17 m at 100 Hz. Beyond this R_{nf} range, the array is assumed to radiate like a directional point source and is treated as such for propagation modelling.

The interactions between individual elements of the array create directionality in the overall acoustic emission. Generally, this directionality is prominent mainly at frequencies in the mid-range between tens of hertz to several hundred hertz. At lower frequencies, with acoustic wavelengths much larger than the inter-airgun separation distances, the directionality is small. At higher frequencies, the pattern of lobes is too finely spaced to be resolved and the effective directivity is less.

2.1.2. Vessel Sound

As discussed in Section 1.2.1.1, if the propulsion system of a vessel is under heavy load (acceleration, dynamic positioning) the sound produced by the cavitation process on the propellers will dominate other sources of vessel sound (machinery, hull vibration, etc.)

A vessel equipped with propellers/thrusters has two primary sound sources that propagate from the drilling rig: the machinery and the propellers. For thrusters operating in the heavily loaded conditions, the acoustic energy generated by the cavitation processes on the propeller blades dominates (Leggat et al. 1981). The sound power from the propellers is proportional to the number of blades, the propeller diameter, and the propeller tip speed.

Based on an analysis of acoustic data, Ross (1976) provided the following formula for the sound levels from a vessel's propeller, operating in calm, open ocean conditions:

$$L_{100} = 155 + 60\log(u/25) + 10\log(B/4), \tag{16}$$

where L_{100} is the spectrum level at 100 Hz, u is the propeller tip speed (m/s), and B is the number of propeller blades. Equation 16 gives the total energy produced by the propeller cavitation at frequencies between 100 Hz and 10 kHz. This equation is valid for a propeller tip speed between 15 and 50 m/s. The spectrum is assumed to be flat below 100 Hz. Its level is assumed to fall off at a rate of −6 dB per octave above 100 Hz (Figure 6).

Another method of predicting the source level of a propeller was suggested by Brown (1977). For propellers operating in heavily loaded conditions, the formula for the sound spectrum level is:

$$\mathrm{SL}_B = 163 + 40\log D + 30\log N + 10\log B - 20\log f + 10\log(A_c/A_D), \tag{17}$$

where D is the propeller diameter (m), N is the propeller revolution rate per second, B is the number of blades, A_C is the area of the blades covered by cavitation, and A_D is the total propeller disc area. Similar to Ross's approach, the spectrum below 100 Hz is assumed to be flat. The tests with a naval propeller operating at off-design heavily loaded conditions showed that Equation 17 should be used with a value of $A_c/A_D = 1$ (Leggat et al. 1981).

If the vessel is equipped with multiple thrusters, the combined source level for a group of thrusters operating together can be estimated using the formula:

$$\mathrm{SL}_{\mathrm{total}} = 10\log_{10}\sum_i 10^{SL_i/10}, \tag{18}$$

where $\mathrm{SL}_{1,\ldots,N}$ are the source levels of individual thrusters. If the vessel is equipped with the same type of thrusters (the source levels are equal), the combined source level can be estimated using the formula:

$$\mathrm{SL}_N = \mathrm{SL} + 10\log N, \tag{19}$$

where N is the total number of thrusters of the same type.

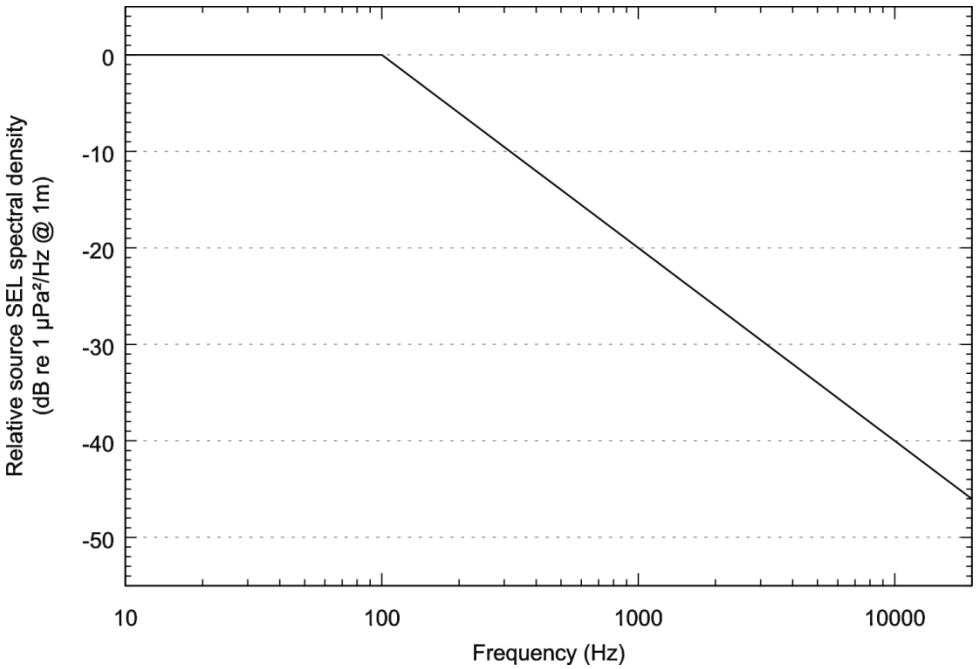

Figure 6. Estimated sound spectrum from cavitating propeller (Leggat et al.1981).

2.2. Sound Propagation Models

The choice of the modelling approach for the acoustic propagation depends on the sound type (continuous, impulsive) and the required output metric for the modelled received levels. Estimation of the received levels from a non-impulsive source in the rms SPL or SEL metric and from an impulsive source in the SEL metric can be performed using the 1/3-octave-band analysis approach (see Section 1.2.3).

The underwater sound propagation (i.e., transmission loss) for the 1/3-octave-band analysis approach was predicted with JASCO's Marine Operations Noise Model (MONM). To achieve the greatest accuracy and computational efficiency, MONM uses two separate models (MONM-PE and MONM-BELLHOP) to estimate transmission loss. The choice between the models depends on the frequency of the acoustic wave being propagated.

The calculation of the rms SPL metric of an acoustic signal from an impulsive source (airgun source array) requires estimation of the 90% energy pulse duration (T_{90}) (see Section 1.2.2). In this study, full waveform modelling was performed that provides acoustic pressure time series for virtual receivers around the source. This approach allows direct calculation of the rms SPL and is more accurate than estimating rms SPL from SEL with a correction function.

2.2.1. Two Frequency Regimes: RAM Versus BELLHOP

At frequencies ≤ 2 kHz, MONM computes acoustic propagation via a wide-angle parabolic equation solution to the acoustic wave equation (Collins 1993) based on a version of the U.S. Naval Research Laboratory's Range-dependent Acoustic Model (RAM), which has been modified to account for an elastic seabed (Zhang and Tindle 1995). The parabolic equation method has been extensively benchmarked and is widely employed in the underwater acoustics community (Collins et al. 1996). The RAM-based component of MONM (MONM-RAM) accounts for the additional reflection loss at the seabed due to partial conversion of incident compressional waves to shear waves at the seabed and sub-bottom interfaces, and it includes wave attenuations in all layers. MONM-RAM incorporates the following site-specific environmental properties: a modeled area bathymetric grid, underwater sound speed as a function of depth, and a geoacoustic profile based on the overall stratified composition of the seafloor.

MONM-RAM accounts for source horizontal directivity. MONM-RAM's predictions have been validated against experimental data in several underwater acoustic measurement programs conducted by JASCO (Hannay and Racca 2005, Aerts et al. 2008, Funk et al. 2008, Ireland et al. 2009, O'Neill et al. 2010, Warner et al. 2010). Comparison with experimental data shows that transmission loss estimated by MONM-RAM is accurate within 3 dB.

At frequencies ≥ 2 kHz, MONM employs the widely used BELLHOP Gaussian beam ray-trace propagation model (Porter and Liu 1994), which accounts for increased sound attenuation due to volume absorption at these higher frequencies following Fisher and Simmons (1977). This type of attenuation is significant for frequencies higher than 5 kHz and cannot be neglected or model results far from the source will noticeably suffer. The BELLHOP component of MONM (MONM-BELLHOP) accounts for the source directivity, specified as a function of both azimuthal angle and depression angle. MONM-BELLHOP incorporates the following site-specific environmental properties: a bathymetric grid of the modeled area and underwater sound speed as a function of depth.

In contrast to MONM-RAM, the geoacoustic input for MONM-BELLHOP consists of only one interface: the sea bottom. This is an acceptable limitation because the influence of the sub-bottom layers on the propagation of acoustic waves with frequencies above 1 kHz is negligible. Both propagation models account for full exposure from a direct acoustic wave, as well as exposure from acoustic wave reflections and refractions (i.e., multipath arrivals at the receiver).

2.2.2. *N*×2-D Volume Approximation

MONM computes acoustic fields in three dimensions by modeling transmission loss within two-dimensional (2-D) vertical planes aligned along radials covering a 360° swath from the source, an approach commonly referred to as *N*×2-D. These vertical radial planes are separated by an angular step size of $\Delta\theta$, yielding $N = 360°/\Delta\theta$ number of planes (Figure 7).

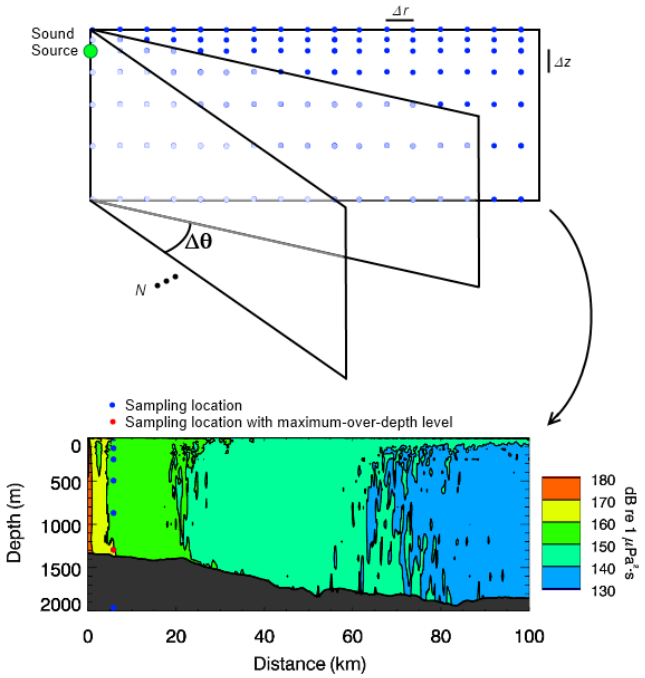

Figure 7. The *N*×2-D and maximum-over-depth modeling approach.

2.2.3. Sound Propagation with FWRAM

For impulsive sounds from an airgun source array, time-domain representations of the pressure waves generated in the water are required to calculate rms SPL and peak SPL. Furthermore, since it consists of multiple source elements, an airgun source array must be represented as a distributed source to accurately characterize vertical directivity effects in the near-field zone. For this study, synthetic pressure waveforms were computed using FWRAM, which is a time-domain acoustic model based on the same wide-angle PE algorithm as MONM. FWRAM computes synthetic pressure waveforms versus range and depth for range-varying marine acoustic environments, and it takes the same environmental inputs as MONM (bathymetry, water sound speed profile, and seabed geoacoustic profile). Unlike MONM, FWRAM computes pressure waveforms via Fourier synthesis of the modelled acoustic transfer function in closely spaced frequency bands. FWRAM employs the array starter method to accurately model sound propagation from a spatially distributed source (MacGillivray and Chapman 2012).

The modelling procedure with FWRAM is significantly more computationally intensive, as it requires smaller frequency steps, therefore more modelling runs for individual frequencies. The maximum frequency step is usualy taken as 1 Hz. The length of output synthetic pressure waveforms (T_{trace}) inversly depends on the modelling frequency step (Δf):

$$\Delta f = \frac{1}{T_{trace}} \tag{20}$$

For deep environments, it is important to produce synthetic pressure waveforms longer than 1 second as the acoustic signal (direct and reflected arrivals) becomes spread in time. In this case, the modelling frequency step can be set smaller than 1 Hz.

2.2.4. Zero-to-peak SPL Estimation for Continuous Sound Sources

For ideal continuous noise sources with a sinusoidal tonal signal, the peak SPL is 1.46 dB higher than the rms SPL. However, for broadband continuous sound sources, the relation can be different. The presence of peaks in the pressure time series of a continuous acoustic source is a random phenomenon and cannot be mathematically modelled. The most robust approach would be to estimate the difference between the peak SPL and rms SPL metric of the signal from empirical data.

The analysis of JASCO's field recorded acoustic data from vessels shows that, on average, the difference between rms SPL and peak SPL values for a signal from a continuous sound source is approximately 10 dB. The field measurements data presented in Kyhn et al. (2011) suggest a constant difference of 12 dB between rms SPL and peak SPL values for a drillship similar to the one considered in this report.

Consequently, the peak SPL field for a continuous sound source was estimated based on the rms SPL field using the formula:

$$L_{pkSPL} = L_{rmsSPL} + 12\,. \tag{21}$$

This approach was used to estimate the peak SPL field for vessel noise.

2.3. Radii Calculation

As previously discussed, the underwater sound fields predicted by the propagation models are sampled so that the received sound level at each point in the horizontal plane are taken to be the maximum value over all modelled depths for that point. The predicted distances to specific levels are then computed from the maximum-over-depth sound fields. Two distances relative to the source are reported for each sound level: (1) R_{max}, the maximum range at which the given sound level was encountered in the modelled maximum-over-depth sound field and (2) $R_{95\%}$, the maximum range at which the given sound level was encountered after the 5% farthest such points are excluded (Figure 8). The $R_{95\%}$ is used because the

maximum-over-depth sound field footprint might not be circular and, along a few azimuths, could extend far beyond the main ensonification zone. Regardless of the geometric shape of the maximum-over-depth footprint, $R_{95\%}$ is the predicted range encompassing at least 95% of the area (in the horizontal plane) that would be exposed to sound at or above that level. The difference between R_{max} and $R_{95\%}$ depends on the source directivity and the heterogeneity of the acoustic environment. The $R_{95\%}$ excludes ends of protruding areas or small isolated acoustic foci not representative of the nominal ensonification zone.

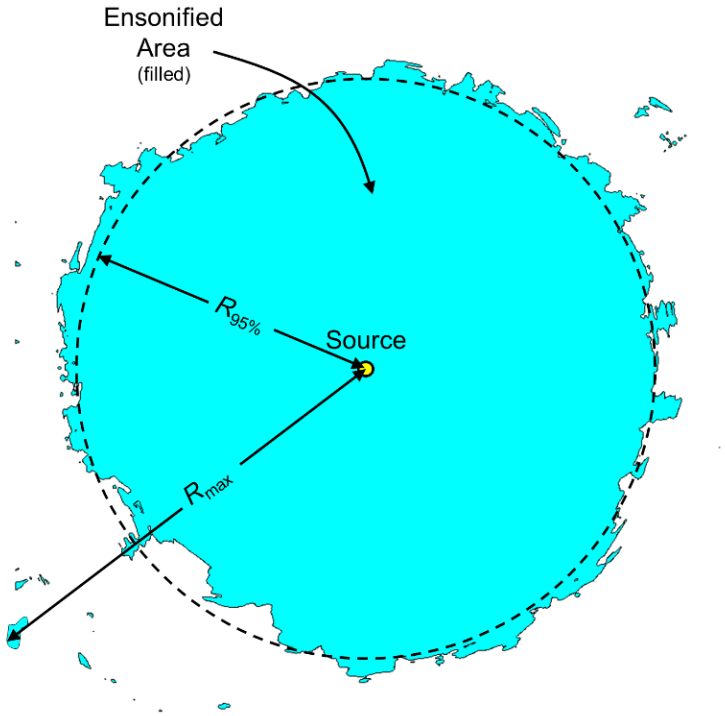

Figure 8. Example of an area ensonified to an arbitrary sound level shown R_{max} and $R_{95\%}$ radii.

3. Model Parameters

3.1. Acoustic Source Parameters

The specifics of the airgun source array and the drilling vessel were unknown at the time of this study. JASCO modelled the most likely parameters for the sources, based on experience modelling similar acoustic operations for BP and other clients. Details of the selected representative sound sources are presented below.

3.1.1. VSP Airgun Source Array

The Schlumberger Dual Magnum 2400 in^3 airgun, previously used by BP in Gulf of Mexico surveys, was modelled as the seismic source for the VSP source. The Schlumberger airgun array consists of four triangular clusters with in-line separations of 2 m. Two clusters are assembled from three 250 in^3 source elements with 0.9 m separation between each element. The two other clusters have three 150 in^3 source elements with 0.6 m separation between each element. The airguns are activated simultaneously at 2000 psi air pressure. The airgun array was modelled at a tow depth of 4.5 m (the centre of the clusters). Figure 9 presents the airgun distribution in the horizontal (*x*-*y*) plane.

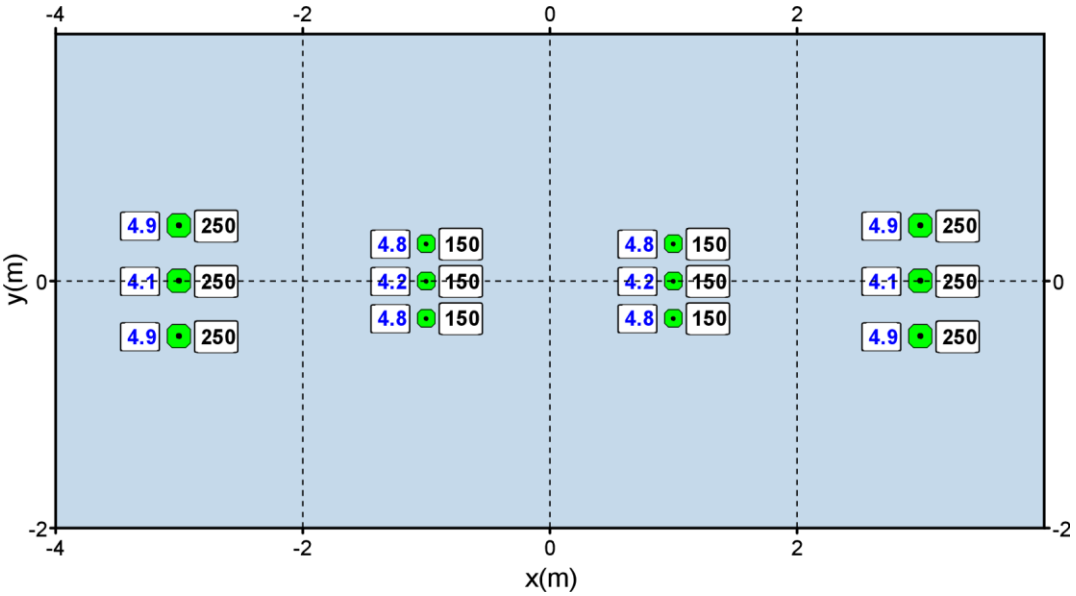

Figure 9. Layout of the suggested airgun array (2400 in^3 total firing volume, 4.5 m depth), composed of 12 airguns. Relative symbol sizes and black numbers indicate airgun firing volume in cubic inches. The blue numbers indicate the depth of the source element relative to the sea surface.

3.1.2. Vessels

Either a drillship or a semi-submersible platform could be used in the Scotian Basin drilling program; therefore, both of these scenarios were modelled, along with the presence of an offshore support vessel. The specific parameters required as modelling input for each vessel are:

- Thruster depth,
- Propeller diameter,
- Propeller revolutions-per-minute (rpm) at nominal power output,

- Number of blades, and
- Thruster locations on the vessel's hull.

3.1.2.1. Drillship

The estimates of the drillship acoustic source levels and sound spectrum were based on the drillship *Deep Ocean Clarion* (Figure 10). *Deep Ocean Clarion* is equipped with six Rolls-Royce UUC 455 thrusters (Det Norske Veritas 2010.). These thrusters have a fixed-pitch propeller in a PV-nozzle. The UUC 455 thruster parameters (Det Norske Veritas. 2010.) are:

- 4.1 m propeller diameter,
- 157 rpm nominal propeller speed, and
- 5500 kW maximum continuous power input.

For modelling, all six thrusters were assumed to operate at nominal speed (i.e., the highest sustainable revolutions-per-minute). The vertical position of the thrusters was 12 m below the sea surface (draft of the vessel during drilling operations). Figure 11 shows the thruster locations.

Figure 10. *Deep Ocean Clarion* drillship.

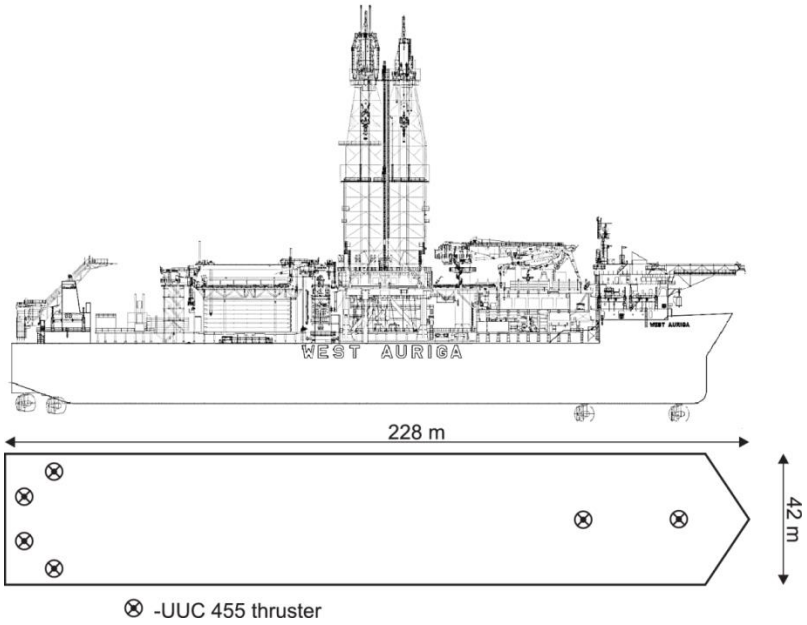

Figure 11. *Deep Ocean Clarion* dimensions and thruster locations (circles).

3.1.2.2. Semi-Submersible Platform

The estimates of the semi-submersible platform acoustic source levels and sound spectrum were based on the *Seadrill West Sirius* (Figure 12). *Seadrill West Sirius* is reportedly equipped with eight Rolls-Royce UUC 355 thrusters. The thruster has a fixed-pitch propeller in a PV-nozzle.

The parameters for the UUC 355 thruster are:

- 3.5 m propeller diameter,
- 177 rpm nominal propeller speed, and
- 3800 kW maximum continuous power input.

For modelling, all eight thrusters were assumed to operate at nominal speed. The vertical position of the thrusters was 18 m below the sea surface (draft of the rig during drilling operations). Figure 13 shows the thruster locations.

Figure 12. *Seadrill West Sirius* semi-submersible platform.

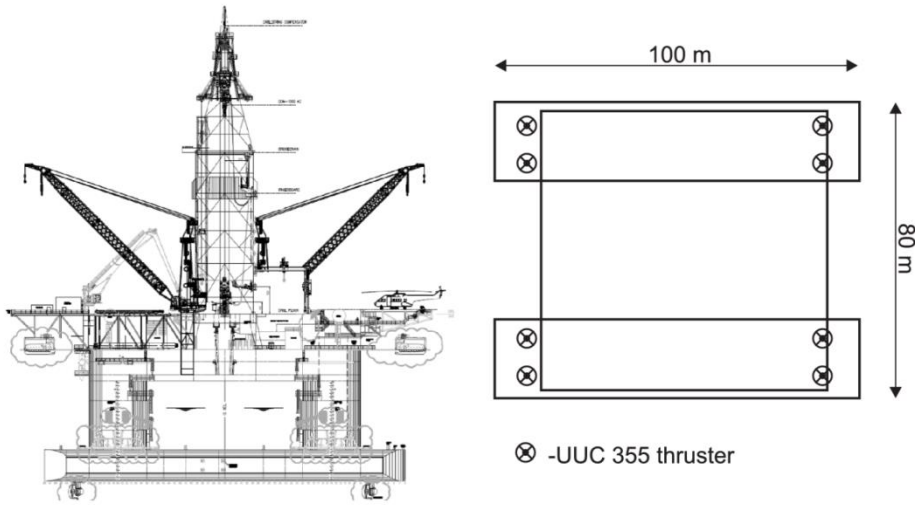

Figure 13. *Seadrill West Sirius* dimensions and thruster locations (circles).

3.1.2.3. Support Vessel

The estimates of acoustic source levels and sound spectrum for the support vessel were based on the Damen platform supply vessel 3300CD (Figure 14). Damen 3300CD is equipped with two main azimuthal thrusters and two bow thrusters. The vertical position of the thrusters is 5 m below the sea surface. This thruster type and configuration is typical for this type of vessel.

The parameters for main thrusters are:

- 2.3 m propeller diameter,
- 250 rpm nominal propeller speed, and
- 2000 kW maximum continuous power input.

The parameters for bow thrusters are:

- 1.7 m propeller diameter,
- 290 rpm nominal propeller speed, and
- 750 kW maximum continuous power input.

For modelling, all four thrusters were assumed to operate at nominal speed. Figure 15 shows the thruster locations.

Figure 14. Damen supply vessel 3300CD.

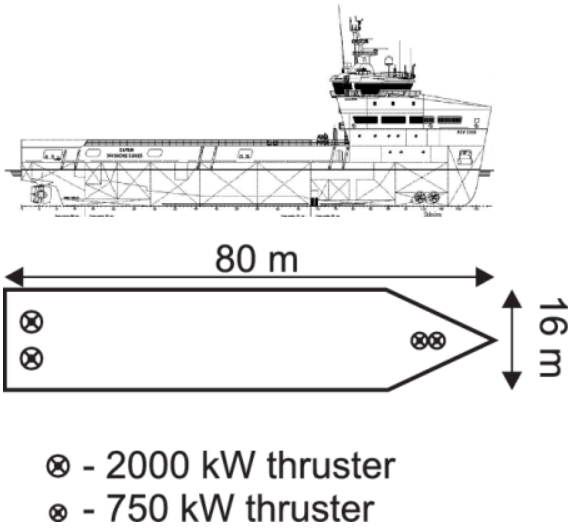

Figure 15. Damen 3300CD dimensions and thruster locations (circles).

3.2. Environmental Parameters

3.2.1. Bathymetry

Water depths throughout the modelled area were obtained from digital bathymetry grid SRTM15+ (Smith et al. 1997, Becker et al. 2009). The bathymetry grid has a resolution of 15 arc-seconds (~ 330 × 460 m at the studied latitude). The data were extracted for a 600 × 600 km area and re-gridded onto a Universal Transverse Mercator (UTM) Zone 20 coordinate projection with a regular grid spacing of 250 × 250 m.

3.2.2. Geoacoustic Properties

The geoacoustic properties of surficial layers depend on the sediment type. As the porosity decreases, the compressional sound speed, sediment bulk density, and compressional attenuation increase.

For each modelled location, MONM assumes a single geoacoustic profile of the seafloor for the entire modelled area. The acoustic properties required by MONM are:

- Sediment bulk density,
- Compressional-wave (or P-wave) speed,
- P-wave attenuation in decibels per wavelength,
- Shear-wave (or S-wave) speed, and
- S-wave attenuation, also in decibels per wavelength.

These geoacoustic parameters for the sediment layer were estimated using a sediment grain-shearing model (Buckingham 2005), which computes the acoustic properties of the sediments from porosity and grain-size measurements. The input parameters required by the geoacoustic model are the bottom type (grain size) and sediment porosity, inferred from the geological description of the modelling region.

The geoacoustic profile (Table 5) was based on data obtained by the Ocean Drilling Program (ODP) at site 905, leg 150 (Shipboard Scientific Party 1994). The well was located at a 2,700 m water depth. The reported porosity for the surficial sediments is 60% and does not change with depth, maintaining the same value of 60% down to 600 metres below the seafloor (mbsf).

Table 5. Geoacoustic properties of the sub-bottom sediments as a function of depth, in metres below the seafloor (mbsf). Within each depth range, each parameter varies linearly within the stated range.

Depth (mbsf)	Material	Density (g/cm³)	P-wave speed (m/s)	P-wave attenuation (dB/λ)	S-wave speed (m/s)	S-wave attenuation (dB/λ)
0–10	Clay	1.70	1560–1613	0.19–0.40	100	0.02
10–50			1613–1683	0.40–0.67		
50–150			1683–1763	0.67–0.93		
150–300			1763–1833	0.93–1.14		
300–600			1833–1925	1.14–1.37		
> 600			2000	1.37		

3.2.3. Sound Speed Profiles

The sound speed profiles for the modelled sites were derived from temperature and salinity profiles from the U.S. Naval Oceanographic Office's *Generalized Digital Environmental Model V 3.0* (GDEM; Teague et al. 1990, Carnes 2009). GDEM provides a climatology data of temperature and salinity for the world's oceans as a latitude-longitude grid with 0.25° spatial resolution, with a temporal resolution of one month, based on global historical observations from the U.S. Navy's Master Oceanographic Observational Data Set (MOODS). The climatology profiles include 78 fixed-depth points to a maximum depth of 6,800 m (where the ocean is that deep). The GDEM temperature-salinity profiles were converted to sound speed profiles according to the equations of Coppens (1981):

$$\begin{aligned} c(z,T,S,\phi) &= 1449.05 + 45.7t - 5.21t^2 - 0.23t^3 \\ &\quad + \left(1.333 - 0.126t + 0.009t^2\right)\left(S - 35\right) + \Delta \\ \Delta &= 16.3Z + 0.18Z^2, \quad Z = \frac{z}{1000}\left[1 - 0.0026\cos\left(2\phi\right)\right], \quad t = \frac{T}{10} \end{aligned} \tag{22}$$

where z is water depth (m), T is temperature (°C), S is salinity (psu), and ϕ is latitude (radians).

Twelve sound speed profiles, one for each month, were calculated based on the data extracted from GDEM database for the location at 43°N 60.25°W (Figure 16, left). Out of the set, two profiles were

selected that are believed to provide the most (February) and the least (August) favourable conditions for the sound propagation (Figure 16, right). The sound speed profile for February represented winter propagation conditions and August represented summer propagation conditions.

The February sound speed profile features a strong surface channel. The thickness of ~ 150 m and the speed difference of more than 20 m/s would effectively trap acoustic energy at frequencies ~100 Hz and higher. The sound speed profile for August also exhibits a sound channel; however, the upper slope shows higher speed gradient and also a larger speed difference between the axis of the channel at 50 m and the sea surface. This geometry will allow a significant amount of acoustic energy to escape from the channel.

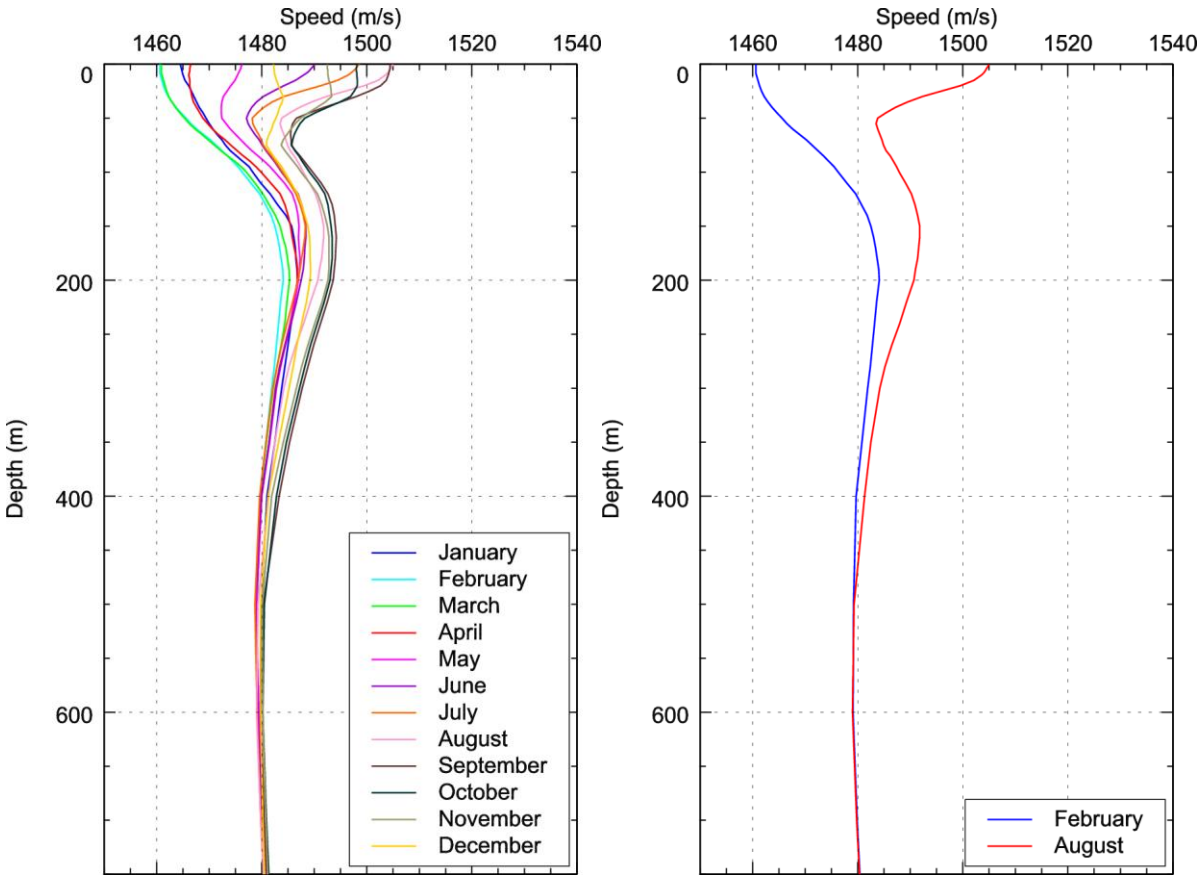

Figure 16. Mean monthly sound speed profiles near the modelling area: (left) All months and (right) months selected for modelling. The profiles were derived from data obtained from *GDEM V 3.0* (Teague et al. 1990, Carnes 2009).

3.3. Modelled Scenarios

The two sites where drilling is expected to occur were used for modelling. Table 6 provides the coordinates (UTM zone 20) and the water depth at each site. The water depth was extracted from the bathymetry grid used for acoustic propagation modelling.

Table 6. Modelling site locations and depths.

Site	UTM North (m)	UTM East (m)	Water depth (m)
A	4,747,165	720,825	2,790
B	4,767,949	708,954	2,100

At each site, a series of acoustic sources were modelled:

- Drillship
- Drillship with support vessel
- Semi-submersible platform
- Semi-submersible platform with support vessel
- VSP airgun source array

Figure 17 shows the geometries of the multi-vessel scenarios. For the vessel scenarios, the actual location of each thruster was taken into account when calculating the combined acoustic field around the vessels.

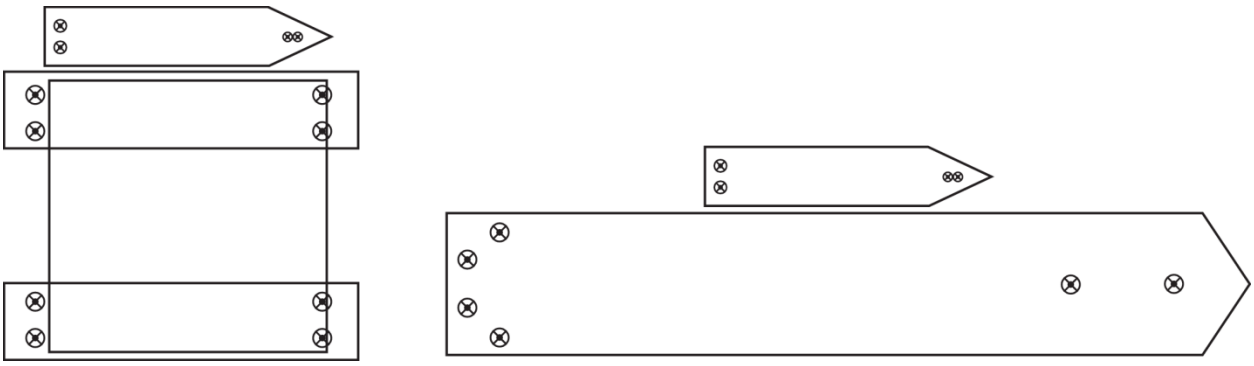

Figure 17. Multi-vessel source geometry: (left) Semi-submersible platform with support vessel and (right) drillship with support vessel. The circles indicate thruster locations.

Table 7 lists acoustic propagation modelling scenarios considered in this study. For each scenario, the rms SPL and the cumulative SEL fields were estimated using nine weighting functions, for a total of 200 acoustic fields.

Table 7. Acoustic propagation modelling scenarios for BP Scotian Basin project. Each scenario was conducted at Sites A and B, in winter and summer.

Scenario	Sound sources	Scenario count
1	Drillship	4
2	Drillship with support vessel	4
3	Semi-submersible platform	4
4	Semi-submersible platform with support vessel	4
5	VSP airgun array source	4
	Total	**20**

3.4. Geometry and Modelled Volumes

As discussed in Section 2.2.2, the modelling of the acoustic field around the sources was performed in N×2-D mode. The deepest diving depth of marine mammals in the area was assumed to be 3,000 m.

3.4.1. MONM Sound Propagation Modelling

The sound propagation was modelled with MONM to estimate the rms SPL and cumulative SEL fields from vessels and cumulative SEL field from the airgun array source out to distances of 150 km. The modelling was performed in 1/3-octave-bands for the frequencies from 10 to 63,000 Hz (39 bands). The transmission loss was modelled in 23 bands (from 10 to 1600 Hz) using MONM-RAM. For higher frequency bands (from 2 kHz to 63 kHz), the transmission loss was modelled using MONM-BELLHOP.

Sound fields were modelled along a series of radial profiles covering 360° with a horizontal angular resolution of $\Delta\theta = 5°$ for a total of N = 72 radial planes. The horizontal step size for virtual receivers along the profiles was 20 m. Each profile extended 150 km from the source.

The transmission loss modelling results were obtained for one to three source depths at each location:

- 5 m (support vessel thruster and VSP airgun source array);
- 12 m (drillship thrusters);
- 18 m (semi-submersible thrusters).

To obtain the vertical distribution of the acoustic field, at each surface sampling location the sound field was sampled at:

- 2 m,
- Every 5 m from 5 to 25 m,
- Every 25 m from 50 to 100 m,
- Every 50 m from 150 to 500 m,
- Every 100 m from 600 to 1200 m, and
- Every 200 m from 1400 to 3,000 m.

3.4.2. FWRAM Sound Propagation Modelling

The sound propagation was modelled with FWRAM to estimate the peak SPL and rms SPL fields around the VSP airgun source array.

Since the propagation modelling with FWRAM, which produces pressure time series, is significantly more computationally expensive, the number of modelling profiles and the maximum modelling distance was less than for MONM modelling.

Sound fields were modelled along a series of radial profiles covering 360° with a horizontal angular resolution of $\Delta\theta$ = 22.5° for a total of N = 16 radial planes. Each profile extended 20 km from the source. The horizontal step size for the distributed virtual receivers varied, increasing with the distance from the source as shown in Table 8.

Table 8. Horizontal step between virtual receivers as function of distance from the source.

Distance from the source (m)	Horizontal step (m)
0–200	10
200–600	20
600–900	30
900–1,300	40
1,300–2,000	50
2,000–10,000	100
10,000–20,000	200

A single source depth of 5 m was modelled, the depth of the VSP airgun source array.

To obtain the vertical distribution of the acoustic field, at each surface sampling location the sound field was sampled at:

- 2.5 m,
- Every 5 m from 5 to 25 m,
- Every 25 m from 50 to 100 m,
- Every 50 m from 150 to 500 m,
- Every 100 m from 600 to 1,200 m, and
- Every 200 m from 1400 to 3,000 m.

The full waveform acoustic propagation modelling was limited to the 10 to 500 Hz frequency band. Most acoustic energy is concentrated in the band below 500 Hz and, unlike cumulative SEL estimation, there are no weighting functions applied that supress the lower frequencies and make the contribution of higher frequencies significant. The reduced modelled bandwidth did not affect the pressure levels or the pulse shape, and the accuracy of the rms SPL field estimation was not decreased.

The modelling was performed with 0.5 Hz frequency steps (981 frequencies were propagated), which allowed synthesize a 2 second long pressure time series to be synthesized.

4. Results

4.1. Acoustic Sources

4.1.1. VSP Airgun Source Array

The source levels and directivity patterns of the airgun source array were modelled using AASM (see Section 2.1.1) in the frequency band from 10 to 25,000 Hz.

Figure 18 and Table 9 show the horizontal overpressure signatures and corresponding power spectrum levels for the 2400 in^3 airgun source array, stationary at a 4.5 m depth (to the vertical centre of the source element clusters), for the broadside (perpendicular to the tow direction) and endfire (parallel to the tow direction) directions. The signatures consist of a strong primary peak related to the initial firing of the airguns, followed by a series of pulses associated with bubble oscillations. Most energy is produced at frequencies below 500 Hz (Figure 18b and Table 9). The spectrum contains peaks and nulls resulting from interference among airguns in the array, where the frequencies at which they occur depend on the volumes of the airguns and their locations within the array. Figure 19 shows the maximum (horizontal) 1/3-octave-band sound levels over all directions for all weighting functions (Sections 1.3.2.1 and 1.3.3.1). Figure 20 shows the horizontal 1/3-octave-band directivities for frequencies up to and including 6,310 Hz.

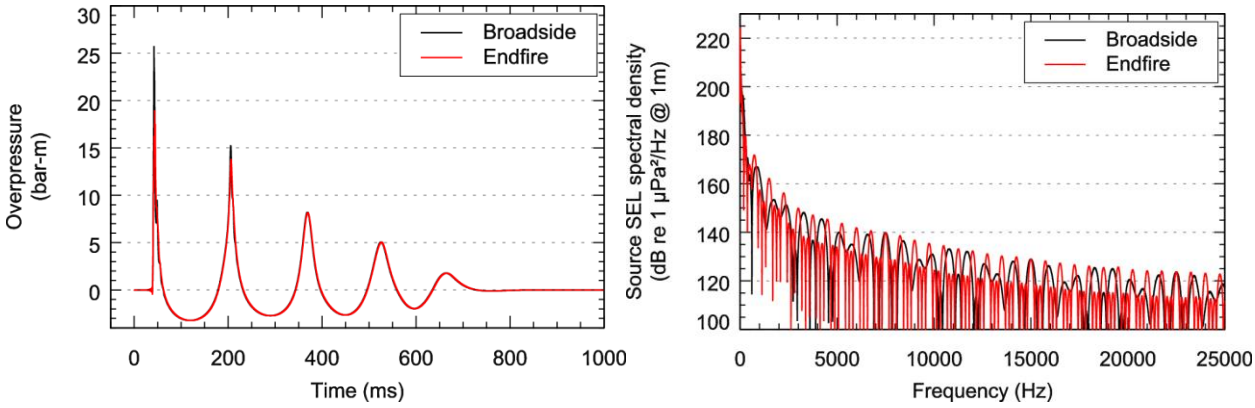

Figure 18. 2400 in^3 VSP airgun source array: Predicted (a) overpressure signature and (b) power spectrum in the broadside and endfire (horizontal) directions. Surface ghosts (effects of the pulse reflection at the water surface) are not included in these signatures as they are accounted for by the MONM propagation model.

Table 9. Horizontal source level specifications for the airgun source array (2400 in^3) at 4.5 m depth, computed with AASM in the broadside and endfire directions. Surface ghost effects are not included as they are accounted for by the MONM propagation model.

Direction	Zero-to-peak SPL (dB re 1 µPa @ 1 m)	SEL (dB re 1 µPa²·s @ 1 m)			
		0.01–63 kHz	0.01–0.5 kHz	0.5–5 kHz	5–63 kHz
Broadside	248.2	224.7	224.7	192.5	171.6
Endfire	245.6	224.1	224.1	195.0	172.2

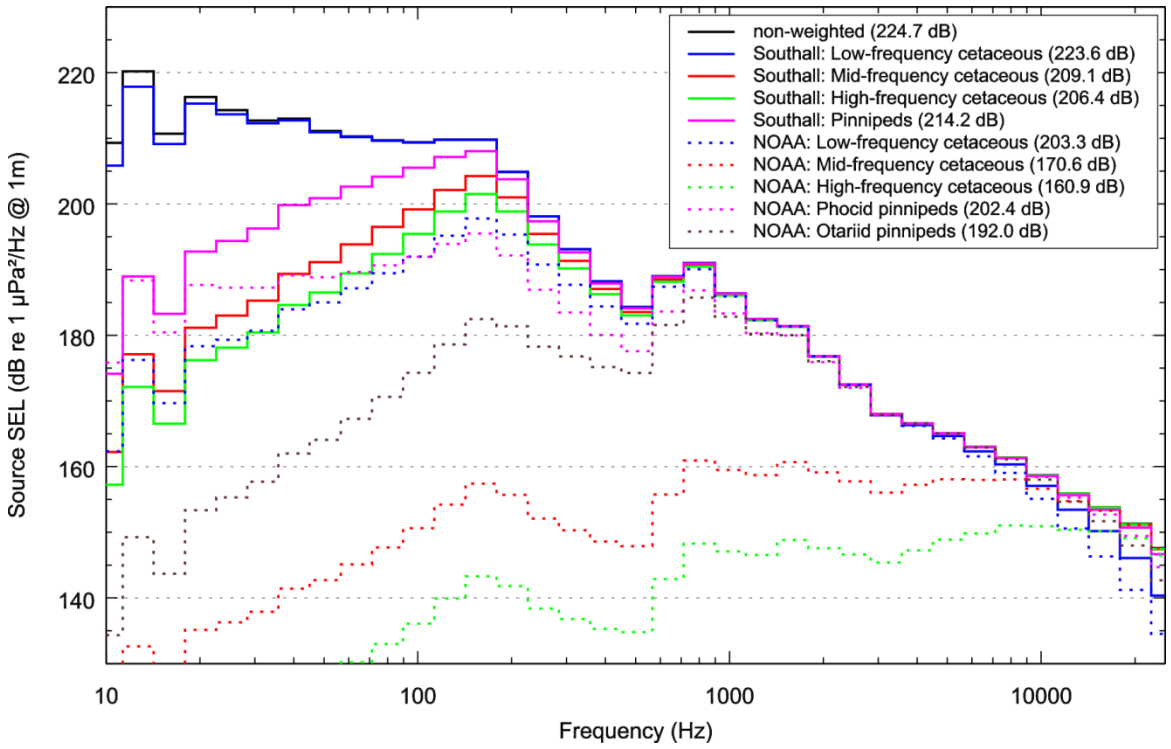

Figure 19. Maximum directional source level in the horizontal plane, in each 1/3-octave-band, for the 2400 in^3 VSP airgun source array (10–25000 Hz). Effective spectrums after application of the weighting functions (Southall et al 2007 and NOAA 2015) are shown as well.Values in brackets show effective broadband source levels.

Analysis of the effective source levels for the airgun seismic array with different M–weighting filters applied shows that the assessment of the exposure for mid- and high-frequency cetaceans (NOAA 2015 criteria) requires consideration of the frequency band extended up to 25 kHz.

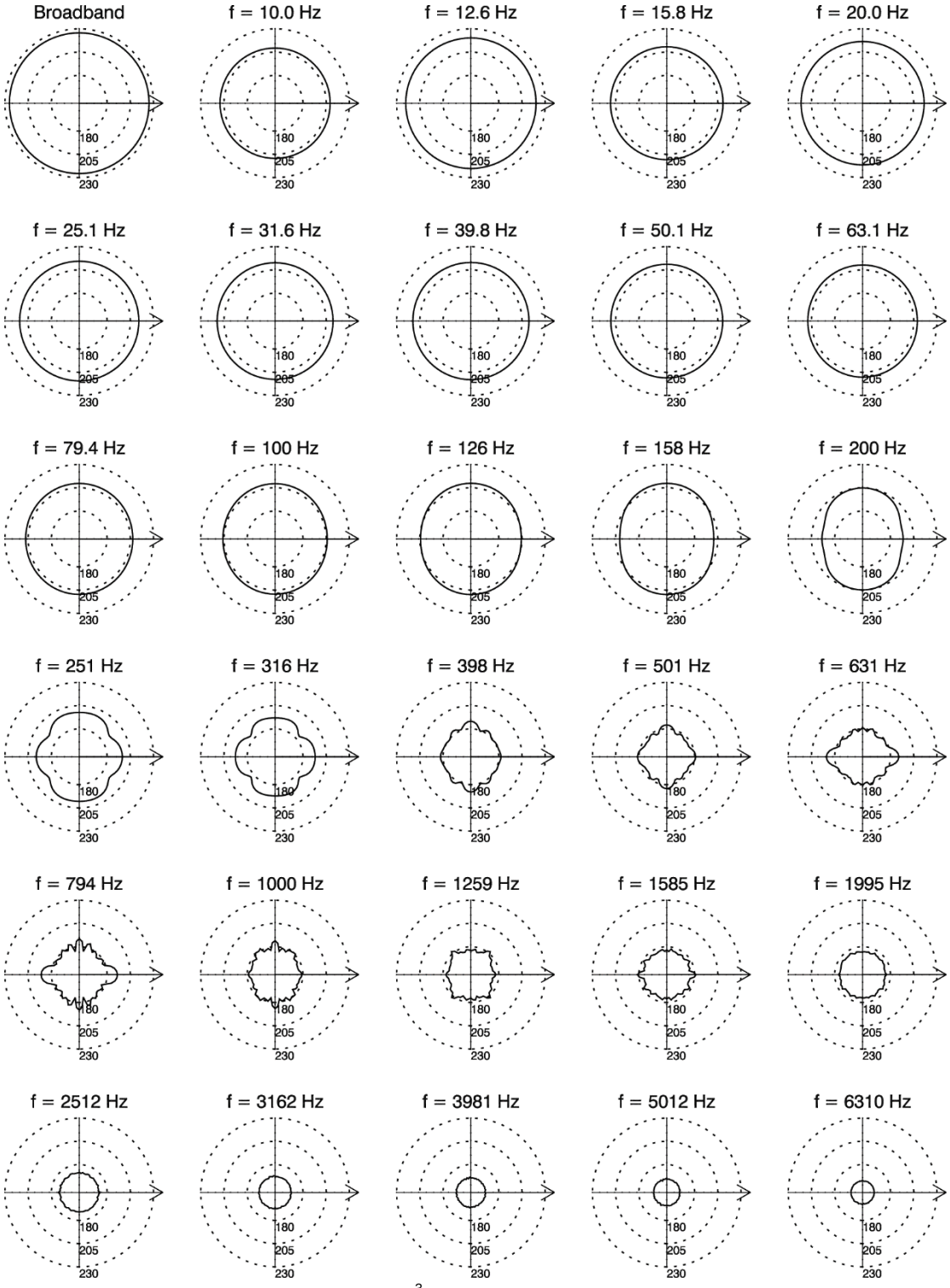

Figure 20. Horizontal directivity of the 2400 in^3 VSP airgun source array. Source levels (SLs, dB re 1 µPa^2·s) in 1/3-octave-bands. The 1/3-octave-band centre frequencies are indicated above each plot.

4.1.2. Vessels

4.1.2.1. Modelled Source Levels

The source levels and the sound spectrum from vessel thrusters were estimated based on the thruster specifications (diameter, rpm) according to the method described in Section 2.1.2. The method assumes that under heavy operation conditions, the sound from the cavitation process on the thruster propellers dominates the sound levels from other components of the vessel (machinery, drilling equipment, hull vibration). The relative spectrum of the sound is identical for all thrusters, as the method only accounts for the change of the broadband source level.

The thrusters are considered as omni-directional sources (i.e., the source levels do not depend on the horizontal azimuth).

Table 10 provides the estimated broadband levels of the individual thrusters, and Figure 21 shows their sound spectra.

Table 10. Estimated broadband levels for individual thrusters.

Thruster type	rms SPL (dB re 1 µPa @ 1 m)
UUC 355	187.7
UUC 455	188.9
SV aft thruster	184.9
SV bow thruster	181.6

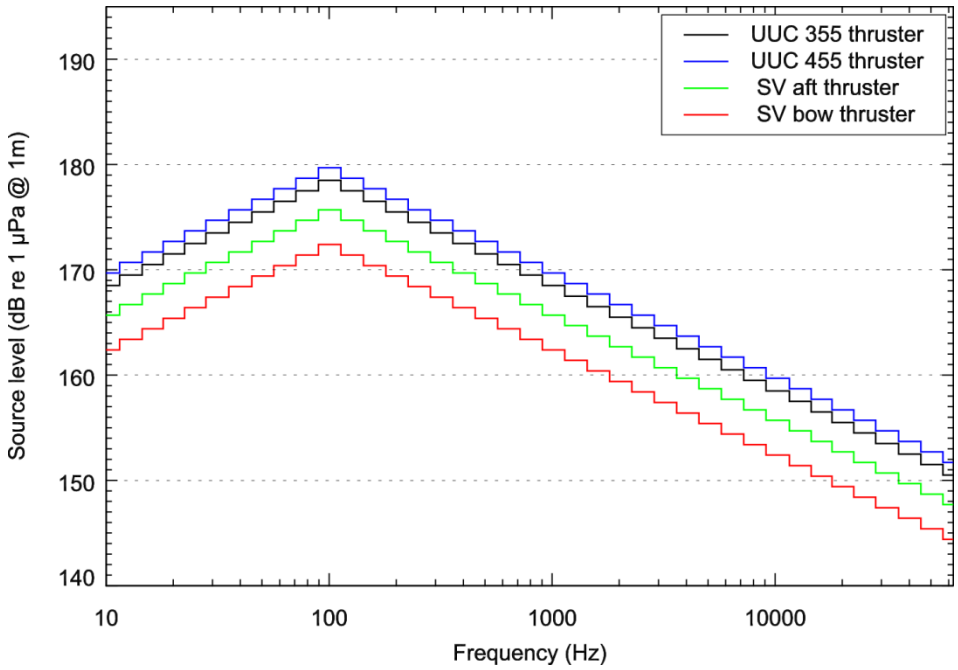

Figure 21. Estimated sound spectra from cavitating propellers of individual thrusters.

If considered as a point source with all thrusters located at the same point, the rms SPL broadband levels for each vessel are:

- 196.7 dB re 1 µPa @ 1 m for the drillship (8 × UUC355 thrusters),
- 196.7 dB re 1 µPa @ 1 m for the semi-submersible platform (6 × UUC455 thrusters), and
- 188.6 dB re 1 µPa @ 1 m for the support vessel (2 × SV aft + 2×SV bow thrusters).

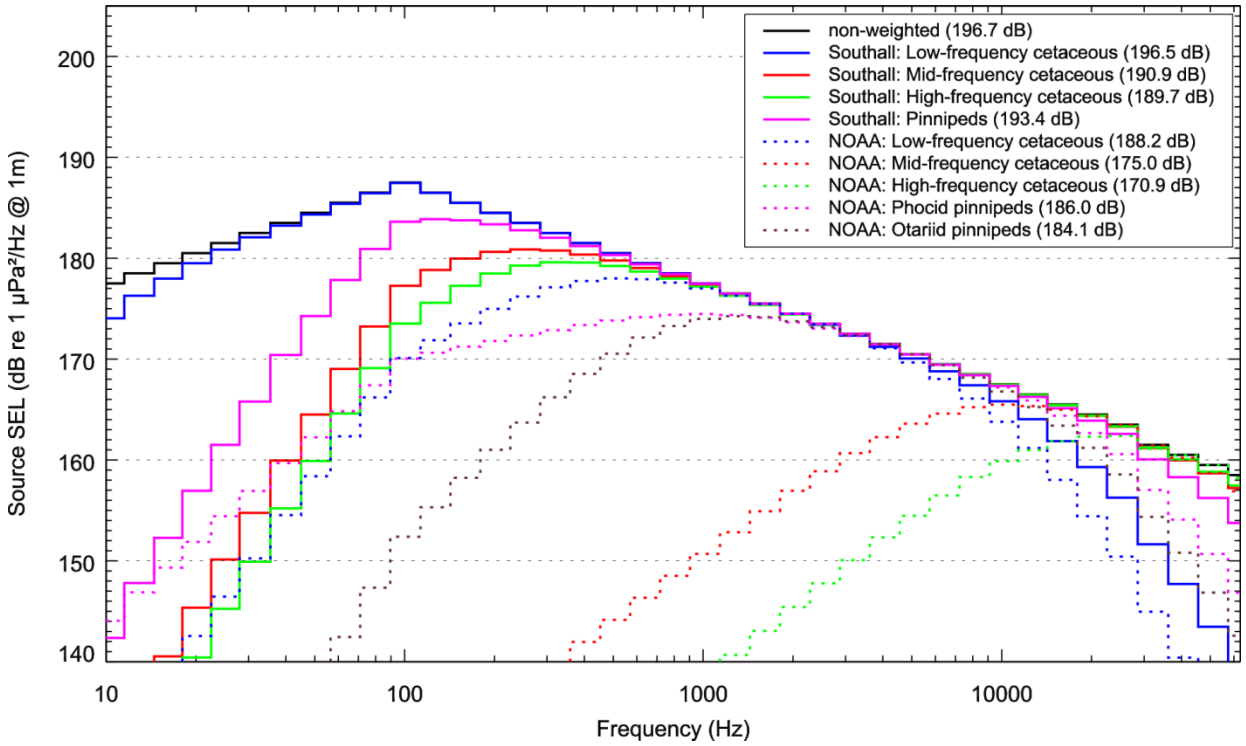

Figure 22. Estimated source level in each 1/3-octave-band for the drillship (10–63000 Hz). Effective spectrums after application of the weighting functions (Southall et al 2007 and NOAA 2015) shown as well.Values in brackets show effective broadband source levels.

The source level were estimated for the operation conditions at which the power output of the thrusters is near the nominal (maximum sustainable).

The analysis of the effective source levels for the vessel noise with different M–weighting filters applied shows that the assessment of the exposure for Mid- and High-frequency cetaceous (NOAA 2015 criteria) requires consideration of the frequency band extended up to 63 kHz.

From the analysis of the acoustic field modelling results, it was established that for accurate sound field assessment at distances less than 500 m, the actual locations of the thrusters on the vessel should be considered.

The estimated broadband source levels for the drillship and the semi-submersible platform are both 196.7 dB re 1 µPa. The drillship is equipped with UUC 355 thrusters that are slightly louder than the UUC 455 thrusters on the semi-submersible platform. The semi-submersible platform, however, is equipped with eight thrusters, while only six are installed on the drillship. The spectrum of the sound is identical for both vessels since the method accounts only for the broadband level value based on the specifications of the thrusters.

4.1.2.2. Modelling Results Validation

To validate the modelling results, the modelled sources levels were compared with the levels from similar vessels that had been directly measured in other studies

First, we compared the estimated sound levels used in this modelling study with the sound levels from measurements studies for similar platforms, which were anchored and did not use dynamic positioning systems. In 2012, JASCO conducted field measurements of two drillships, the *Noble Discoverer* (*Discoverer*) in the Chukchi Sea and *Kulluk* in the Beaufort Sea (Austin 2014). The acoustic recorders were located as close as 1 km from the drilling site. The sound levels were measured during drilling activities. The source levels were derived from the received levels by the back propagation method. The transmission loss between the source and receiver was computed using acoustic propagation with MONM.

The drillships in the Austin (2014) study were anchored; therefore, the recorded acoustic signal represents the sound from regular drilling activities without the dynamic positioning system. Figure 23 shows the frequency spectrum for the modelled drillship with dynamic positioning in use in this study and measured source spectrum for the anchored drillships without dynamic positioning (Austin 2014). The modelled drillship source spectrum is consistently 10–15 dB higher compared to the measured results in Austin (2014). There are similarities between the spectra. The maximum band level for the *Discoverer* is close to 100 Hz. The slope of the band level decrease at higher frequencies is also similar.

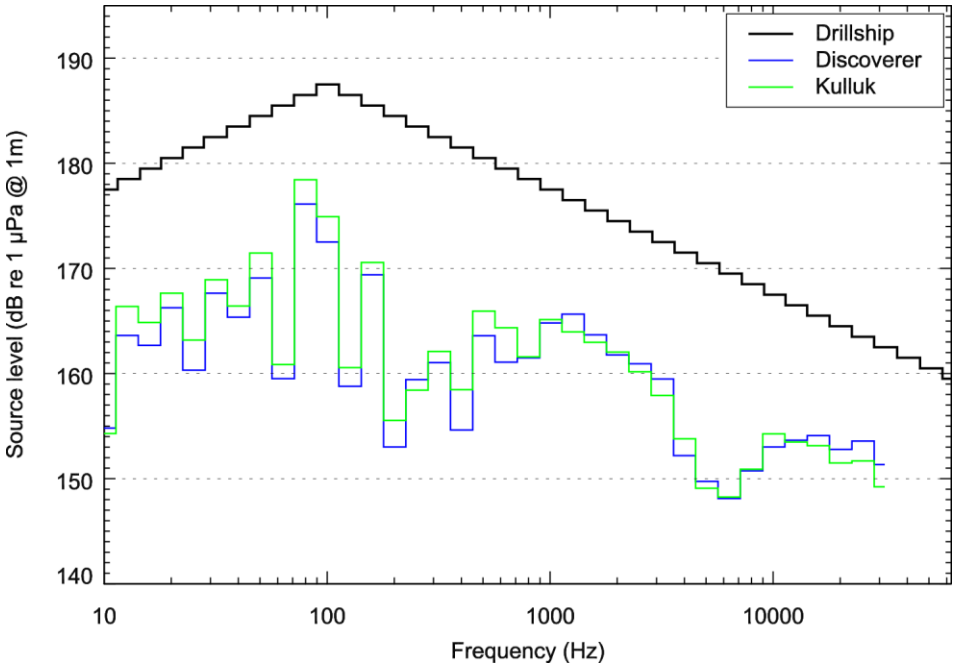

Figure 23. Acoustic source spectra comparison: Estimated for the drillship in this study and measured for anchored drillships.

Kyhn et al. (2011) conducted measurements on a drillship in Baffin Bay, Greenland, at a 500 m water depth. The measured drillship (*Stena Forth*) is 228 m long and 42 m wide equipped with six UUC 455 thrusters. The specifications of the *Stena Forth* are identical to the specifications of a generic drillship considered in this study. The measurements were conducted at distances as close as 500 m and at longer ranges from the vessel. Drilling and maintenance operations were measured while the dynamic positioning system was on duty. The monitoring was performed at sea state two or less.

Separate received sound spectra in 1/3-octave-bands were provided for each operation condition. Also, the broadband source levels were estimated as 190 dB re 1 µPa rms SPL for maintenance mode and 184 dB re 1 µPa for drilling mode. To perform the comparison, the received level spectra for the data

recorded at 500 m from the vessel were digitized and constant shift was applied to match the corresponding broadband source level (Figure 24).

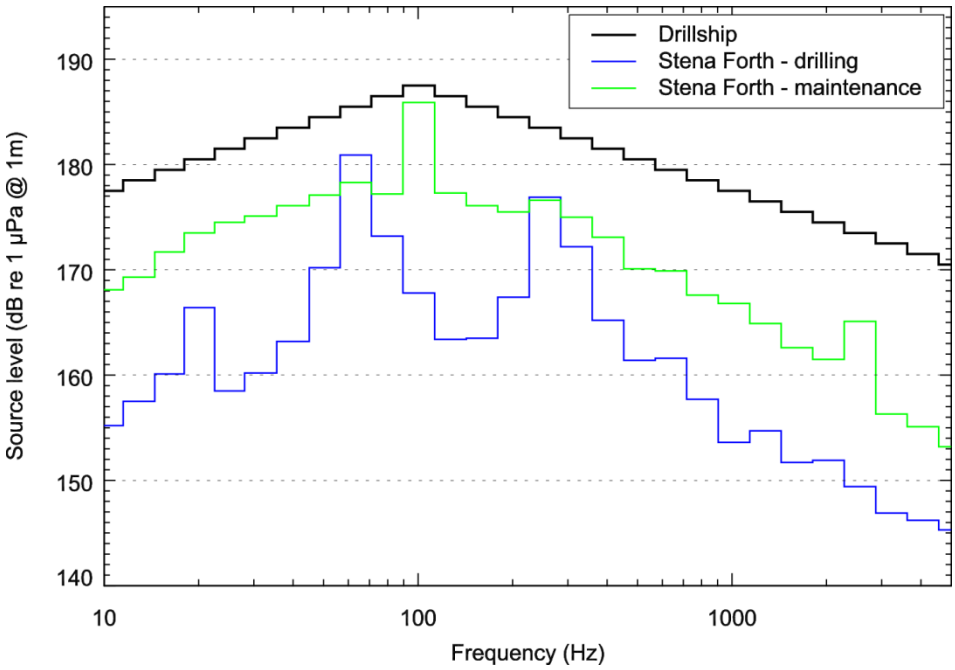

Figure 24. Acoustic source spectra comparison: Estimated for the drillship in this study and measured for the *Stena Forth*. The source level spectra for the *Stena Forth* were estimated based on information provided in Kyhn et al. 2011.

The vessel comparison shown on Figure 24 reveals good agreement of the main features of the modelled source level spectra for the drillship used in this study and measured spectra for the *Stena Forth*. Again, the maximum of the measured spectrum for maintenance mode is the same as for the modelled drillship, at 100 Hz. The band level roll off rates on either side of the maximum also match.

In summary, the comparison of modelled and measured results show:

1. Estimated source sound levels based on field measurements for a vessel using dynamic positioning were lower than the modelled source sound levels for the vessels in this study.
2. The main features of the spectrum graph (position of the maximum, slopes) for the modelled sources were similar to those obtained by field measurements.
3. Measured sound levels from a drilling activity without dynamic positioning system were lower than the modelled sound levels with dynamic positioning systems alone.

4.2. Acoustic Fields

Three types of acoustic field metrics were assessed for each source: rms SPL, cumulative SEL, and peak SPL. The acoustic fields from vessels were estimated based on the acoustic field of each individual thruster. The combined acoustic field from a vessel takes into account the actual location of each thruster on the vessel.

Maps of the horizontal acoustic field footprints were plotted and the ranges to specific thresholds were calculated based on a 2-D Cartesian grid representing horizontal distribution of the acoustic field around a source. The vertical dimension was reduced using the maximum-over-depth rule. The received sound level at a surface sampling location was taken as the maximum value that occurred over all samples

within the water column below. This provides a conservative prediction of the received sound level around the source, independent of depth.

The resultant N×1D dataset was gridded using triangulation method. Prior to gridding smoothing was applied to the data along each individual 1-D radial. The smoothing method was boxcar average with a 200 m width and affected the data points that were 200 m from the source and further. No smoothing was applied to the data points located closer than 200 m to the source.

In addition to maximum and 95% horizontal distances (see Section 2.3), the affected area was also calculated. The affected area calculations were performed by counting the number of grid nodes with levels higher than the specific threshold and multiplying it by the area of the grid cell. The affected area size was provided only for the thresholds, for which contours were fully enclosed within the modelled area.

The variation of the rms SPLs with range from the source was also analyzed. The grid of maximum-over-depth rms SPL field was taken and all grid nodes were binned based on the distance to the source regardless of the azimuth. Average and maximum values were calculated for all the nodes in each bin. The results of this analysis are presented as average and maximum rms SPLs compared to range graphs and also as tables of average and maximum rms SPLs at specific ranges from the source. For the purpose of average and maximum rms SPLs compared to range calculations, the bins within ±5% of the range of interest were taken into account.

4.2.1. rms SPL

The rms SPL metric was estimated based on an un-weighted acoustic field (i.e., without application of any of the M-weighting filters as discussed in Sections 1.3.2.1 and 1.3.3.1).

4.2.1.1. VSP Airgun Source Array

The rms SPL field for the VSP airgun source array was estimated based on the results of the full waveform modelling in the frequency band from 10 to 500 Hz. The reduction of the modelled frequency band was justified, as the amount of acoustic energy carried by the waves with frequencies above 500 Hz was 32 dB less than within 10 to 500 Hz band (see Table 9).

The full waveform modelling was performed to the maximum distance of 20 km from the source. The 90% rms SPL metric of the acoustic signal was calculated according to Equation 3 using a pressure time series. Table 11 lists the ranges to thresholds for Sites A and B in winter and summer. Figure 25 shows a small scale contour map of modelled maximum-over-depth rms SPLs at Site A in winter. Figure 26 provides larger scale maps of modelled maximum-over-depth rms SPLs for Sites A and B in winter and summer.

The graphs of average and maximum rms SPLs compared to range from the airgun source array for both sites and both seasons are provided in Figure 27. The graphs of average and maximum 0-to-peak SPLs compared to range from the airgun source array for both sites and both seasons are provided in Figure 28. The bin widths were set to 20 m.

Table 12 provides the average and maximum rms SPLs at specific ranges from the airgun source array for Sites A and B in winter and summer. Table 13 provides the average and maximum 0-to-peak SPLs at specific ranges from the airgun source array for sites A and B in winter and summer.

Table 11. VSP airgun source array: Maximum (R_{max}, km) and 95% ($R_{95\%}$, km) horizontal distances from the modelled maximum-over-depth rms SPL thresholds and affected area (A, km²). Bolded values represent distances over which the various NMFS interim criteria for marine mammal injury and sensory disturbance from an impulsive source are exceeded (i.e., 190 dB re 1 µPa rms SPL for pinniped injury; 180 dB re 1 µPa rms SPL for cetacean injury; 160 dB re 1 µPa rms SPL for pinniped and cetacean sensory disturbance) (see Section 1.3.1).

rms SPL (dB re 1 µPa)	**Site A**						**Site B**					
	Winter			Summer			Winter			Summer		
	R_{max}	$R_{95\%}$	A	R_{max}	$R_{95\%}$	A	R_{max}	$R_{95\%}$	A	R_{max}	$R_{95\%}$	A
210	<0.02	<0.02		<0.02	<0.02		<0.02	<0.02		<0.02	<0.02	
200	0.04	0.04	0.01	0.04	0.04	0.01	0.04	0.04	0.01	0.04	0.04	0.01
190	0.1	0.1	0.03	0.1	0.09	0.02	0.1	0.1	0.03	0.1	0.09	0.02
180	0.3	0.28	0.2	0.3	0.28	0.19	0.3	0.28	0.19	0.3	0.28	0.19
170	1.96	1.78	9.34	1.9	1.74	9.18	1.64	1.52	7.33	1.65	1.52	7.29
160	**3.54**	**3.19**	**33.3**	**3.46**	**3.17**	**32.8**	**3.57**	**2.83**	**21.7**	**8.44**	**2.95**	**22.3**
150	>20	>20		>20	>20		>20	>20		>20	>20	

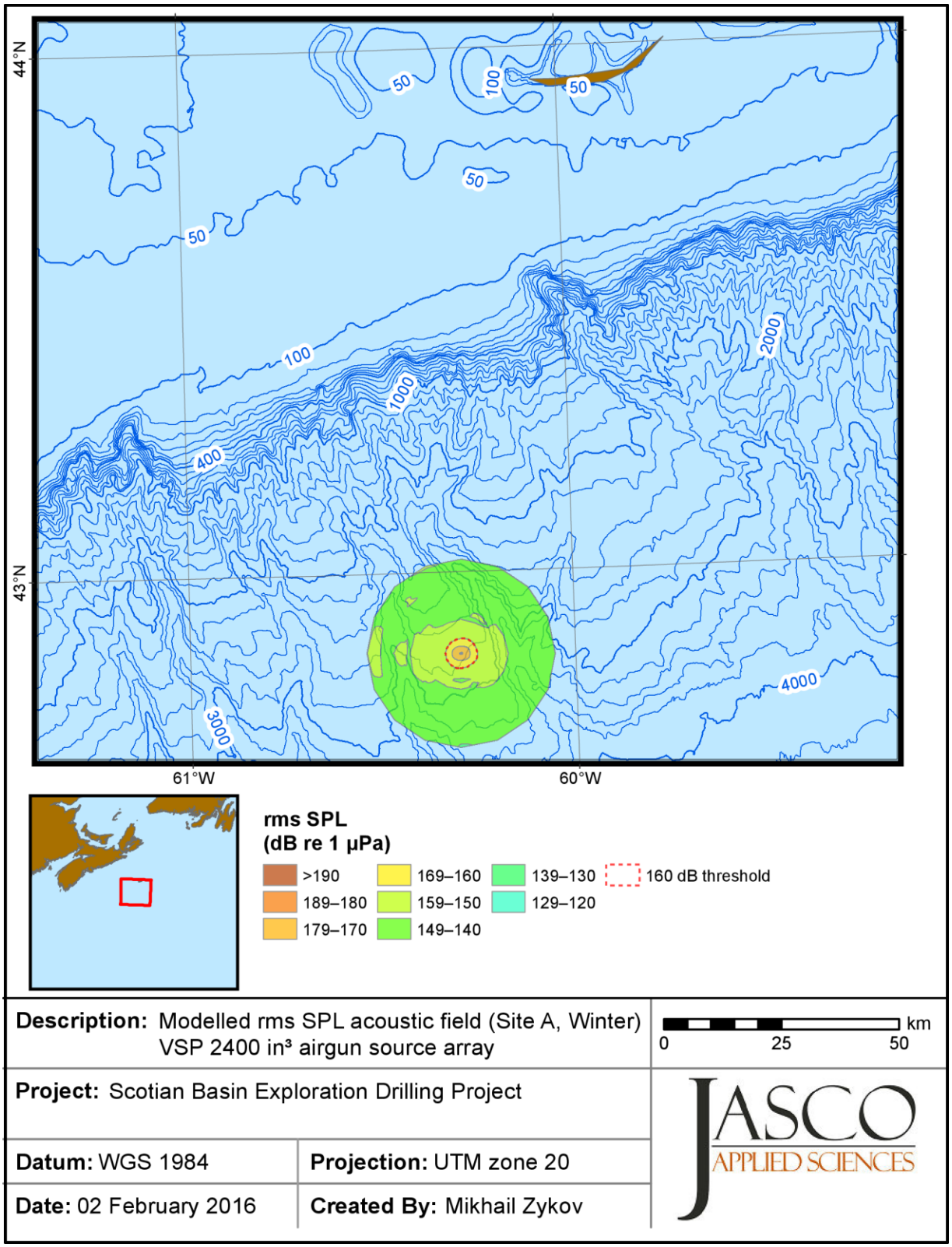

Figure 25. VSP airgun source array: Maximum-over-depth rms SPLs at Site A in winter. Source depth is 5 m; orientation azimuth is 0°.

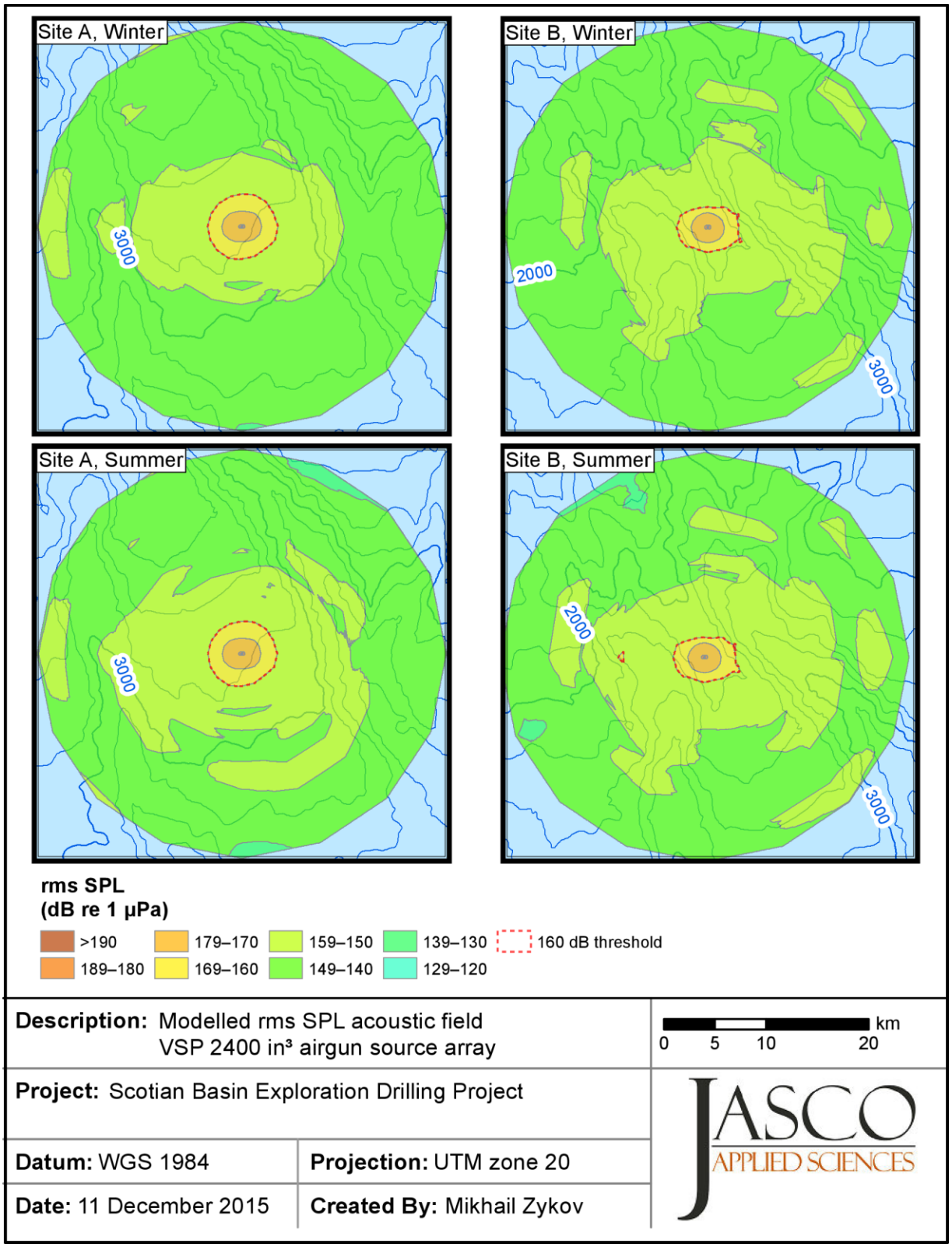

Figure 26. VSP airgun source array: Maximum-over-depth rms SPLs at Sites A and B in winter and summer (zoomed in). Source depth is 5 m; orientation azimuth is 0°.

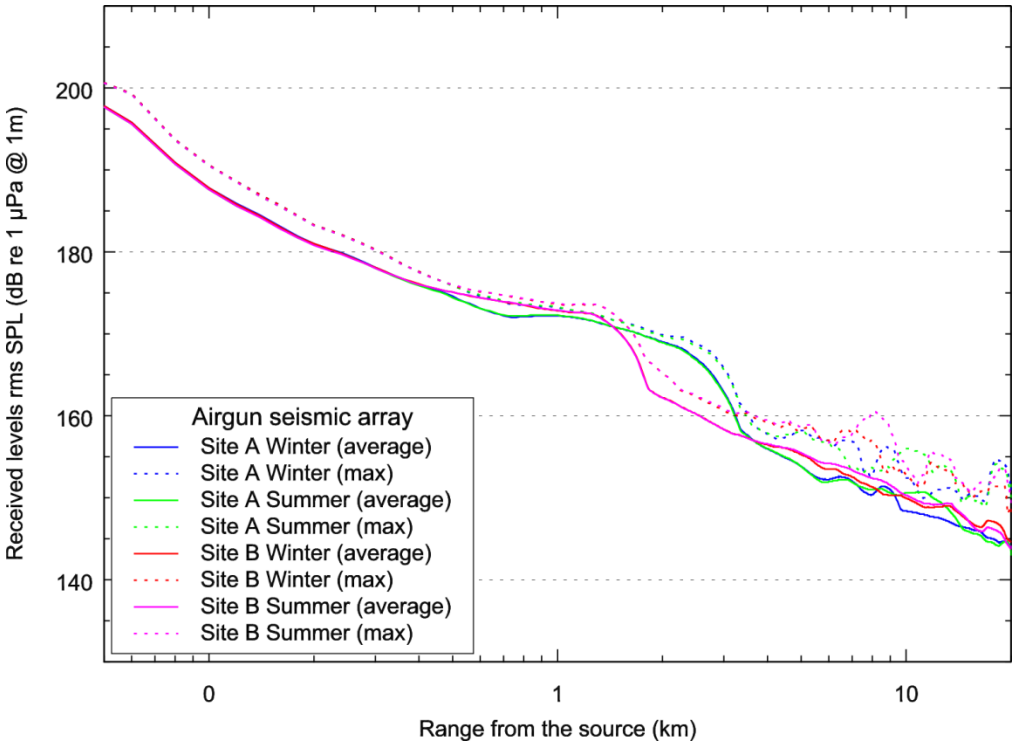

Figure 27. Airgun source array: Variation of the average and maximum rms SPLs compared to distance at Sites A and B in winter and summer.

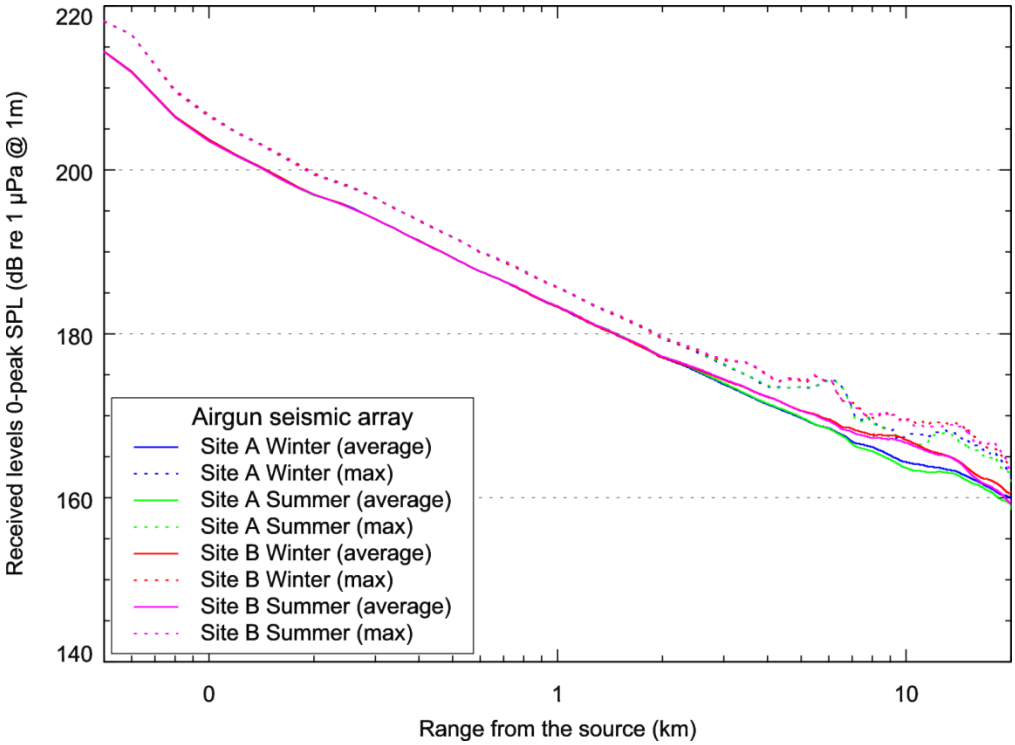

Figure 28. Airgun seismic array: Variation of the average and maximum 0-peak SPLs compared to distance at Sites A and B in winter and summer.

Table 12. VSP airgun source array: Maximum (L_{max}, dB re 1 µPa) and average (L_{avg}, dB re 1 µPa) maximum-over-depth rms SPL at specific ranges from the source.

Range (km)	Site A				Site B			
	Winter		Summer		Winter		Summer	
	L_{max}	L_{avg}	L_{max}	L_{avg}	L_{max}	L_{avg}	L_{max}	L_{avg}
0.1	190.6	187.8	190.5	187.6	190.6	187.8	190.5	187.6
0.25	181.8	179.6	181.7	179.5	181.8	179.5	181.7	179.4
0.5	175.9	174.6	175.9	174.4	176	175.1	176	175.1
1	173.2	172.2	173.3	172.3	173.6	172.8	173.7	172.9
2.5	168.8	167	168.5	166.8	162.3	160.2	162.4	160.2
5	158.1	153.8	158	153.8	158.4	155.3	158.8	155.5
10	152.7	148.5	155.9	150.5	152.8	149.9	153.9	150.3
20	153.1	144.5	152.4	144.4	149.6	145.1	152	144.4

Table 13. VSP airgun source array: Maximum (L_{max}, dB re 1 µPa) and average (L_{avg}, dB re 1 µPa) maximum-over-depth 0-peak SPL at specific ranges from the source.

Range (km)	Site A				Site B			
	Winter		Summer		Winter		Summer	
	L_{max}	L_{avg}	L_{max}	L_{avg}	L_{max}	L_{avg}	L_{max}	L_{avg}
0.1	206.7	203.7	206.5	203.5	206.7	203.7	206.5	203.5
0.25	198.1	195.6	197.9	195.5	198.1	195.6	197.9	195.5
0.5	191.8	189.3	191.8	189.3	191.8	189.3	191.8	189.3
1	185.6	183.3	185.7	183.3	185.6	183.3	185.7	183.4
2.5	177.8	175.4	178	175.6	177.9	175.7	178.2	175.8
5	173.5	169.7	173.5	169.8	174.2	170.6	174.4	170.6
10	167.5	164.4	166.9	163.7	169.5	167.1	169.4	166.7
20	163.4	160.2	163.1	159.5	164.3	160.7	164.2	159.7

4.2.1.2. Vessels

The rms SPL fields for the vessel scenarios were estimated based on the results of per-second SEL modelling. For continuous sources, the rms SPL is equal to the SEL, since the integration time in both cases is equal to 1 s (see Equations 2 and 4). The modelling was performed to the maximum distance of 150 km from the source.

The ranges to thresholds for the four vessel scenarios at Sites A and B are provided in Table 14 and Table 15, respectively. Figures 29 to 32 show the contour maps of maximum-over-depth rms SPL fields

for the entire modelling area. Each figure is dedicated for a single scenario and provides a set of four fields representing each site and season. To show the structure of the acoustic field near the sources, Figure 33 provides a set of four maps zoomed in on the vessels. The maps show the field modelled at Site A in winter. Since the water depth and sound speed profile variation have virtually no effect on sound propagation at close ranges, this map can also be referred to for the other site and season.

The graphs of average and maximum rms SPLs vs. range from the source for both sites and both seasons are provided in Figure 34 (drillship), Figure 35(drillship with support vessel), Figure 36 (semi-submersible platform), and Figure 37 (semi-submersible platform with support vessel). The bin widths were set to 50 m.

The average and maximum rms SPLs at specific ranges from the source for four vessel scenarios at Sites A and B are provided in Table 16 and Table 17, respectively.

Table 14. Vessels at Site A: Maximum (R_{max}, km) and 95% (R_{95}%, km) horizontal distances from the modelled maximum-over-depth rms SPL thresholds. Bolded values represent distances over which the NMFS interim criteria for marine mammal injury and sensory disturbance from a non-impulsive source are exceeded (i.e., 190 dB re 1 µPa rms SPL for pinniped injury; 180 dB re 1 µPa rms SPL for cetacean injury; 120 dB re 1 µPa rms SPL for pinniped and cetacean sensory disturbance) (see Section 1.3.1).

rms SPL (dB re 1 µPa)	**Drillship**				**Drillship w/ support vessel**				**Semi-submersible**				**Semi-submersible w/ support vessel**			
	Winter		Summer		Winter		Summer		Winter		Summer		Winter		Summer	
	R_{max}	$R_{95\%}$	R_{max}	$R_{95\%}$	R_{max}	$R_{95\%}$	R_{max}	$R_{95\%}$	R_{max}	$R_{95\%}$	R_{max}	$R_{95\%}$	R_{max}	$R_{95\%}$	R_{max}	$R_{95\%}$
190	<0.15	<0.15	<0.15	<0.15	<0.15	<0.15	<0.15	<0.15	<0.1	<0.1	<0.1	<0.1	<0.1	<0.1	<0.1	<0.1
180	**<0.15**	**<0.15**	**<0.15**	**<0.15**	**<0.15**	**<0.15**	**<0.15**	**<0.15**	**<0.1**	**<0.1**	**<0.1**	**<0.1**	**<0.1**	**<0.1**	**<0.1**	**<0.1**
170	<0.15	<0.15	<0.15	<0.15	<0.15	<0.15	<0.15	<0.15	<0.1	<0.1	<0.1	<0.1	<0.1	<0.1	<0.1	<0.1
160	0.18	0.16	0.18	0.16	0.19	0.16	0.18	0.16	0.11	0.11	0.11	0.11	0.13	0.12	0.12	0.11
150	0.38	0.34	0.38	0.34	0.39	0.35	0.39	0.36	0.33	0.32	0.33	0.32	0.35	0.34	0.36	0.34
140	0.99	0.93	1.06	0.98	1.99	1.93	1.11	1.05	2.06	2.02	1.07	1.04	2.45	2.37	1.13	1.1
130	14.9	12.8	3.5	3.4	17.3	14.5	3.8	3.6	19.1	17.4	3.7	3.6	21.6	19.0	4.0	3.8
120	>150	>150	51.3	23.1	>150	>150	51.6	50.4	>150	>150	51.3	24	>150	>150	51.6	27.8

Table 15. Vessels at Site B: Maximum (*Rmax*, km) and 95% (*R95*%, km) horizontal distances from the modelled maximum-over-depth rms SPL thresholds. Bolded values represent distances over which the NMFS interim criteria for marine mammal injury and sensory disturbance from a non-impulsive source are exceeded (i.e., 190 dB re 1 µPa rms SPL for pinniped injury; 180 dB re 1 µPa rms SPL for cetacean injury; 120 dB re 1 µPa rms SPL for pinniped and cetacean sensory disturbance) (see Section 1.3.1).

rms SPL (dB re 1 µPa)	**Drillship**				**Drillship w/ support vessel**				**Semi-submersible**				**Semi-submersible w/ support vessel**			
	Winter		Summer		Winter		Summer		Winter		Summer		Winter		Summer	
	R_{max}	$R_{95\%}$	R_{max}	$R_{95\%}$	R_{max}	$R_{95\%}$	R_{max}	$R_{95\%}$	R_{max}	$R_{95\%}$	R_{max}	$R_{95\%}$	R_{max}	$R_{95\%}$	R_{max}	$R_{95\%}$
190	<0.15	<0.15	<0.15	<0.15	<0.15	<0.15	<0.15	<0.15	<0.1	<0.1	<0.1	<0.1	<0.1	<0.1	<0.1	<0.1
180	<0.15	<0.15	<0.15	<0.15	<0.15	<0.15	<0.15	<0.15	<0.1	<0.1	<0.1	<0.1	<0.1	<0.1	<0.1	<0.1
170	<0.15	<0.15	<0.15	<0.15	<0.15	<0.15	<0.15	<0.15	<0.1	<0.1	<0.1	<0.1	<0.1	<0.1	<0.1	<0.1
160	0.18	0.16	0.18	0.16	0.19	0.16	0.18	0.16	0.11	0.11	0.11	0.11	0.13	0.12	0.12	0.11
150	0.38	0.34	0.38	0.34	0.39	0.35	0.4	0.36	0.33	0.32	0.33	0.32	0.35	0.34	0.36	0.34
140	1.0	0.93	1.06	0.98	2.0	1.94	1.12	1.05	2.07	2.02	1.07	1.04	2.46	2.38	1.14	1.1
130	15.9	14.1	6.6	5.8	19.4	14.9	7.0	6.6	21.8	18.5	6.5	5.2	22.2	19.2	7.1	6.5
120	144	128	50.8	25.5	>150	>150	60.7	27.0	>150	>150	60.8	26.7	>150	>150	61.0	28.5

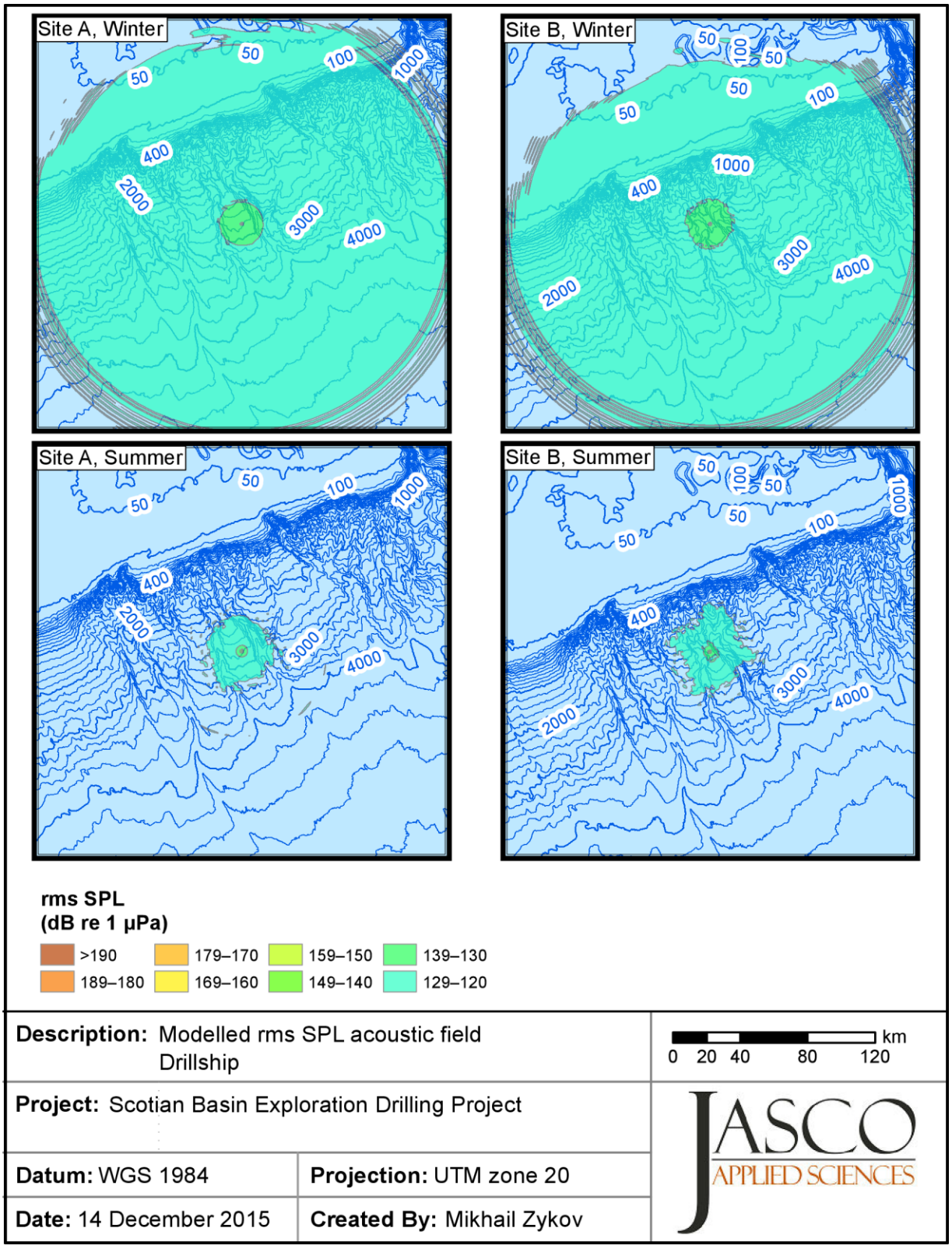

Figure 29. Drillship: Maximum-over-depth rms SPLs at Sites A and B in winter and summer (zoomed in).

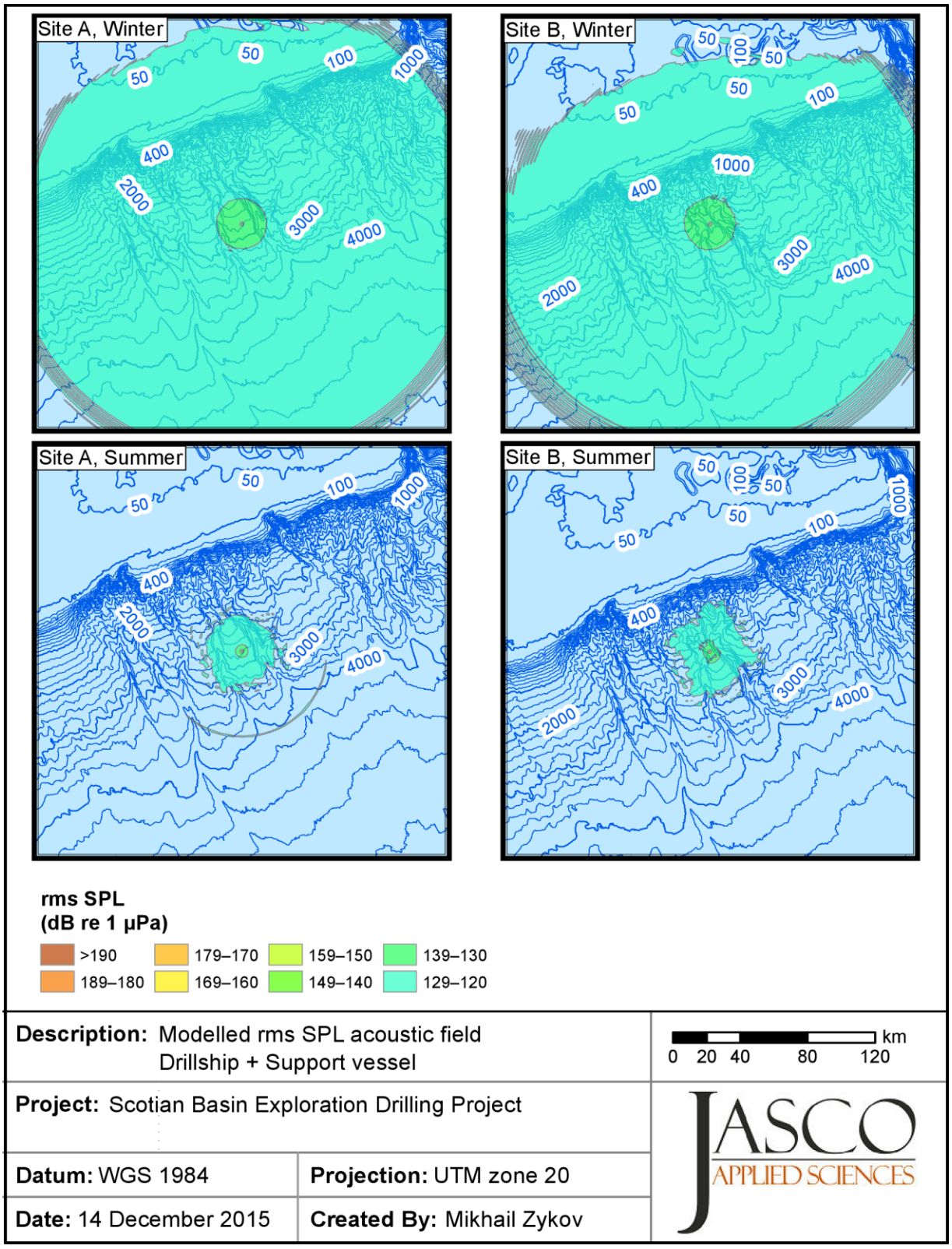

Figure 30. Drillship with support vessel: Maximum-over-depth rms SPLs at Sites A and B in winter and summer (zoomed in).

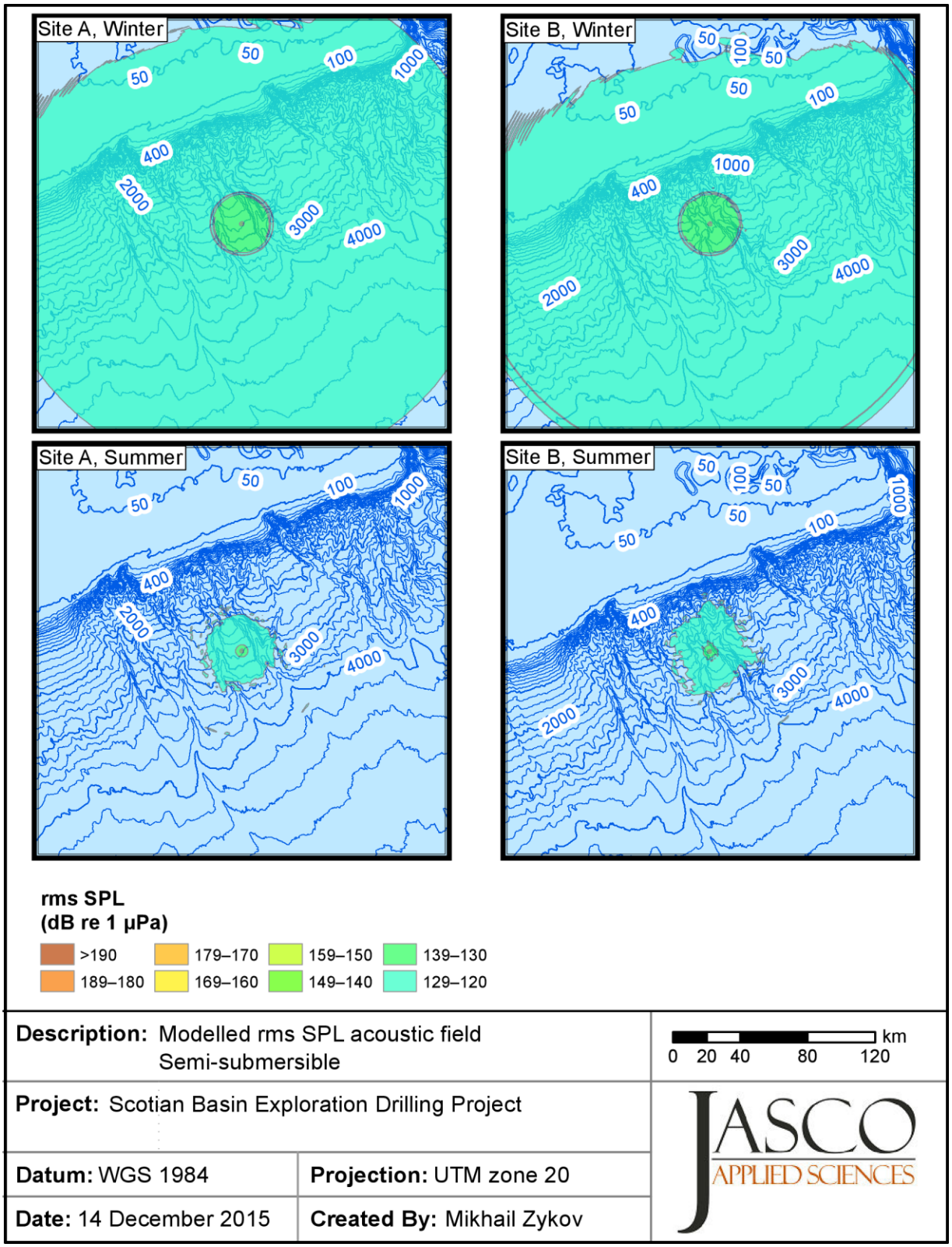

Figure 31. Semi-submersible platform: Maximum-over-depth rms SPLs at Sites A and B in winter and summer (zoomed in).

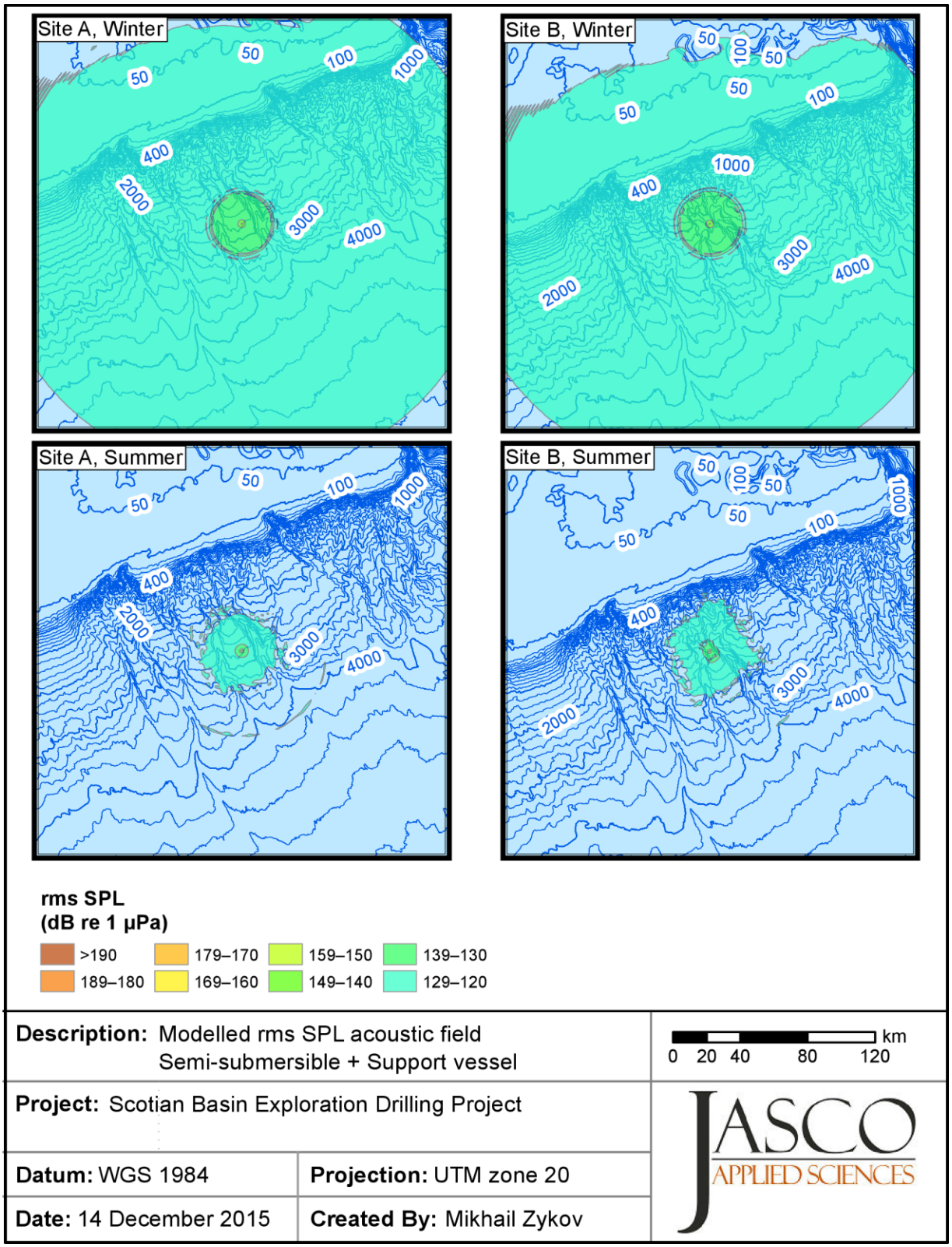

Figure 32. Semi-submersible platform with support vessel: Maximum-over-depth rms SPLs at Sites A and B in winter and summer (zoomed in).

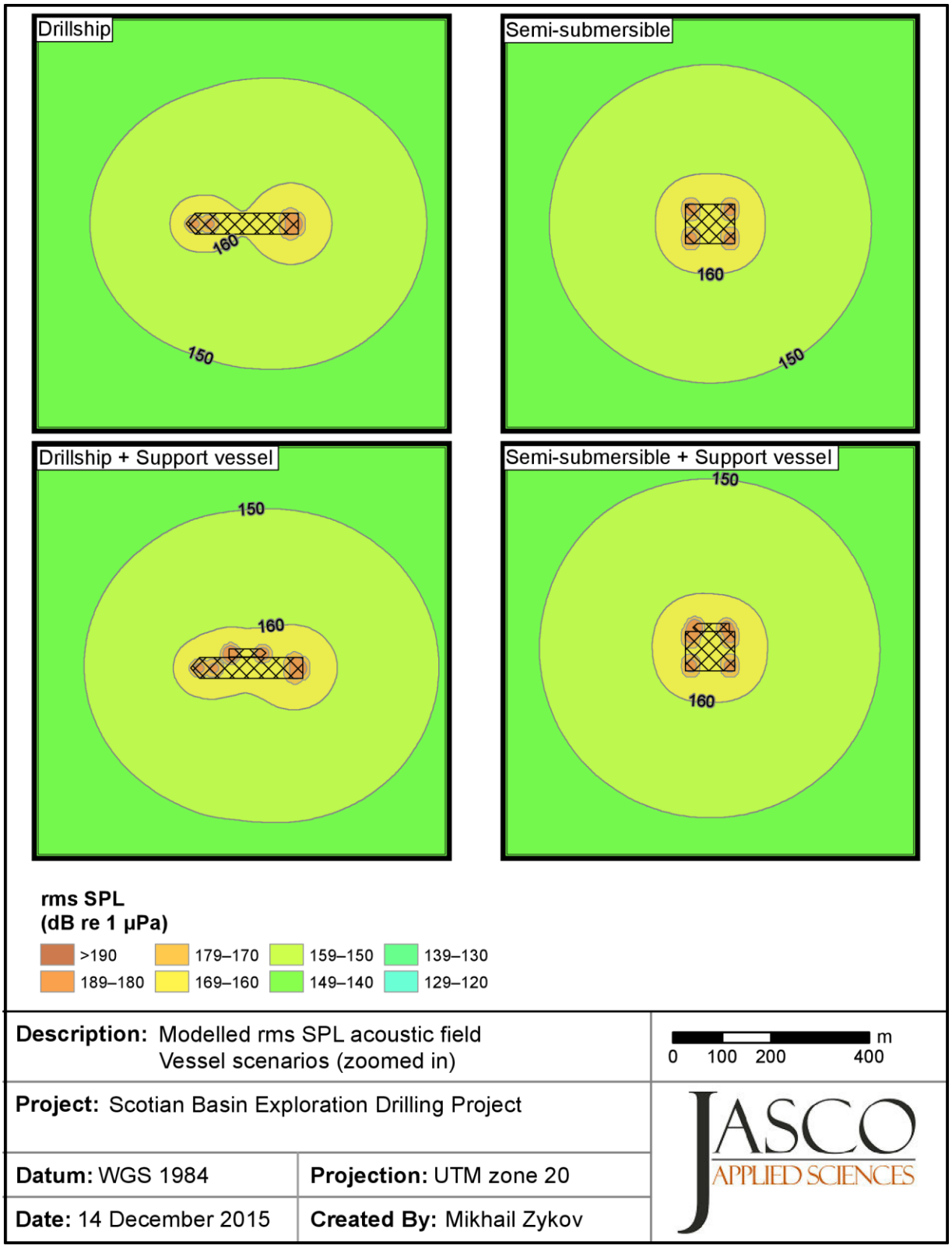

Figure 33. Vessel scenarios (zoomed in): Maximum-over-depth rms SPLs at Site A in winter.

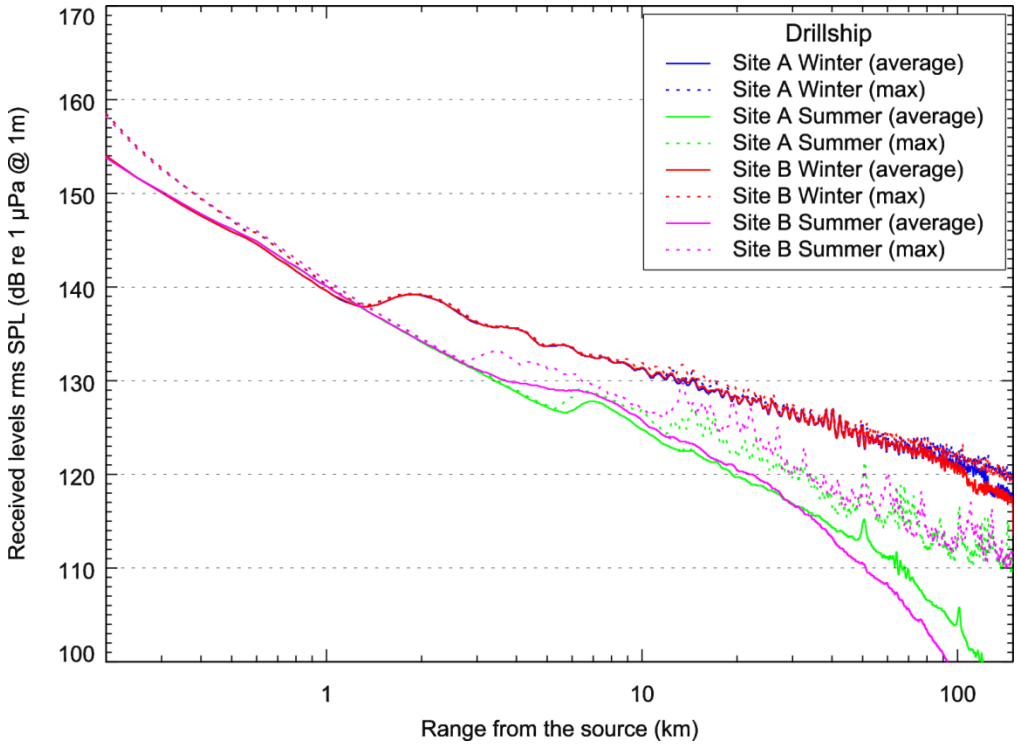

Figure 34. Drillship: Variation of the average and maximum rms SPLs compared to distance at Sites A and B in winter and summer.

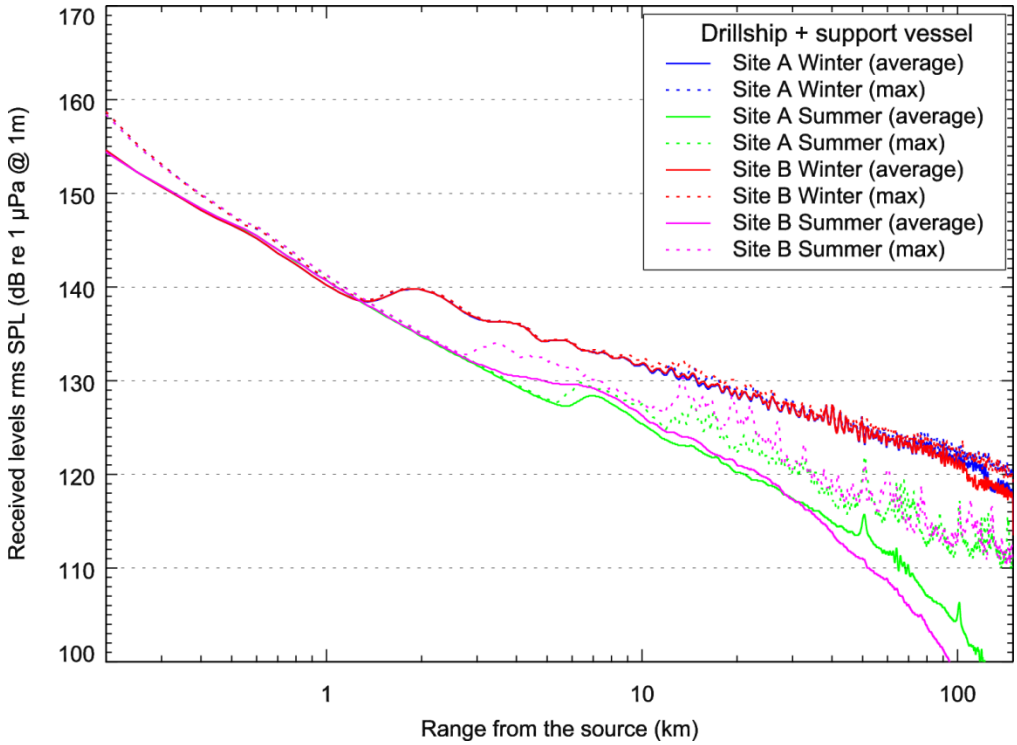

Figure 35. Drillship with support vessel: Variation of the average and maximum rms SPLs compared to distance at Sites A and B in winter and summer.

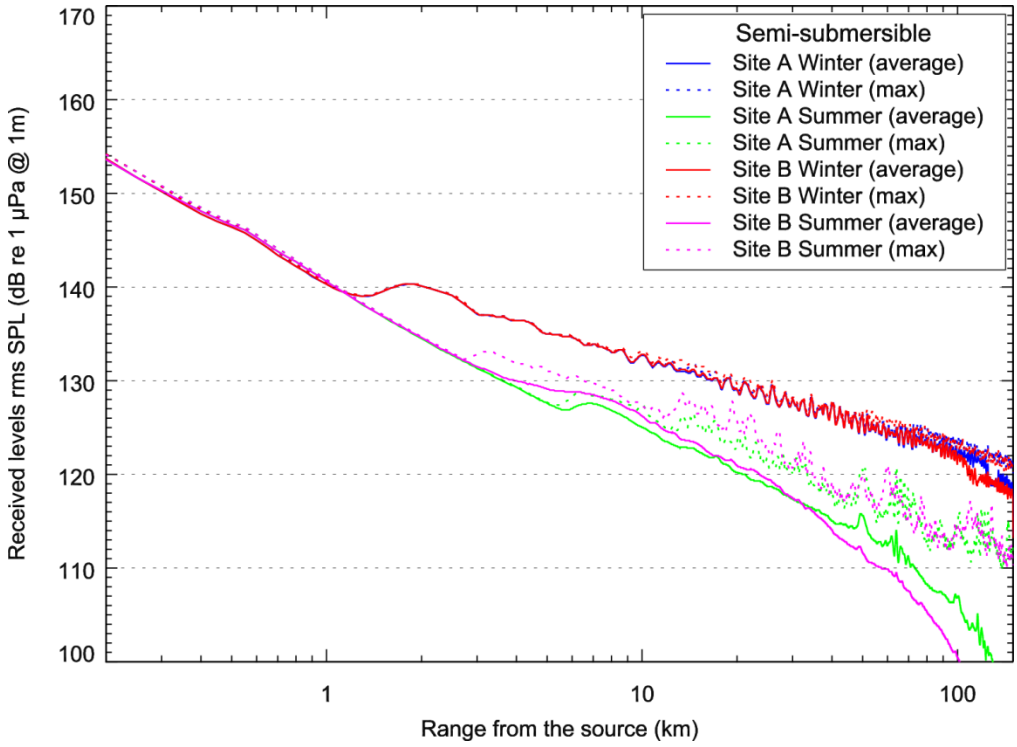

Figure 36. Semi-submersible platform: Variation of the average and maximum rms SPLs compared to distance at Sites A and B in winter and summer.

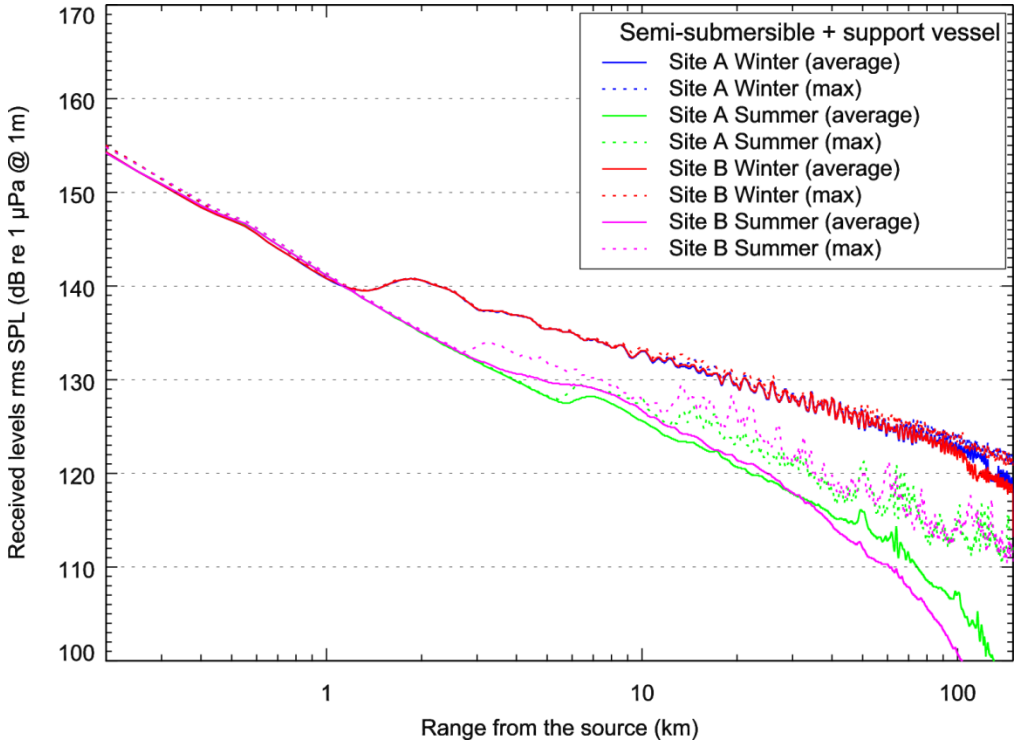

Figure 37. Semi-submersible platform with support vessel: Variation of the average and maximum rms SPLs compared to distance at Sites A and B in winter and summer.

Table 16. Vessels at Site A: Maximum (L_{max}, dB re 1 µPa) and average (L_{avg}, dB re 1 µPa) maximum-over-depth rms SPL at specific ranges from the source.

Range (km)	Drillship				Drillship w/ support vessel				Semi-submersible				Semi-submersible w/ support vessel			
	Winter		Summer		Winter		Summer		Winter		Summer		Winter		Summer	
	L_{max}	L_{avg}	L_{max}	L_{avg}	L_{max}	L_{avg}	L_{max}	L_{avg}	L_{max}	L_{avg}	L_{max}	L_{avg}	L_{max}	L_{avg}	L_{max}	L_{avg}
0.25	155	151.7	154.8	151.7	155.3	152.3	155.1	152.3	152.3	151.7	152.3	151.7	153.1	152.3	153	152.3
0.5	147.1	145.9	147.2	146.2	147.6	146.6	147.7	146.8	146.7	146.4	146.9	146.6	147.3	147.0	147.5	147.2
1	140.3	139.6	140.7	140.1	140.8	140.2	141.3	140.7	140.5	140.3	140.8	140.6	141.0	140.8	141.4	141.1
2.5	138.0	137.7	132.6	132.4	138.4	138.2	133.2	133.0	139.1	139.0	132.8	132.7	139.5	139.4	133.4	133.3
5	133.8	133.7	127.3	127.2	134.3	134.2	128.0	127.8	135.1	135.1	127.7	127.6	135.5	135.4	128.3	128.2
10	131.2	131.1	126.7	124.8	131.7	131.6	127.2	125.4	132.5	132.5	127.0	125.0	132.9	132.8	127.5	125.6
25	127.6	127.2	121.2	118.4	128.1	127.7	121.8	119.0	128.8	128.5	121.3	118.8	129.2	128.8	121.8	119.3
50	124.4	124.0	118.6	113.7	124.9	124.5	119.0	114.2	125.7	125.3	119.4	114.9	126.1	125.7	119.8	115.2
100	122.2	121.0	112.8	104.1	122.6	121.5	113.3	104.5	123.4	122.3	113.9	106.2	123.8	122.7	114.2	106.5
150	119.8	117.6	111.7	96.4	120.3	118.1	112.1	96.7	121.1	118.7	112.6	98.1	121.5	119.0	113.0	98.2

Table 17. Vessels at Site B: Maximum (L_{max}, dB re 1 µPa) and average (L_{avg}, dB re 1 µPa) maximum-over-depth rms SPL at specific ranges from the source.

Range (km)	Drillship				Drillship w/ support vessel				Semi-submersible				Semi-submersible w/ support vessel			
	Winter		Summer		Winter		Summer		Winter		Summer		Winter		Summer	
	L_{max}	L_{avg}	L_{max}	L_{avg}	L_{max}	L_{avg}	L_{max}	L_{avg}	L_{max}	L_{avg}	L_{max}	L_{avg}	L_{max}	L_{avg}	L_{max}	L_{avg}
0.25	155	151.7	154.8	151.7	155.3	152.3	155.1	152.3	152.3	151.7	152.3	151.7	153.1	152.3	153	152.3
0.5	147.1	145.9	147.2	146.2	147.6	146.6	147.7	146.8	146.7	146.4	146.9	146.6	147.3	147	147.5	147.2
1	140.3	139.6	140.7	140.1	140.9	140.2	141.3	140.7	140.5	140.3	140.8	140.6	141.1	140.9	141.4	141.1
2.5	138	137.7	132.7	132.5	138.5	138.2	133.3	133.1	139.2	139.1	133	132.8	139.5	139.4	133.6	133.4
5	133.9	133.7	131.5	129.2	134.4	134.3	132.3	129.9	135.2	135.1	131.2	129.1	135.5	135.4	132	129.8
10	131.8	131.2	127	125.7	132.3	131.7	127.6	126.3	132.9	132.5	127.3	126.2	133.3	132.9	127.8	126.7
25	128	127.3	122.9	119	128.5	127.8	123.5	119.5	129.1	128.5	122.9	119.5	129.5	128.9	123.4	120
50	124.9	124	118	110.3	125.4	124.5	118.4	110.8	126.3	125.4	118.6	111.6	126.6	125.7	119	112
100	122	120.6	113.4	98.0	122.4	121.1	113.9	98.5	123.2	121.8	113.7	100.4	123.5	122.2	114.1	100.7
150	119.7	117.2	110.9	94.0	120.1	117.7	111.4	94.3	121.1	117.9	111.2	95.3	121.4	118.3	111.6	95.5

4.2.2. Cumulative SEL

The cumulative SELs were based on per-pulse SELs for the impulsive source (VSP airgun source array) and per-second SELs for the continuous sound sources (vessels). The cumulative integration time was 24 h.

The cumulative SEL fields were calculated for each of the four functional hearing groups by Southall et al. (2007) and five functional hearing groups from NOAA (2015) using the applicable M-weighting filters.

4.2.2.1. VSP Airgun Source Array

The VSP airgun source array is expected to be activated 2040 times in a 24 hour period during the VSP survey. According to Equation 5, $cSEL_{24hr}$ is estimated by adding 33.1 dB to the modelled per-pulse SEL.

The ranges to specific thresholds based on un-weighted fields for both sites and both seasons are provided in Table 18. The maximum-over-depth un-weighted 24 hour cumulative SELs are displayed as contour maps in Figure 38. Figure 39 provides a map of criteria threshold contours zoomed in on the source. The map is based on the fields modelled at Site A in winter. Since the water depth and sound speed profile variation have virtually no effect on sound propagation at close ranges, this map can be used to represent the other site and season.

Table 18. VSP airgun source array: Maximum (R_{max}, km) and 95% ($R_{95\%}$, km) horizontal distances to modelled maximum-over-depth cumulative SEL thresholds, un-weighted field.

cSEL (dB re 1 µPa²·s)	**Site A**				**Site B**			
	Winter		Summer		Winter		Summer	
	R_{max}	$R_{95\%}$	R_{max}	$R_{95\%}$	R_{max}	$R_{95\%}$	R_{max}	$R_{95\%}$
230	<0.02	<0.02	<0.02	<0.02	<0.02	<0.02	<0.02	<0.02
220	0.04	0.04	0.04	0.04	0.04	0.04	0.04	0.04
210	0.17	0.16	0.17	0.16	0.17	0.16	0.17	0.16
200	0.55	0.5	0.54	0.5	0.55	0.51	0.54	0.5
190	1.79	1.63	1.79	1.64	3.25	1.7	3.27	1.7
180	14.6	8.13	12.7	7.65	22.1	12.4	19.5	8.34
170	>50	>50	39.8	27.1	>50	>50	>50	>50

Table 19. VSP airgun source array: Maximum (R_{max}, km), 95% ($R_{95\%}$, km) horizontal distances from the source to PTS onset acoustic threshold levels and affected area (A, km²) for 24 hour cumulative SEL.

Marine mammal group	Threshold (dB)	Site A						Site B					
		Winter			Summer			Winter			Summer		
		R_{max}	$R_{95\%}$	A	R_{max}	$R_{95\%}$	A	R_{max}	$R_{95\%}$	A	R_{max}	$R_{95\%}$	A
Southall et al. *(2007)*													
Low-frequency cetaceans	198	0.67	0.62	1.1	0.67	0.61	1.1	0.67	0.62	1.1	0.67	0.62	1.1
Mid-frequency cetaceans	198	0.26	0.24	0.12	0.26	0.24	0.12	0.26	0.24	0.12	0.26	0.24	0.12
High-frequency cetaceans	198	0.18	0.17	0.06	0.18	0.16	0.06	0.18	0.17	0.06	0.18	0.16	0.06
Pinnipeds	186	1.65	1.51	5.2	1.7	1.55	5.41	1.67	1.53	5.3	1.73	1.58	5.5
NOAA (2015)													
Low-frequency cetaceans	192	0.26	0.24	0.19	0.26	0.24	0.19	0.26	0.24	0.18	0.26	0.24	0.19
Mid-frequency cetaceans	187	<0.02	<0.02	—	<0.02	<0.02	—	<0.02	<0.02	—	<0.02	<0.02	—
High-frequency cetaceans	154	0.14	0.13	0.13	0.13	0.13	0.13	0.14	0.13	0.13	0.13	0.13	0.13
Phocid pinnipeds	186	0.4	0.37	0.32	0.4	0.37	0.32	0.4	0.37	0.32	0.4	0.37	0.32
Otariid pinnipeds	203	<0.02	<0.02	—	<0.02	<0.02	—	<0.02	<0.02	—	<0.02	<0.02	—

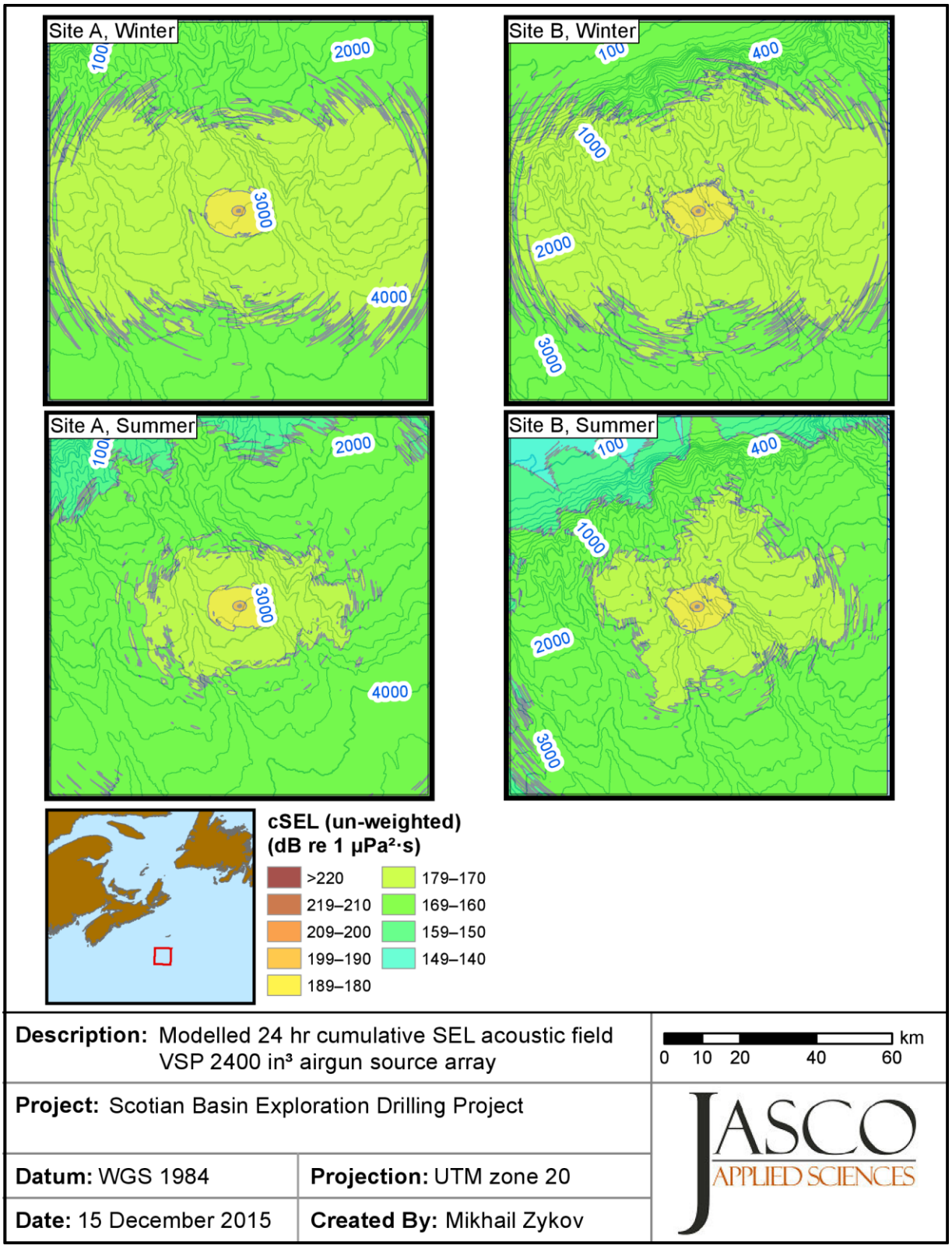

Figure 38. VSP airgun source array: Maximum-over-depth 24 hour cumulative SEL at Sites A and B in winter and summer for the un-weighted field.

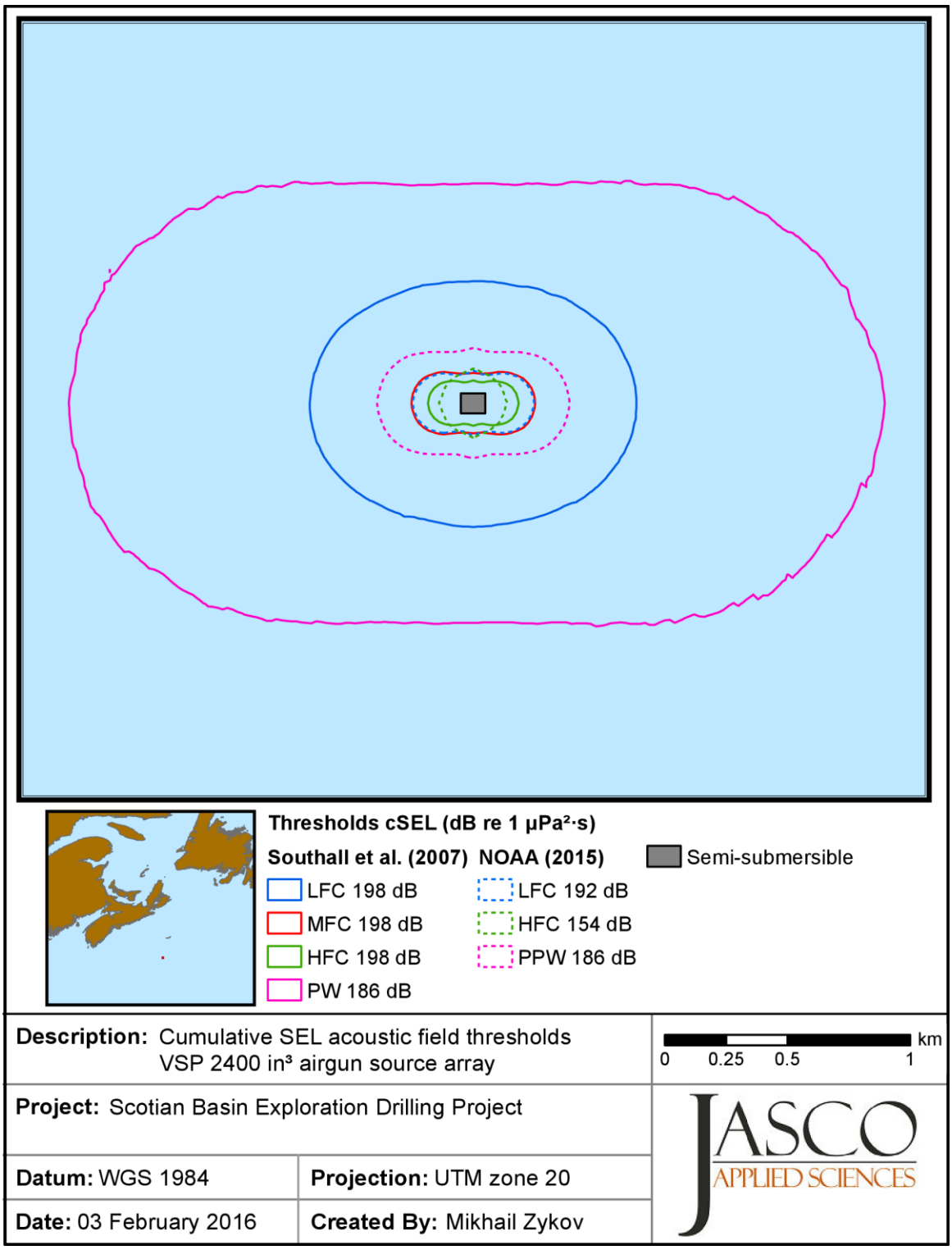

Figure 39. VSP airgun source array: Maximum-over-depth 24 hour cumulative SEL threshold contours at Site A in winter for the Southall et al. (2007) and NOAA (2015) criteria. Marine mammal hearing groups: LFC–low-frequency cetaceous, MFC–mid-frequency cetaceous, HFC–high-frequency cetaceous, PW–pinnipeds in water (Southall), PPW–phocid pinnipeds in water (NOAA), and OPW–otariid pinnipeds in water (NOAA). The thresholds contours for MFC (NOAA) and OPW (NOAA) are smaller than 20 m and not shown on the map.

4.2.2.2. Vessels

The cumulative sound field from vessels was calculated based on an assumption that all the thrusters of the vessels are performing at nominal output power continuously 24 hours a day (86400 seconds). According to Equation 5, $cSEL_{24hr}$ is estimated by adding 49.4 dB to the modelled per-second SEL.

The ranges to specific thresholds based on un-weighted fields for Site A and B (both seasons) are provided in Table 20 and Table 21, respectively. The maximum-over-depth un-weighted 24 hour cumulative SELs for vessel scenarios are displayed as contour maps in Figure 40 (drillship), Figure 41 (drillship with support vessel), Figure 42 (semi-submersible platform), and Figure 43 (semi-submersible platform with support vessel). The contour maps of un-weighted cumulative SEL are plotted based on acoustic field grids with grid cell size of 100 m.

The ranges to the criteria thresholds based on the weighted 24 hour cumulative SEL field for both sites and both seasons are provided in Table 22 (drillship), Table 23 (drillship with support vessel), Table 24 (semi-submersible platform), and Table 25 (semi-submersible platform with support vessel). All the ranges are relative to the geometric centre of the largest vessel in the group.

Maps of criteria threshold contours for all four vessel scenarios at Site A in winter are presented in Figure 44. At the ranges at which the threshold contours occur, the water depth and the sound speed profile have no effect on the acoustic field; therefore, the position of the criteria contours at Site B and in summer are virtually identical to those in Figure 44. The threshold contour maps are plotted based on acoustic field grids with grid cell size of 20 m.

Table 20. Vessels at Site A: Maximum (R_{max}, km) and 95% ($R_{95\%}$, km) horizontal distances to modelled maximum-over-depth cumulative SEL thresholds, un-weighted field.

cSEL (dB re 1 µPa²·s)	**Drillship**				**Drillship w/ support vessel**				**Semi-submersible**				**Semi-submersible w/ support vessel**			
	Winter		Summer		Winter		Summer		Winter		Summer		Winter		Summer	
	R_{max}	$R_{95\%}$	R_{max}	$R_{95\%}$	R_{max}	$R_{95\%}$	R_{max}	$R_{95\%}$	R_{max}	$R_{95\%}$	R_{max}	$R_{95\%}$	R_{max}	$R_{95\%}$	R_{max}	$R_{95\%}$
210	0.16	0.16	0.16	0.16	0.16	0.16	0.16	0.16	0.1	0.1	0.1	0.1	0.11	0.11	0.11	0.11
200	0.35	0.32	0.35	0.32	0.36	0.34	0.36	0.34	0.3	0.29	0.3	0.3	0.32	0.32	0.32	0.32
190	0.96	0.9	1.01	0.94	1.01	0.96	1.06	1.01	0.97	0.96	1.02	1	2.01	1.98	1.08	1.05
180	14.7	11.4	3.24	3.11	14.9	12.6	3.48	3.36	17.4	14.7	3.37	3.26	19.1	16.9	3.65	3.53
170	144	117	51.2	20.9	>150	>150	51.3	25.9	>150	>150	64.2	21.4	>150	>150	64.2	24.8
160	>150	>150	>150	>150			>150	>150			>150	>150			>150	>150

Table 21. Vessels at Site B: Maximum (R_{max}, km) and 95% ($R_{95\%}$, km) horizontal distances to modelled maximum-over-depth cumulative SEL thresholds, un-weighted field.

cSEL (dB re 1 µPa²·s)	Drillship				Drillship w/ support vessel				Semi-submersible				Semi-submersible w/ support vessel			
	Winter		Summer		Winter		Summer		Winter		Summer		Winter		Summer	
	R_{max}	$R_{95\%}$	R_{max}	$R_{95\%}$	R_{max}	$R_{95\%}$	R_{max}	$R_{95\%}$	R_{max}	$R_{95\%}$	R_{max}	$R_{95\%}$	R_{max}	$R_{95\%}$	R_{max}	$R_{95\%}$
210	0.16	0.16	0.16	0.16	0.16	0.16	0.16	0.16	0.1	0.1	0.1	0.1	0.11	0.11	0.11	0.11
200	0.35	0.32	0.35	0.32	0.36	0.34	0.36	0.34	0.3	0.29	0.3	0.3	0.32	0.32	0.32	0.32
190	0.96	0.9	1.01	0.95	1.02	0.96	1.07	1.01	0.98	0.96	1.02	1	2.02	1.98	1.08	1.06
180	14.8	12.4	6.29	4.81	16.8	14.3	6.43	5.9	19.2	15.5	5.43	4.55	21.4	17.4	6.41	5.41
170	140	117	33.2	24.1	144	127	51.1	25.6	>150	>150	60.8	25.2	>150	>150	60.9	26.5
160	>150	>150	>150	>150	>150	>150	>150	>150			>150	>150			>150	>150

Table 22. Drillship: Maximum (R_{max}, km) and 95% ($R_{95\%}$, km) horizontal distances to PTS onset acoustic threshold levels and affected area (A, km²) for 24 hour cumulative SEL (dB re 1 µPa²·s). Distances are calculated from the geometric centre of the Drillship.

Marine mammal group	Threshold (dB)	Site A						Site B					
		Winter			Summer			Winter			Summer		
		R_{max}	$R_{95\%}$	A	R_{max}	$R_{95\%}$	A	R_{max}	$R_{95\%}$	A	R_{max}	$R_{95\%}$	A
Southall et al. *(2007)*													
Low-frequency cetaceans	215	0.14	0.14	0.01	0.14	0.14	0.01	0.14	0.14	0.01	0.14	0.14	0.01
Mid-frequency cetaceans	215	0.12	0.12	<0.01	0.12	0.12	<0.01	0.12	0.12	<0.01	0.12	0.12	<0.01
High-frequency cetaceans	215	0.12	0.12	<0.01	0.12	0.12	<0.01	0.12	0.12	<0.01	0.12	0.12	<0.01
Pinnipeds	203	0.22	0.21	0.08	0.22	0.2	0.08	0.22	0.21	0.08	0.22	0.2	0.08
NOAA (2015)													
Low-frequency cetaceans	207	0.14	0.12	0.01	0.14	0.12	0.01	0.14	0.12	0.01	0.14	0.12	0.01
Mid-frequency cetaceans	199	0.12	0.12	<0.01	0.12	0.12	<0.01	0.12	0.12	<0.01	0.12	0.12	<0.01
High-frequency cetaceans	171	0.48	0.44	0.58	0.47	0.42	0.54	0.48	0.44	0.58	0.47	0.42	0.54
Phocid pinnipeds	201	0.16	0.15	0.02	0.16	0.15	0.02	0.16	0.15	0.02	0.16	0.15	0.02
Otariid pinnipeds	218	0.12	0.12	<0.01	0.12	0.12	<0.01	0.12	0.12	<0.01	0.12	0.12	<0.01

Table 23. Drillship with support vessel: Maximum (R_{max}, km) and 95% ($R_{95\%}$, km) horizontal distances to PTS onset acoustic threshold levels and affected area (A, km²) for 24 hour cumulative SEL (dB re 1 µPa²·s). Distances are calculated from the geometric centre of the drillship.

Marine mammal group	Threshold (dB)	Site A						Site B					
		Winter			Summer			Winter			Summer		
		R_{max}	$R_{95\%}$	A	R_{max}	$R_{95\%}$	A	R_{max}	$R_{95\%}$	A	R_{max}	$R_{95\%}$	A
Southall et al. *(2007)*													
Low-frequency cetaceans	215	0.14	0.14	0.02	0.14	0.14	0.01	0.14	0.14	0.02	0.14	0.14	0.01
Mid-frequency cetaceans	215	0.12	0.12	0.01	0.12	0.12	0.01	0.12	0.12	0.01	0.12	0.12	0.01
High-frequency cetaceans	215	0.12	0.12	0.01	0.12	0.12	0.01	0.12	0.12	0.01	0.12	0.12	0.01
Pinnipeds	203	0.23	0.21	0.1	0.22	0.2	0.09	0.23	0.21	0.1	0.22	0.2	0.09
NOAA (2015)													
Low-frequency cetaceans	207	0.14	0.12	0.01	0.14	0.12	0.01	0.14	0.12	0.01	0.14	0.12	0.01
Mid-frequency cetaceans	199	0.12	0.12	0.01	0.12	0.12	0.01	0.12	0.12	0.01	0.12	0.12	0.01
High-frequency cetaceans	171	0.52	0.47	0.69	0.49	0.45	0.63	0.52	0.47	0.69	0.49	0.45	0.63
Phocid pinnipeds	201	0.16	0.15	0.03	0.16	0.14	0.03	0.16	0.15	0.03	0.16	0.14	0.03
Otariid pinnipeds	218	0.12	0.12	<0.01	0.12	0.12	<0.01	0.12	0.12	<0.01	0.12	0.12	<0.01

Table 24. Semi-submersible platform: Maximum (R_{max}, km) and 95% ($R_{95\%}$, km) horizontal distances from the source to PTS onset acoustic threshold levels and affected area (A, km²) for 24 hour cumulative SEL (dB re 1 µPa²·s). Distances are calculated from the geometric centre of the semi-submersible platform.

Marine mammal group	Threshold (dB)	Site A						Site B					
		Winter			Summer			Winter			Summer		
		R_{max}	$R_{95\%}$	A	R_{max}	$R_{95\%}$	A	R_{max}	$R_{95\%}$	A	R_{max}	$R_{95\%}$	A
Southall et al. *(2007)*													
Low-frequency cetaceans	215	0.07	0.07	0.01	0.07	0.07	0.01	0.07	0.07	0.01	0.07	0.07	0.01
Mid-frequency cetaceans	215	0.06	0.06	<0.01	0.06	0.06	<0.01	0.06	0.06	<0.01	0.06	0.06	<0.01
High-frequency cetaceans	215	0.06	0.06	<0.01	0.06	0.06	<0.01	0.06	0.06	<0.01	0.06	0.06	<0.01
Pinnipeds	203	0.16	0.16	0.08	0.15	0.15	0.07	0.16	0.16	0.08	0.15	0.15	0.07
NOAA (2015)													
Low-frequency cetaceans	207	0.06	0.06	0.01	0.06	0.06	0.01	0.06	0.06	0.01	0.06	0.06	0.01
Mid-frequency cetaceans	199	0.06	0.06	<0.01	0.06	0.06	<0.01	0.06	0.06	<0.01	0.06	0.06	<0.01
High-frequency cetaceans	171	0.42	0.41	0.56	0.42	0.4	0.54	0.42	0.41	0.56	0.42	0.4	0.54
Phocid pinnipeds	201	0.09	0.09	0.02	0.09	0.09	0.02	0.09	0.09	0.02	0.09	0.09	0.02
Otariid pinnipeds	218	0.06	0.06	<0.01	0.06	0.06	<0.01	0.06	0.06	<0.01	0.06	0.06	<0.01

Table 25. Semi-submersible platform with support vessel: Maximum (R_{max}, km) and 95% ($R_{95\%}$, km) horizontal distances from the source to PTS onset acoustic threshold levels and affected area (A, km²) for 24 hour cumulative SEL (dB re 1 µPa²·s). Distances are calculated from the geometric centre of the semi-submersible platform.

Marine mammal group	Threshold (dB)	Site A						Site B					
		Winter			Summer			Winter			Summer		
		R_{max}	$R_{95\%}$	A	R_{max}	$R_{95\%}$	A	R_{max}	$R_{95\%}$	A	R_{max}	$R_{95\%}$	A
Southall et al. *(2007)*													
Low-frequency cetaceans	215	0.09	0.07	0.02	0.09	0.07	0.02	0.09	0.07	0.02	0.09	0.07	0.02
Mid-frequency cetaceans	215	0.07	0.07	0.01	0.07	0.07	0.01	0.07	0.07	0.01	0.07	0.07	0.01
High-frequency cetaceans	215	0.07	0.07	0.01	0.07	0.07	0.01	0.07	0.07	0.01	0.07	0.07	0.01
Pinnipeds	203	0.17	0.17	0.09	0.17	0.16	0.09	0.17	0.17	0.09	0.17	0.16	0.09
NOAA (2015)													
Low-frequency cetaceans	207	0.09	0.07	0.01	0.09	0.07	0.01	0.09	0.07	0.01	0.09	0.07	0.01
Mid-frequency cetaceans	199	0.07	0.07	0.01	0.07	0.07	0.01	0.07	0.07	0.01	0.07	0.07	0.01
High-frequency cetaceans	171	0.47	0.46	0.68	0.46	0.44	0.65	0.47	0.46	0.68	0.46	0.44	0.65
Phocid pinnipeds	201	0.1	0.1	0.03	0.1	0.1	0.03	0.1	0.1	0.03	0.1	0.1	0.03
Otariid pinnipeds	218	0.07	0.07	<0.01	0.07	0.07	<0.01	0.07	0.07	<0.01	0.07	0.07	<0.01

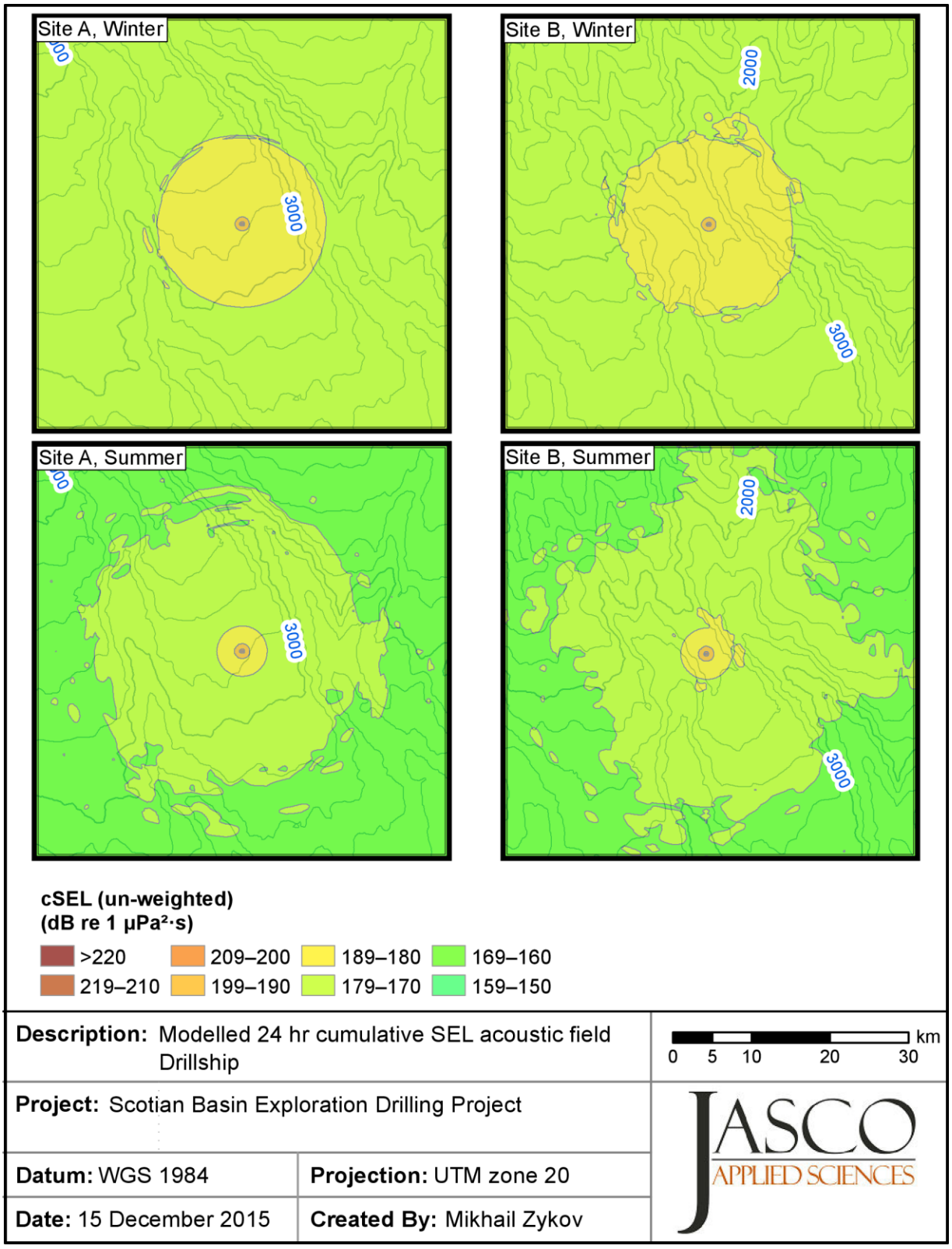

Figure 40. Drillship: Maximum-over-depth 24 hour cumulative SEL for at Sites A and B in winter and summer for the un-weighted field.

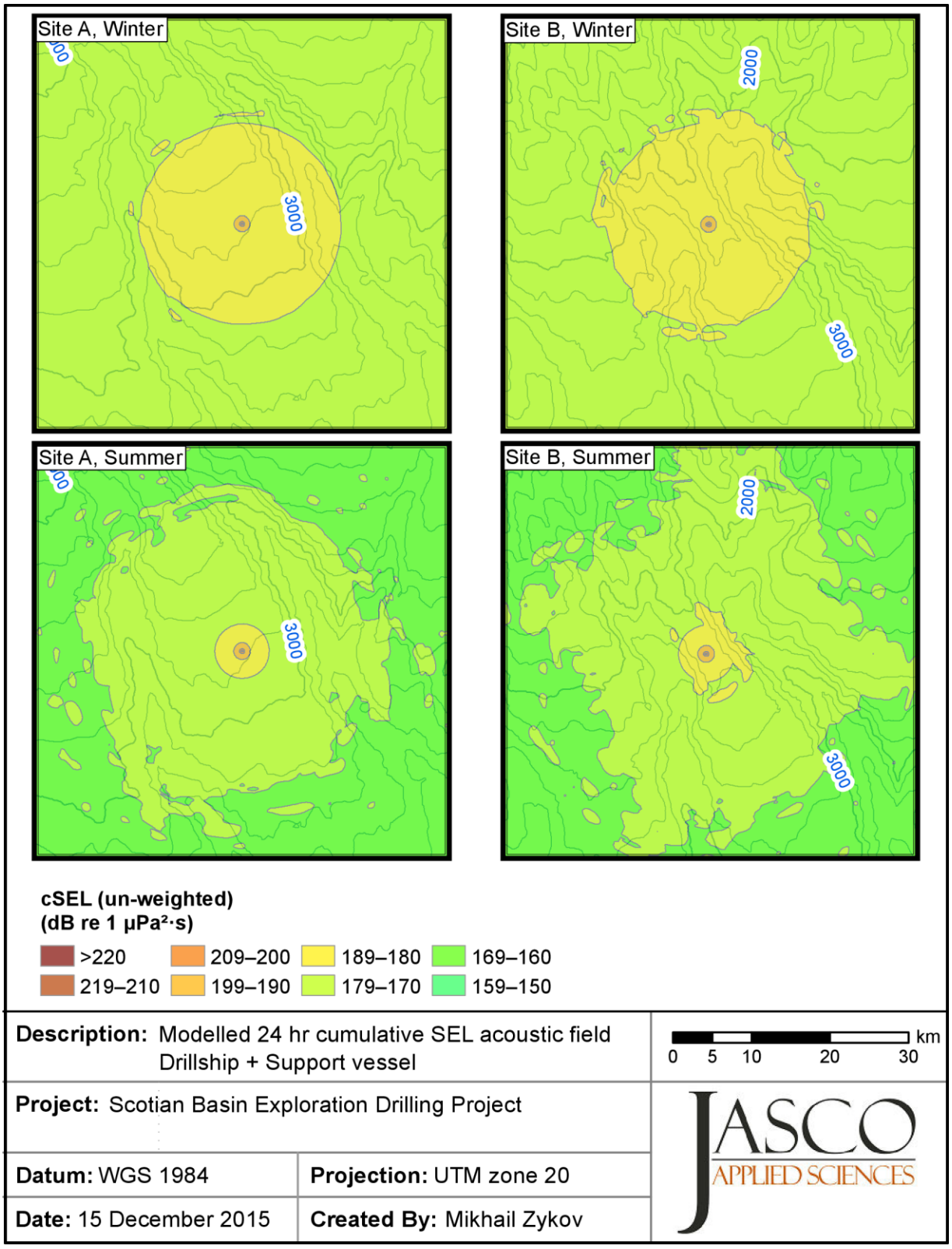

Figure 41. Drillship with support vessel: Maximum-over-depth 24 hour cumulative SEL for at Sites A and B in winter and summer for un-weighted field.

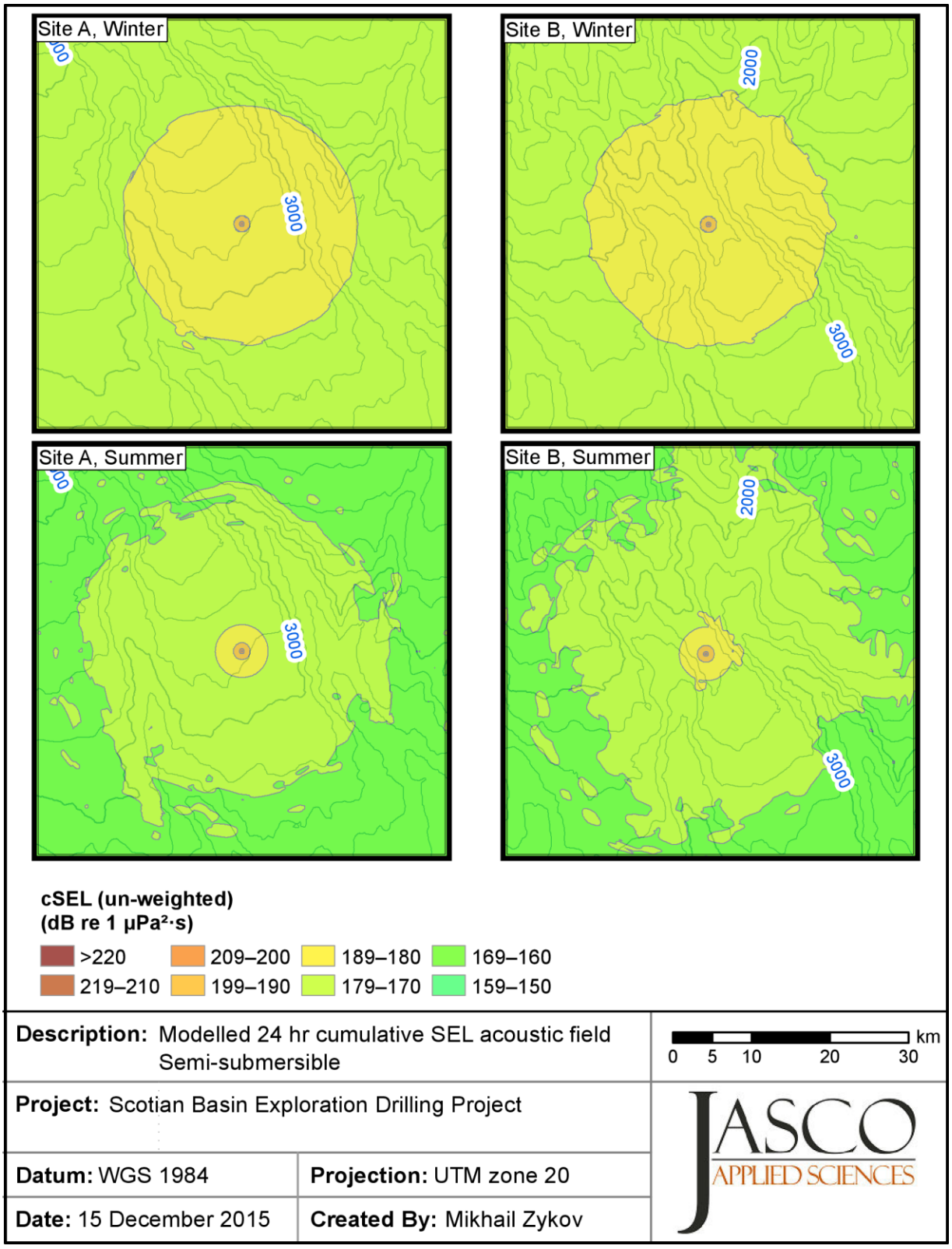

Figure 42. Semi-submersible platform: Maximum-over-depth 24 hour cumulative SEL for at Sites A and B in winter and summer for un-weighted field.

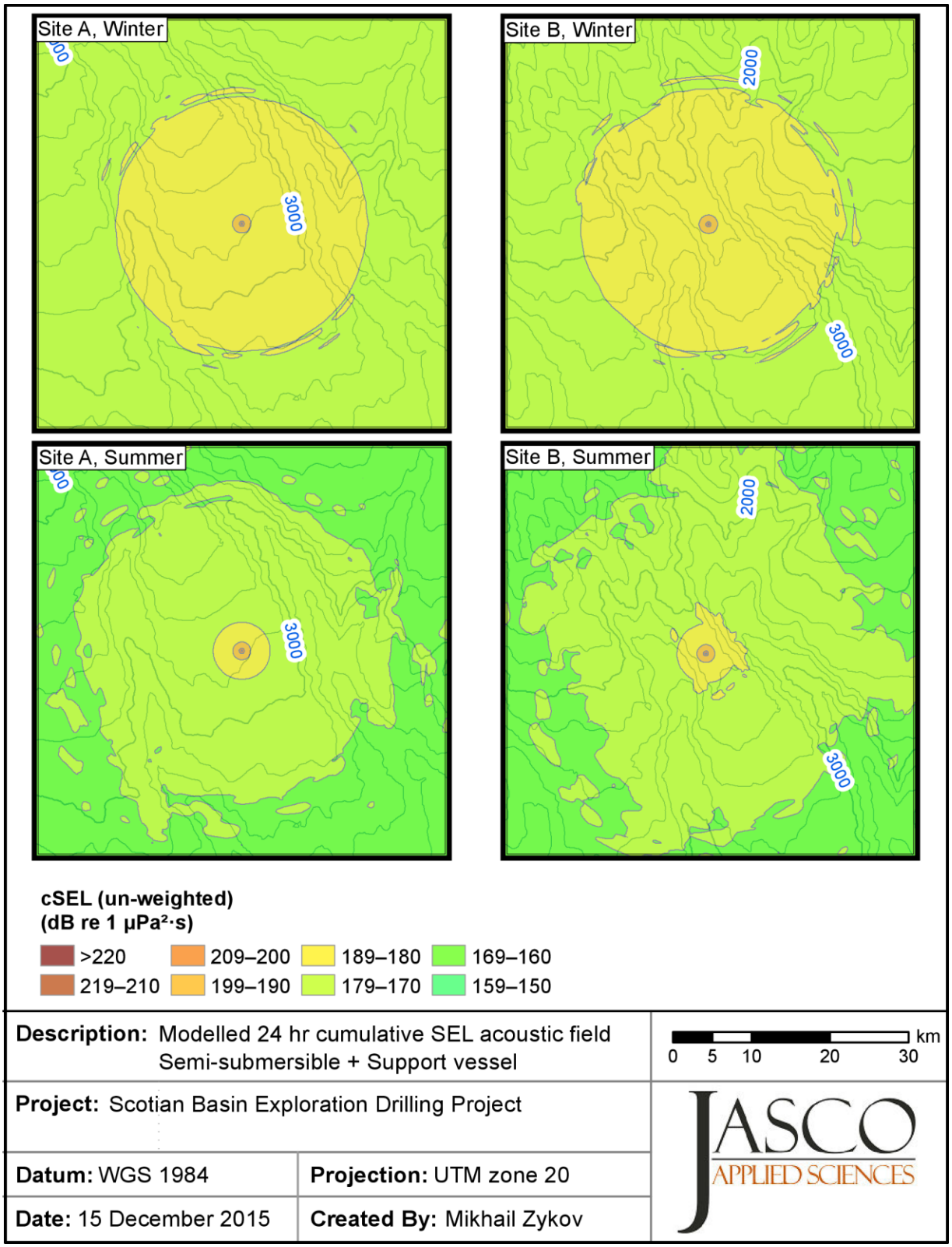

Figure 43. Semi-submersible platform with support vessel: Maximum-over-depth 24 hour cumulative SEL for at Sites A and B in winter and summer for the un-weighted field.

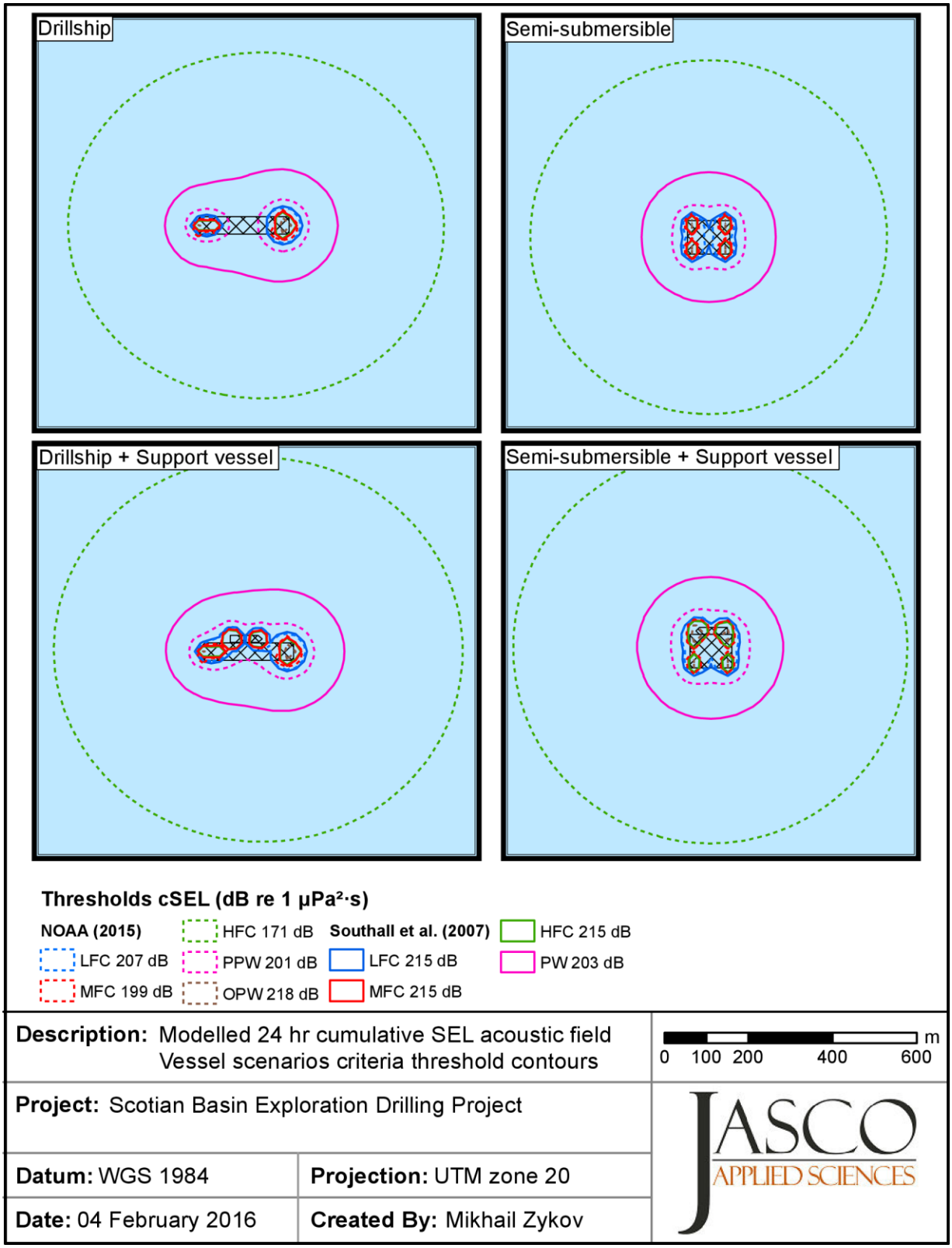

Figure 44. Vessel scenarios: cSEL threshold contours at Site A in winter for Southall et al. (2007) and NOAA (2015) criteria. Marine mammal hearing groups: LFC–low-frequency cetaceous, MFC–mid-frequency cetaceous, HFC–high-frequency cetaceous, PW–pinnipeds in water (Southall), PPW–phocid pinnipeds in water (NOAA), and OPW–otariid pinnipeds in water (NOAA).

4.2.3. Peak SPL

The zero-to-peak SPL metric was estimated based on an un-weighted acoustic field (i.e., without application of any of the M-weighting filters discussed in Sections 1.3.2.1 and 1.3.3.1).

4.2.3.1. VSP Airgun Source Array

The zero-to-peak SPL field for the VSP airgun source array was estimated based on the results of the full waveform modelling (Section 2.2.3). The modelling was performed to the maximum distance of 20 km from the source. The calculations were done according to Equation 1, using modelled pressure time series. The ranges to thresholds for both sites and both seasons are provided in Table 26. Maximum-over-depth zero-to-peak SPLs are displayed as contour maps in Figure 45.

Table 26. VSP airgun source array: Maximum (R_{max}, km) and 95% ($R_{95\%}$, km) horizontal distances from the modelled maximum-over-depth 0-to-peak SPL thresholds. Rows in bold are for the criteria threshold: 230 dB–all marine mammal hearing groups for both Southall et al. (2007) and NOAA (2015) except pinnipeds in water (Southall) and high-frequency cetaceous (NOAA) groups; 218 dB–pinnipeds in water (Southall); 202 dB–high-frequency cetaceous (NOAA).

0-Pk SPL (dB re 1 µPa)	**Site A**				**Site B**			
	Winter		Summer		Winter		Summer	
	R_{max}	$R_{95\%}$	R_{max}	$R_{95\%}$	R_{max}	$R_{95\%}$	R_{max}	$R_{95\%}$
230	**<0.02**	**<0.02**	**<0.02**	**<0.02**	**<0.02**	**<0.02**	**<0.02**	**<0.02**
220	0.04	0.04	0.04	0.04	0.04	0.04	0.04	0.04
218	**0.04**	**0.04**	**0.04**	**0.04**	**0.04**	**0.04**	**0.04**	**0.04**
210	0.07	0.07	0.07	0.07	0.07	0.07	0.07	0.07
202	**0.15**	**0.14**	**0.15**	**0.14**	**0.15**	**0.14**	**0.15**	**0.14**
200	0.18	0.18	0.18	0.17	0.18	0.18	0.18	0.17
190	0.58	0.54	0.6	0.55	0.58	0.54	0.6	0.55
180	1.88	1.73	1.92	1.76	1.88	1.72	1.9	1.75
170	7.11	6.03	7.08	6	9.42	6.83	9.38	6.69
160	>20	>20	>20	>20	>20	>20	>20	>20

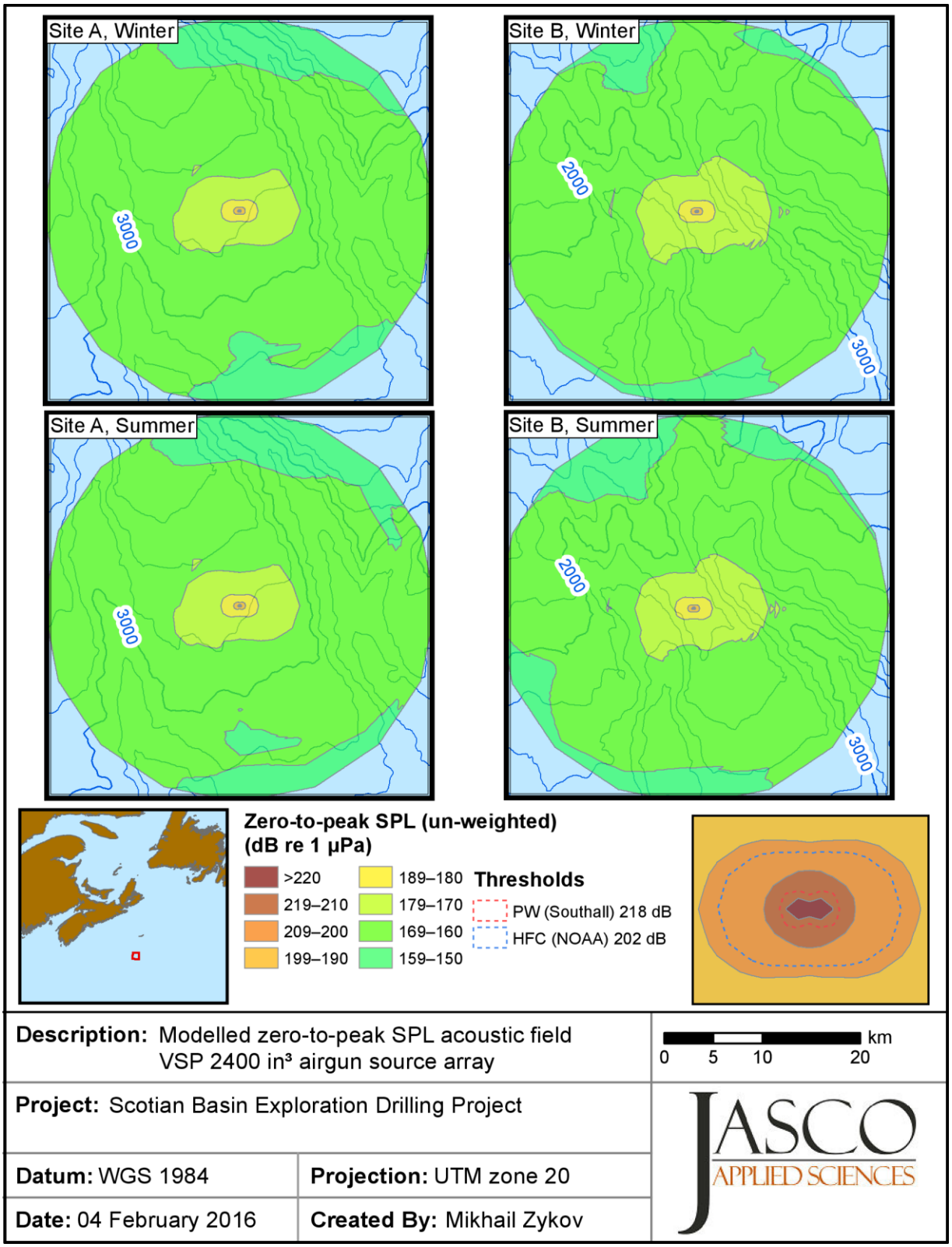

Figure 45. VSP airgun source array: Maximum-over-depth zero-to-peak SPLs for Sites A and B in winter and summer. Marine mammal hearing groups: HFC–high-frequency cetaceous, PW–pinnipeds in water (Southall et al. 2007). The 230 dB threshold contour is less than 20 m from the source and is not shown. Source depth is 5 m; orientation azimuth is 0.

4.2.3.2. Vessels

The zero-to-peak SPL field for vessels can be estimated based on the rms SPL field in conjunction with Equation 21. According to that equation, the zero-to-peak values for a continuous source are approximately 12 dB more than the rms SPL.

The ranges to the criteria thresholds for the zero-to-peak metric of the acoustic signal can be estimated using the source levels of the thrusters. Even if considered as a point source, the rms SPL source level for both the drillship and semi-submersible platform is 196.7 dB re 1 µPa at 1 m rms SPL and, consequently, 208.7 dB re 1 µPa at 1 m zero-to-peak SPL. The lowest threshold for the zero-to-peak SPL metric is 202 dB re 1 µPa. The most conservative cylindrical spreading law predicts a 10 dB decrease in the sound levels at 10 m from the source; therefore, the lowest criteria threshold of 202 dB would occur closer than 10 m from the source.

5. Discussion

5.1. Factors Influencing Sound Propagation

Generally, several factors affect sound propagation in a marine environment:

- Water depth at the sound source,
- Structure of the sound speed profile (e.g., presence or absence of sound channel),
- Vertical position of the source

Considering the graphs of received level variation with distance from the for the modelled vessel scenarios at two sites and two seasons (see Figure 29), the area around the acoustic sources can be divided into two zones based on the range from the source:

- Near zone (< 1 km)
- Far zone (**>** 1 km).

In the near zone, the water depth at the source had little influence on the sound field, since the range of the zone was at least two times smaller than the shallowest site. The sound speed profile also had little influence on the sound propagation at close ranges. As a result, the ranges to specific thresholds (see Table 14 and Table 15) that fall within 1 km from the source had virtually no variation if the site or season changed.

In the far zone, where the ranges were greater than the water depth, the water depth of the source had a greater influence.

Shallower Site B had longer ranges to the same threshold levels compared to Site A. The variation was ~ 10%. However, the greatest variation in ranges to the threshold levels was for the seasonal change of the sound speed profile. The strong surface duct in winter trapped acoustic energy, where it propagated without any bottom interaction, hence minimizing the transmission loss. Conversely, the sound speed profile in the summer was downwardly refracting, which maximized the acoustic wave interaction with the bottom and the acoustic energy loss due to this interaction. The ranges to the same threshold levels could be as much as 300% greater in winter than in summer.

In addition, the influence of the vertical position of the source can be noted when comparing the threshold ranges for the drillship (12 m water depth) and the semi-submersible platform (18 m water depth). Despite both vessels having the same total broadband source level (196.7 dB rms SPL), the range to 130 dB rms SPL threshold was greater for the semi-submersible platform. In winter, the range was about 30% greater, and about 10% in summer. This shows that the variation of the acoustic field with the source depth occurs due to specific features of the sound speed profile.

5.2. Conservativeness of the Exposure Estimations

The usual approach for representing an estimate for a physical parameter is to provide an average value with confidence interval. The actual value has 50% chance of being larger than the average value and 50% chance of being lower (in case of normal distribution). The conservative approach provides such value that the probability of the actual value being larger than that is low (5% or less).

The acoustic propagation modelling combines large variety of inputs (e.g., source levels, propagation environment properties) as well as data processing techniques. Each input bears its own level of uncertainty (the confidence interval), which contributes to the uncertainty of the output value. Due to complexity and non-linearity of the acoustic propagation problem, large variety of input data, it is often too difficult to define the confidence interval for the end result.

The acoustic modelling study for this project was conducted exercising a ‘conservative approach’, i.e., when necessary the choices were made to produce an overestimate relative to an average, or expected, value. This approach ensures that the probability of providing an underestimated end result is lower than the individual probabilities of underestimation related to each specific input parameter.

One of such conservative choice is the estimates for the source levels of the vessels. The source level for the thrusters in this study were estimated for the power output close to the nominal value (the maximum sustainable). It is highly unlikely, that the all the thrusters of all vessels will be operated at such conditions for a prolonged time.

Another factor that contributed to the conservativeness of the exposure estimates in this study, is the time period considered for the cumulative SEL assessment. NOAA (2015) suggests an accumulation period of 1 h if animal movement is not considered (such as in this study). The ranges to the specific thresholds in this report were estimated based on accumulation period of 24 h. The reduction of accumulation period from 24 h to 1 h would provide reduction in the cumulative SEL of 13.8 dB for both vessel scenarios and airgun source array.

Glossary

1/3-octave-band
Non-overlapping passbands that are one-third of an octave wide (where an octave is a doubling of frequency). Three adjacent 1/3-octave-bands make up one octave. One-third-octave-bands become wider with increasing frequency. See also octave.

90%-energy time window
The time interval over which the cumulative energy rises from 5% to 95% of the total pulse energy. This interval contains 90% of the total pulse energy. Symbol: T_{90}.

90% root-mean-square sound pressure level (90% rms SPL)
The root-mean-square sound pressure levels calculated over the 90%-energy time window of a pulse. Used only for pulsed sounds.

attenuation
The gradual loss of acoustic energy from absorption and scattering as sound propagates through a medium.

auditory weighting function (frequency-weighting function)
Auditory weighting functions account for marine mammal hearing sensitivity. They are applied to sound measurements to emphasize frequencies that an animal hears well and de-emphasize frequencies they hear less well or not at all (Southall et al. 2007, Finneran and Jenkins 2012, NOAA and US Dept of Commerce 2013).

azimuth
A horizontal angle relative to a reference direction, which is often magnetic north or the direction of travel. In navigation it is also called bearing.

bar
Unit of pressure equal to 100 kPa, which is approximately equal to the atmospheric pressure on Earth at sea level. 1 bar is equal to 10^{6} Pa or 10^{11} µPa.

broadband sound level
The total sound pressure level measured over a specified frequency range. If the frequency range is unspecified, it refers to the entire measured frequency range.

cavitation
A rapid formation and collapse of vapor cavities (i.e., bubbles or voids) in water, most often caused by a rapid change in pressure. Fast-spinning vessel propellers typically cause cavitation, which creates a lot of noise.

cetacean
Any animal in the order Cetacea. These are aquatic, mostly marine mammals and include whales, dolphins, and porpoises.

compressional wave
A mechanical vibration wave in which the direction of particle motion is parallel to the direction of propagation. Also called primary wave or P-wave.

continuous sound
A sound whose sound pressure level remains above ambient sound during the observation period (ANSI/ASA S1.13-2005 R2010). A sound that gradually varies in intensity with time, for example, sound from a marine vessel.

decibel (dB)
One-tenth of a bel. Unit of level when the base of the logarithm is the tenth root of ten, and the quantities concerned are proportional to power (ANSI S1.1-1994 R2004).

endfire direction
Parallel to the travel direction of a source. See also broadside direction.

ensonified
Exposed to sound.

far-field
The zone where, to an observer, sound originating from an array of sources (or a spatially-distributed source) appears t

fast Fourier transform (FFT)
A computationally efficiently algorithm for computing the discrete Fourier transform.

frequency
The rate of oscillation of a periodic function measured in cycles-per-unit-time. The reciprocal of the period. Unit: hertz (Hz). Symbol: *f*. 1 Hz is equal to 1 cycle per second.

functional hearing group
Grouping of marine mammal species with similar estimated hearing ranges. Southall et al. (2007) proposed the following functional hearing groups: low-, mid-, and high-frequency cetaceans, pinnipeds in water, and pinnipeds in air.

geoacoustic
Relating to the acoustic properties of the seabed.

hearing threshold
The sound pressure level that is barely audible for a given individual in the absence of significant background noise during a specific percentage of experimental trials.

hertz (Hz)
A unit of frequency defined as one cycle per second.

high-frequency cetacean
The functional hearing group that represents odontocetes specialized for using high-frequencies.

impulsive sound
Sound that is typically brief and intermittent with rapid (within a few seconds) rise time and decay back to ambient levels (NOAA and US Dept of Commerce 2013, ANSI S12.7-1986 R2006). For example, seismic airguns and impact pile driving.

low-frequency cetacean
The functional hearing group that represents mysticetes (baleen whales).

mid-frequency cetacean
The functional hearing group that represents some odontocetes (dolphins, toothed whales, beaked whales, and bottlenose whales).

M-weighting
The process of band-pass filtering loud sounds to reduce the importance of inaudible or less-audible frequencies for broad classes of marine mammals. “Generalized frequency weightings for various

functional hearing groups of marine mammals, allowing for their functional bandwidths and appropriate in characterizing auditory effects of strong sounds" (Southall et al. 2007).

non-impulsive sound
Sound that is broadband, narrowband or tonal, brief or prolonged, continuous or intermittent, and typically does not have a high peak pressure with rapid rise time (typically only small fluctuations in decibel level) that impulsive signals have (ANSI/ASA S3.20-1995 R2008). For example, marine vessels, aircraft, machinery, construction, and vibratory pile driving.

otariid
A common term used to describe members of the Otariidae, eared seals, commonly called sea lions and fur seals. Otariids are adapted to a semi-aquatic life; they use their large fore flippers for propulsion. Their ears distinguish them from phocids. Otariids are one of the three main groups in the superfamily Pinnipedia; the other two groups are phocids and walrus.

parabolic equation method
A computationally-efficient solution to the acoustic wave equation that is used to model transmission loss. The parabolic equation approximation omits effects of back-scattered sound, simplifying the computation of transmission loss. The effect of back-scattered sound is negligible for most ocean-acoustic propagation problems.

peak sound pressure level (peak SPL)
The maximum instantaneous sound pressure level, in a stated frequency band, within a stated period. Also called zero-to-peak sound pressure level. Unit: decibel (dB).

permanent threshold shift (PTS)
A permanent loss of hearing sensitivity caused by excessive noise exposure. PTS is considered auditory injury.

phocid
A common term used to describe all members of the family Phocidae. These true/earless seals are more adapted to in-water life than are otariids, which have more terrestrial adaptations. Phocids use their hind flippers to propel themselves. Phocids are one of the three main groups in the superfamily Pinnipedia; the other two groups are otariids and walrus.

pinniped
A common term used to describe all three groups that form the superfamily Pinnipedia: phocids (true seals or earless seals), otariids (eared seals or fur seals and sea lions), and walrus.

point source
A source that radiates sound as if from a single point (ANSI S1.1-1994 R2004).

power spectrum density
The acoustic signal power per unit frequency as measured at a single frequency. Unit: $\mu Pa^2/Hz$, or $\mu Pa^2 \cdot s$.

power spectral density level
The decibel level ($10\log_{10}$) of the power spectrum density, usually presented in 1 Hz bins. Unit: dB re 1 $\mu Pa^2/Hz$.

pressure, acoustic
The deviation from the ambient hydrostatic pressure caused by a sound wave. Also called overpressure. Unit: pascal (Pa). Symbol: *p*.

received level (RL)
The sound level measured at a receiver.

rms
root-mean-square.

rms sound pressure level (rms SPL)
The root-mean-square average of the instantaneous sound pressure as measured over some specified time interval. For continuous sound, the time interval is one second. See also sound pressure level (SPL) and 90% rms SPL.

signature
Pressure signal generated by a source.

sound
A time-varying pressure disturbance generated by mechanical vibration waves travelling through a fluid medium such as air or water.

sound exposure
Time integral of squared, instantaneous frequency-weighted sound pressure over a stated time interval or event. Unit: pascal-squared second ($Pa^2 \cdot s$) (ANSI S1.1-1994 R2004).

sound exposure level (SEL)
A measure related to the sound energy in one or more pulses. Unit: dB re 1 $\mu Pa^2 \cdot s$.

sound field
Region containing sound waves (ANSI S1.1-1994 R2004).

sound pressure level (SPL)
The decibel ratio of the time-mean-square sound pressure, in a stated frequency band, to the square of the reference sound pressure (ANSI S1.1-1994 R2004).

For sound in water, the reference sound pressure is one micropascal (p_0 = 1 µPa) and the unit for SPL is dB re 1 µPa:

$$\text{SPL} = 10\log_{10}\left(p^2/p_0^2\right) = 20\log_{10}\left(p/p_0\right)$$

Unless otherwise stated, SPL refers to the root-mean-square sound pressure level (rms SPL).

sound speed profile
The speed of sound in the water column as a function of depth below the water surface.

source level (SL)
The sound pressure level measured 1 metre from a theoretical point source that radiates the same total sound power as the actual source. Unit: dB re 1 µPa @ 1 m.

spectrum
An acoustic signal represented in terms of its power (or energy) distribution versus frequency.

surface duct
The upper portion of a water column within which the sound speed profile gradient causes sound to refract upward and therefore reflect off the surface resulting in relatively long range sound propagation with little loss.

temporary threshold shift (TTS)
Temporary loss of hearing sensitivity caused by excessive noise exposure.

transmission loss (TL)
The decibel reduction in sound level between two stated points that results from sound spreading away from an acoustic source subject to the influence of the surrounding environment. Also called propagation loss.

Literature Cited

[MMC] Marine Mammal Commission. 2007. M*arine mammals and noise: A sound approach to research and management. A Report to Congress from the Marine Mammal Commission*. http://www.mmc.gov/reports/workshop/pdf/fullsoundreport.pdf.

[NMFS] National Marine Fisheries Service. 20*14. Marine Mammals: Interim Sound Threshold Guidance (webpage).* National Marine Fisheries Service, National Oceanic and Atmospheric Administration, U.S. Department of Commerce. http://www.westcoast.fisheries.noaa.gov/protected_species/marine_mammals/threshold_guidance.html.

[NMFS] National Marine Fisheries Service. 2016. *Marine Mammals: Interim Sound Threshold Guidance* (webpage). National Marine Fisheries Service, National Oceanic and Atmospheric Administration, U.S. Department of Commerce. http://www.westcoast.fisheries.noaa.gov/protected_species/marine_mammals/threshold_guidance.html.

[NOAA] National Oceanic and Atmospheric Administration and U.S. Department of Commerce. 2013. *Draft Guidance for Assessing the Effects of Anthropogenic Sound on Marine Mammals: Acoustic Threshold Levels for Onset of Permanent and Temporary Threshold Shifts*. In: National Oceanic and Atmospheric Administration and U.S. Department of Commerce. 76 pp. http://www.nmfs.noaa.gov/pr/acoustics/draft_acoustic_guidance_2013.pdf.

[NOAA] National Oceanic and Atmospheric Administration. 2013. *Effects of Oil and Gas Activities in the Arctic Ocean: Supplemental Draft Environmental Impact Statement*. Prepared by United States Department of Commerce, National Oceanic and Atmospheric Administration, National Marine Fisheries Service, Office of Protected Resources. 60 pp.

[NOAA] National Oceanic and Atmospheric Administration. 2015. *Draft Guidance for Assessing the Effects of Anthropogenic Sound on Marine Mammal Hearing: Underwater Acoustic Threshold Levels for Onset of Permanent and Temporary Threshold Shifts*. In: National Oceanic and Atmospheric Administration and U.S. Department of Commerce. Revised version for Second Public Comment Period. 180 pp. http://www.nmfs.noaa.gov/pr/acoustics/draft%20acoustic%20guidance%20July%202015.pdf.

Aerts, L., M. Blees, S. Blackwell, C. Greene, K. Kim, D. Hannay, and M. Austin. 2008. M*arine mammal monitoring and mitigation during BP Liberty OBC seismic survey in Foggy Island Bay, Beaufort Sea, July-August 2008: 90-day report.* Document Number LGL Report P1011-1. Report by LGL Alaska Research Associates Inc., LGL Ltd., Greeneridge Sciences Inc. and JASCO Applied Sciences for BP Exploration Alaska. 199 pp. http://www.nmfs.noaa.gov/pr/pdfs/permits/bp_liberty_monitoring.pdf.

ANSI S12.7-1986. R2006. *American National Standard Methods for Measurements of Impulse Noise*. American National Standards Institute, New York.

ANSI S1.1-1994. R2004. *American National Standard Acoustical Terminology*. American National Standards Institute, New York.

ANSI/ASA S1.13-2005. R2010. *American National Standard Measurement of Sound Pressure Levels in Air*. American National Standards Institute and Acoustical Society of America, New York.

ANSI/ASA S3.20-1995. R2008. *American National Standard Bioacoustical Terminology*. American National Standards Institute and Acoustical Society of America, New York.

Austin, M. 2014. Underwater noise emissions from drillships in the arctic. UA2014 - 2nd International Conference and Exhibition on Underwater Acoustics, Greece.

Brown, N.A. 1977. Cavitation noise problems and solutions. *International Symposium of Shipboard Acoustics 1976*. TNO Delft, Elsevier Publishing Company, Amsterdam.

Burdic, W.S. 1984. *Underwater acoustic system analysis*. 1st edition. Prentice Hall, Englewood Cliffs, NJ. 445.

Collins, M.D. 1993. A split-step Padé solution for the parabolic equation method. J*ournal of the Acoustical Society of America* 93: 1736-1742.

Collins, M.D., R.J. Cederberg, D.B. King, and S. Chin-Bing. 1996. Comparison of algorithms for solving parabolic wave equations. *Journal of the Acoustical Society of America* 100(1): 178-182.

Det Norske Veritas. 2010. Type Approval Certificate: Certificate No. M−11399. Høvik, Norway. 3 p.

Dragoset, W.H. 1984. A comprehensive method for evaluating the design of airguns and airgun arrays. P*roceedings, 16th Annual Offshore Technology Conference* Volume 3, May 7-9, 1984. OTC 4747, Houston, Houston. 75–84 pp.

Finneran, J.J. and A.K. Jenkins. 2012. *Criteria and thresholds for U.S. Navy acoustic and explosive effects analysis.* SPAWAR Systems Centre Pacific, San Diego, California.

Fisher, F.H. and V.P. Simmons. 1977. Sound absorption in sea water. *Journal of the Acoustical Society of America* 62(3): 558-564. http://link.aip.org/link/?JAS/62/558/1.

Fletcher, J.L. and R.G. Busnel. 1978. *Effects of noise on wildlif*e. Academic Press, New York.

Funk, D., D. Hannay, D. Ireland, R. Rodrigues, and W. Koski (eds.). 2008. *Marine mammal monitoring and mitigation during open water seismic exploration by Shell Offshore Inc. in the Chukchi and Beaufort Seas, July–November 2007: 90-day report.* LGL Report P969-1. Prepared by LGL Alaska Research Associates Inc., LGL Ltd., and JASCO Research Ltd. for Shell Offshore Inc., National Marine Fisheries Service (US), and US Fish and Wildlife Service. 218 pp.

Hannay, D. and R. Racca. 2005. *Acoustic Model Validation*. Document Number 0000-S-90-04-T-7006-00-E, Revision 02. Technical report for Sakhalin Energy Investment Company Ltd. by JASCO Research Ltd. 34 pp.

Ireland, D.S., R. Rodrigues, D. Funk, W. Koski, and D. Hannay. 2009. *Marine mammal monitoring and mitigation during open water seismic exploration by Shell Offshore Inc. in the Chukchi and Beaufort Seas, July–October 2008: 90-Day Report.* Document Number LGL Report P1049-1. 277 pp.

Kyhn, L.A., J. Tougaard, and S. Sveegaard. 2011: Underwater noise from the drillship Stena Forth in Disko West, Baffin Bay, Greenland. National Environmental Research Institute, Aarhus University, Denmark. 30 pp.– NERI Technical Report No. 838. http://www.dmu.dk/Pub/FR838.pdf

Landro, M. 1992. *Modelling of GI gun signatures*. Geophysical Prospecting 40: 721–747.

Laws, M., L. Hatton, and M. Haartsen. 1990. Computer modelling of clustered airguns. *First Break* 8: 331–338.

Leggat, L.J., H.M. Merklinger, and J.L. Kennedy. 1981. *LNG Carrier underwater noise study for Baffin Bay*. DREA Report–81/3, 32 p.

Lurton, X. 2002. *An Introduction to Underwater Acoustics: Principles and Applications*. Springer, Chichester, U.K. 347.

MacGillivray, A.O. 2006. *Acoustic Modelling Study of Seismic Airgun Noise in Queen Charlotte Basin*. MSc Thesis. University of Victoria, Victoria, BC. 98 pp.

MacGillivray, A.O. and N.R. Chapman. 2012. Modelling underwater sound propagation from an airgun array using the parabolic equation method. *Canadian Acoustics* 40(1): 19-25. http://jcaa.caa-aca.ca/index.php/jcaa/article/view/2502.

Mattsson, A. and M. Jenkerson. 2008. *Single Airgun and Cluster Measurement Project*. Joint Industry Programme (JIP) on Exploration and Production Sound and Marine Life Programme Review, October 28-30. International Association of Oil and Gas Producers, Houston, TX.

Nedwell, J.R. and A.W. Turnpenny. 1998. The use of a generic frequency weighting scale in estimating environmental effect. *Workshop on Seismics and Marine Mammals*. 23–25th June 1998, London, U.K.

Nedwell, J.R., A.W.H. Turnpenny, J. Lovell, S.J. Parvin, R. Workman, and J.A.L. Spinks. 2007. *A validation of the dBht as a measure of the behavioural and auditory effects of underwater noise*. Report No. 534R1231 prepared by Subacoustech Ltd. for the UK Department of Business, Enterprise and Regulatory Reform under Project No. RDCZ/011/0004. www.subacoustech.com/information/downloads/reports/534R1231.pdf.

Nowacek, D.P., L.H. Thorne, D.W. Johnston, and P.L. Tyack. 2007. Responses of cetaceans to anthropogenic noise. *Mammal Review* 37(2): 81-115.

O'Neill, C., D. Leary, and A. McCrodan. 2010. Sound Source Verification. (Chapter 3) In Blees, M.K., K.G. Hartin, D.S. Ireland, and D. Hannay (eds.). *Marine mammal monitoring and mitigation during open water seismic exploration by Statoil USA E&P Inc. in the Chukchi Sea, August-October 2010: 90-day report*. LGL Report P1119. Prepared by LGL Alaska Research Associates Inc., LGL Ltd., and JASCO Applied Sciences Ltd. for Statoil USA E&P Inc., National Marine Fisheries Service (US), and US Fish and Wildlife Service. pp 1-34.

Payne, R. and D. Webb. 1971. Orientation by means of long range acoustic signaling in baleen whales. *Annals of the New York Academy of Sciences* 188: 110-142.

Racca, R.G. and J.A. Scrimger. 1986. *Underwater Acoustic Source Characteristics of Air and Water Guns*. Document Number DREP Tech. Rep. 06SB 97708-5-7055. Report by JASCO Research Ltd. for Defence Research Establishment Pacific (Canada), Victoria, BC.

Richardson, W.J., C.R. Greene, Jr., C.I. Malme, and D.H. Thomson. 1995. *Marine Mammals and Noise*. Academic Press, San Diego, California. 576.

Ross, D. 1976. *Mechanics of Underwater Noise*, Pergamon Press, New York, 375 p.

Shipboard Scientific Party. 1994. Site 905. *In*: Mountain, G.S., K.G. Miller, P. Blum, P.-G. Aim, M.-P. Aubry, L.H. Burckle, B.A. Christensen, J. Compton, J.E. Damuth, J.-F. Deconinck, L. de Verteuil, C.S. Fulthorpe, S. Gartner, G. Guèrin, S.P. Hesselbo, B. Hoppie, M.E. Katz, N. Kotake, J.M. Lorenzo, S. McCracken, C.M. McHugh, W.C. Quayle, Y. Saito, S.W. Snyder, W.G. ten Kate, M. Urbat, M.C. Van Fossen, and A. Vecsei. *Proceedings of the Ocean Drilling Program, Initials Reports*. 150:255–308. College Station, TX (Ocean Drilling Program). Available at: doi:10.2973/odp.proc.ir.150.109.1994. Accessed September 28, 2011.

Southall, B.L., A.E. Bowles, W.T. Ellison, J.J. Finneran, R.L. Gentry, C.R. Greene, Jr., D. Kastak, D.R. Ketten, J.H. Miller, et al. 2007. Marine mammal noise exposure criteria: Initial scientific recommendations. *Aquatic Mammals* 33(4): 411-521.

Southall, B.L., A.E. Bowles, W.T. Ellison, J.J. Finneran, R.L. Gentry, C.R. Greene, Jr., D. Kastak, D.R. Ketten, J.H. Miller, et al. 2007. Marine mammal noise exposure criteria: Initial scientific recommendations. *Aquatic Mammals* 33(4): 411-521.

Spence, J., R. Fischer, M. Bahtiarian, L. Boroditsky, N. Jones, and R. Dempsey. 2007. *Review of Existing and Future Potential Treatments for Reducing Underwater Sound from Oil and Gas Industry Activitie*s. NCE REPORT 07-001. Report prepared by Noise Control Engineering, Inc., for Joint Industry Programme on E&P Sound and Marine Life.

Tyack, P.L. 2008. Implications for marine mammals of large-scale changes in the marine acoustic environment. *Journal of Mammology* 89(3): 549-558.

Warner, G., C. Erbe, and D. Hannay. 2010. Underwater Sound Measurements. (Chapter 3) *In* Reiser, C.M., D.W. Funk, R. Rodrigues, and D. Hannay (eds.). *Marine Mammal Monitoring and Mitigation during Open Water Shallow Hazards and Site Clearance Surveys by Shell Offshore Inc. in the Alaskan Chukchi Sea, July-October 2009: 90-Day Report*. LGL Report P1112-1. Report by LGL Alaska Research Associates Inc. and JASCO Applied Sciences for Shell Offshore Inc., National Marine Fisheries Service (US), and US Fish and Wildlife Service. pp 1-54.

Weilgart, L.S. 2007. The impacts of anthropogenic ocean noise on cetaceans and implications for management. *Canadian Journal of Zoology* 85: 1091-1116.

Zhang, Y. and C. Tindle. 1995. Improved equivalent fluid approximations for a low shear speed ocean bottom. *Journal of the Acoustical Society of America* 98(6): 3391-3396. http://scitation.aip.org/content/asa/journal/jasa/98/6/10.1121/1.413789.

Ziolkowski, A. 1970. A method for calculating the output pressure waveform from an airgun. *Geophysical Journal of the Royal Astronomical Society* 21(2): 137-161.

Appendix A. Maps of Cumulative SEL Fields around Vessels

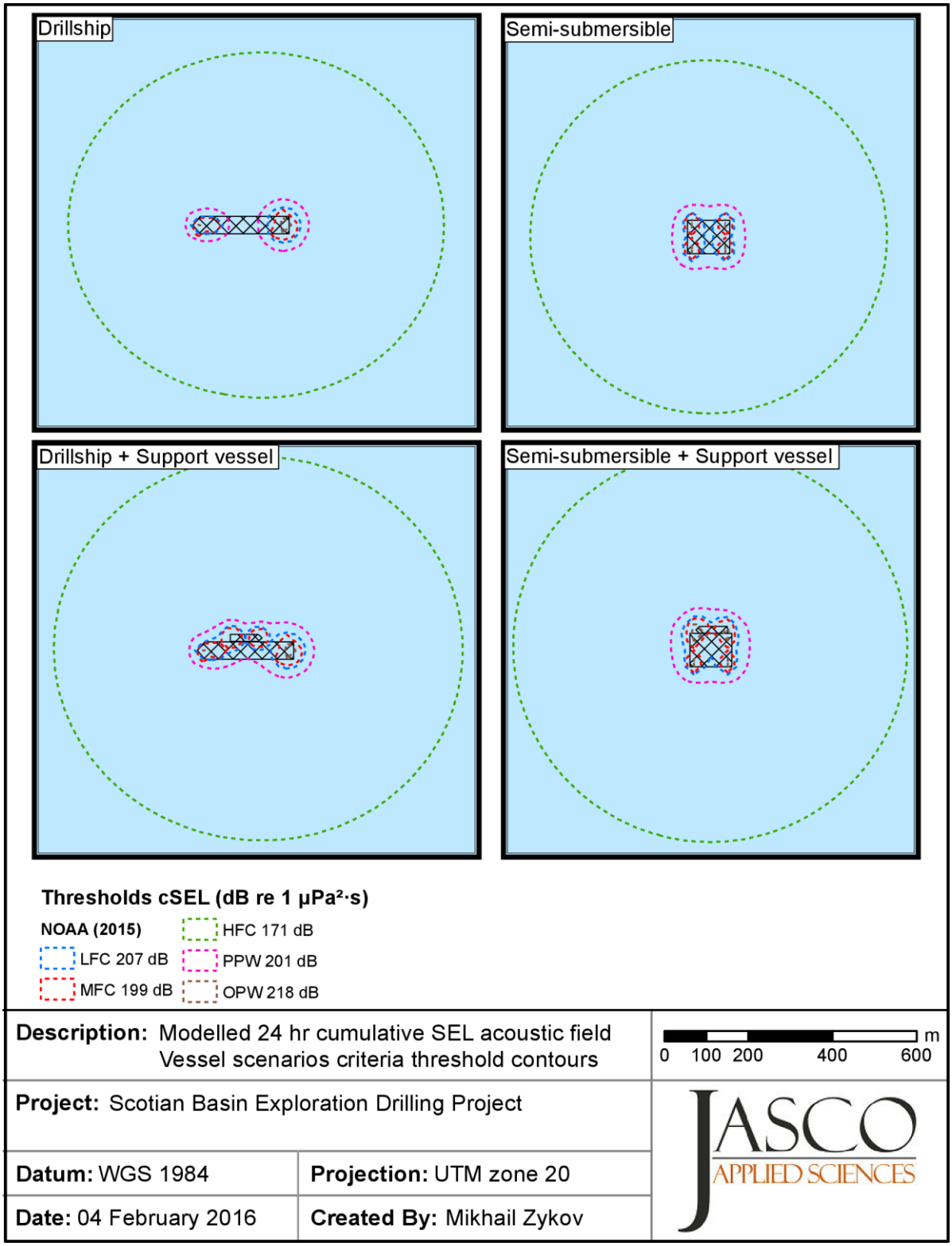

Figure 46. Vessel scenarios: cSEL threshold contours at Site A in winter for the NOAA (2015) criteria. Marine mammal hearing groups: LFC–low-frequency cetaceous, MFC–mid-frequency cetaceous, HFC–high-frequency cetaceous, PPW–phocid pinnipeds in water, and OPW–otariid pinnipeds in water.

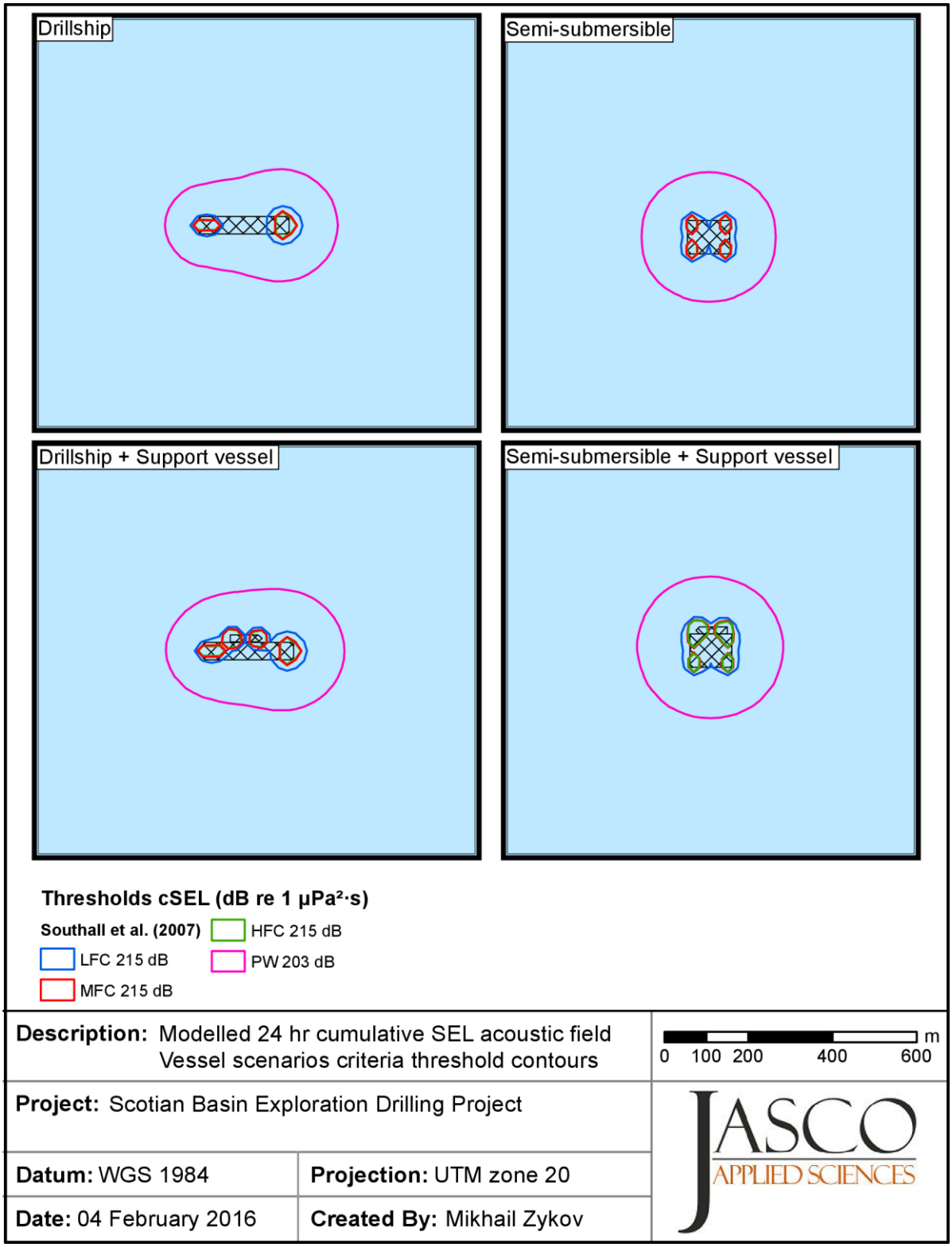

Figure 47. Vessel scenarios: cSEL threshold contours at Site A in winter for the Southall et al. (2007) criteria. Marine mammal hearing groups: LFC–low-frequency cetaceous, MFC–mid-frequency cetaceous, HFC–high-frequency cetaceous, and PW–pinnipeds in water.

.

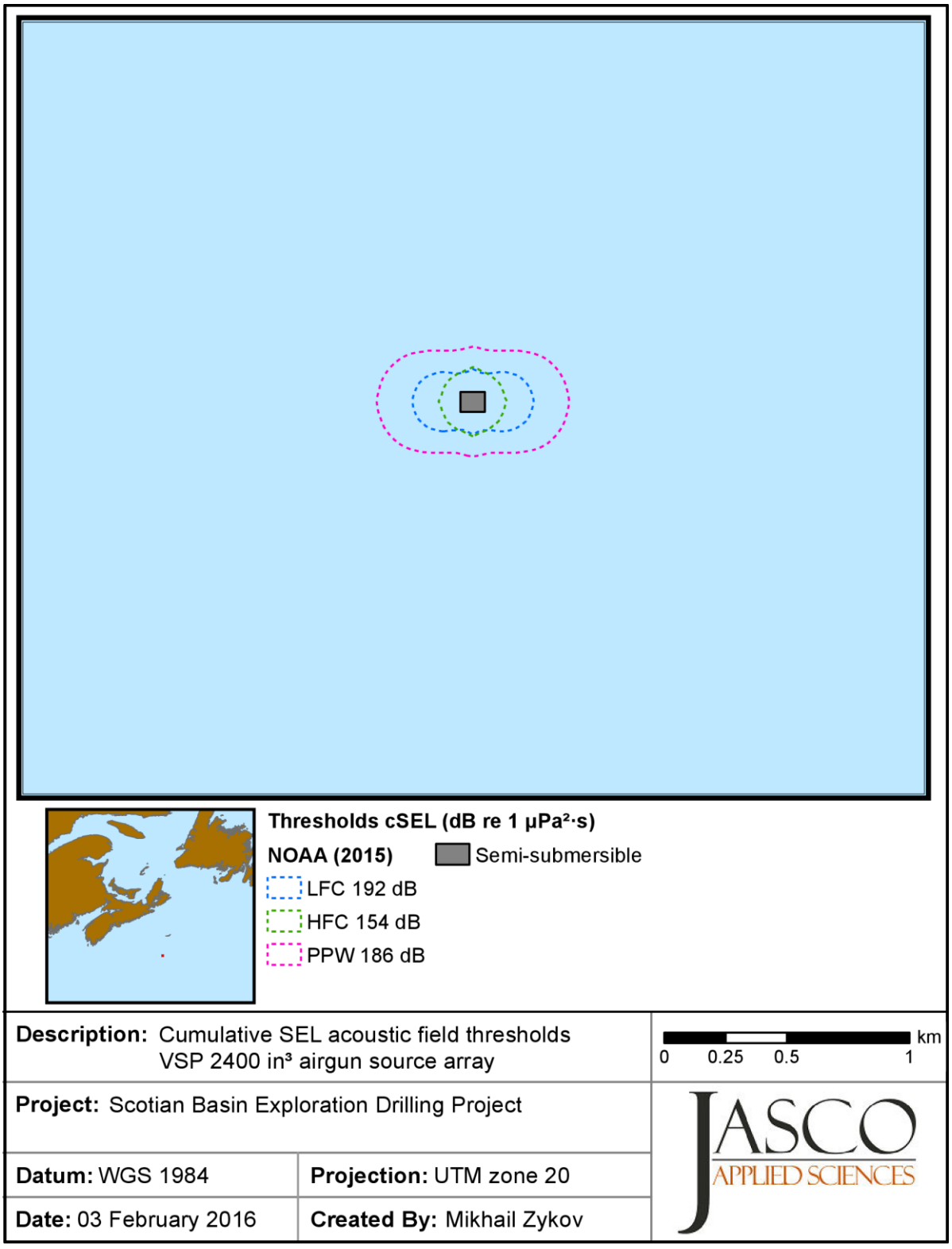

Figure 48. VSP airgun source array: cSEL threshold contours at Site A in winter for the NOAA (2015) criteria. Marine mammal hearing groups: LFC–low-frequency cetaceous, MFC–mid-frequency cetaceous, HFC–high-frequency cetaceous, PPW–phocid pinnipeds in water, and OPW–otariid pinnipeds in water. The thresholds contours for MFC and OPW are smaller than 20 m and not shown on the map.

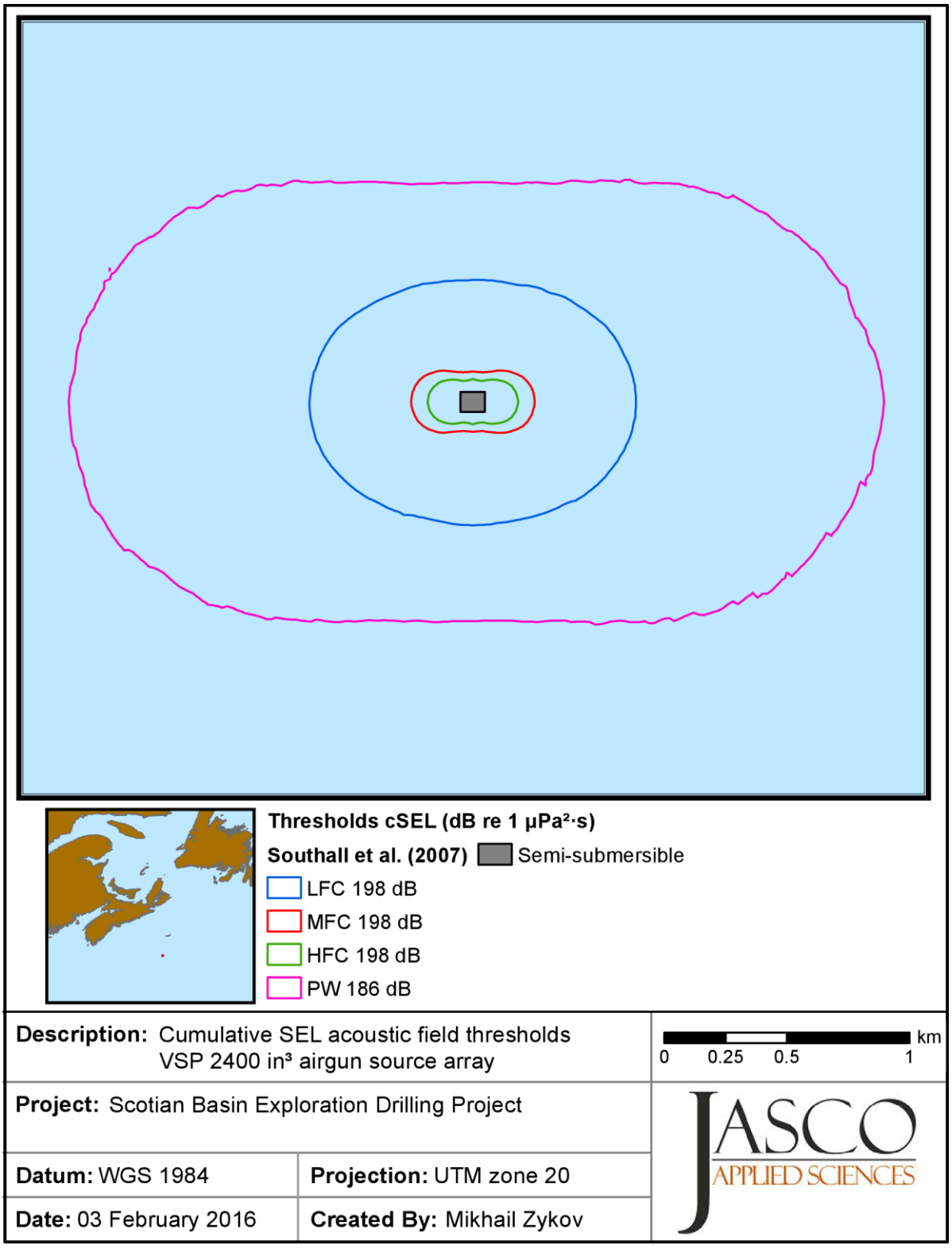

Figure 49. VSP airgun source array: cSEL threshold contours at Site A in winter for the Southall et al. (2007) criteria. Marine mammal hearing groups: LFC–low-frequency cetaceous, MFC–mid-frequency cetaceous, HFC–high-frequency cetaceous, PW–pinnipeds in water.